CENTRAL RESEARCH LIBRARY
DOCUMENT COLLECTION

2

OAK RIDGE NATIONAL LABORATORY
operated by
UNION CARBIDE CORPORATION
for the
U.S. ATOMIC ENERGY COMMISSION

OAK RIDGE NATIONAL LABORATORY LIBRARIES
3 4456 0549211 5

ORNL-TM-1105

TRANSITION RADIATION AND LOW-ENERGY BREMSSTRAHLUNG

Harry James Howe, Jr.

(Thesis)

CENTRAL RESEARCH LIBRARY
DOCUMENT COLLECTION
LIBRARY LOAN COPY
DO NOT TRANSFER TO ANOTHER PERSON
If you wish someone else to see this document, send in name with document and the library will arrange a loan.

Submitted to the Faculty of the Graduate School of Vanderbilt University in partial fulfillment of the requirements for the degree of Master of Science in Physics.

LEGAL NOTICE

This report was prepared as an account of Government sponsored work. Neither the United States, nor the Commission, nor any person acting on behalf of the Commission:

A. Makes any warranty or representation, expressed or implied, with respect to the accuracy, completeness, or usefulness of the information contained in this report, or that the use of any information, apparatus, method, or process disclosed in this report may not infringe privately owned rights; or

B. Assumes any liabilities with respect to the use of, or for damages resulting from the use of any information, apparatus, method, or process disclosed in this report.

As used in the above, "person acting on behalf of the Commission" includes any employee or contractor of the Commission, or employee of such contractor, to the extent that such employee or contractor of the Commission, or employee of such contractor prepares, disseminates, or provides access to, any information pursuant to his employment or contract with the Commission, or his employment with such contractor.

ERRATA

P. 36 EQUATION (3.6) The integrand should be multiplied by $e^{i\omega t}$.

P. 36 EQUATION (3.7) Sign of second term in square brackets in the integral should be positive.

P. 36 EQUATION (3.8) The factor $(\cos\theta_i)^{-2}$ multiplying the integral should be changed to $(\cos\theta_i)^{-1}$, the sign of the second term in the square brackets in the integral should be positive and the following term should be added to the right hand side:

$$\left(k_x \sin\theta_i - \frac{\omega}{v}\right) \frac{\tan^2\theta_i}{v\cos\theta_i}\, \theta_x(z_o/v\cos\theta_i) \int_{-\infty}^{z_o/v\cos\theta_i} \theta_x(z'_o/v\cos\theta_i)\, dz'_o$$

P. 37 EQUATION (3.10) Add the following to the expression for δ

$$(k_x \sin\theta_i - \omega/v)\tan^2\theta_i\, \theta_x(z_o/v\cos\theta_i) \int_{-\infty}^{z_o/v\cos\theta_i} \theta_x(z'_o/v\cos\theta_i \frac{dz'_o}{\cos\theta_i}$$

P. 38 EQUATION (3.13b). Add the above term to the expression for $B(\theta^2)$.

P. 38 EQUATION (3.36c). Replace the third term inside braces, i.e.,

$$\gamma\cos^2\theta_i, \text{ by } \gamma.$$

P. 53 EQUATION (3.39c). Replace last term of equation, i.e.,

$$\gamma\cos^2\theta_i, \text{ by } \gamma.$$

P. 55 EQUATION (3.41c). Delete $\cos^2\theta_i$ the last line of the equation.

ORNL-TM-1105

Contract No. W-7405-eng-26

HEALTH PHYSICS DIVISION

TRANSITION RADIATION AND LOW-ENERGY BREMSSTRAHLUNG

H. J. Howe, Jr. and R. H. Ritchie

Submitted as a thesis to the Graduate School of Vanderbilt University in partial fulfillment of the requirements for the degree of Master of Science

AUGUST 1965

OAK RIDGE NATIONAL LABORATORY
Oak Ridge, Tennessee
operated by
UNION CARBIDE CORPORATION
for the
U.S. ATOMIC ENERGY COMMISSION

OAK RIDGE NATIONAL LABORATORY LIBRARIES

3 4456 0549211 5

ACKNOWLEDGEMENTS

The authors are pleased to acknowledge the assistance of L. C. Emerson and R. N. Hamm in connection with the writing of the computer codes necessary for the numerical analysis of this work. Appreciation is also expressed to J. E. Turner for his fine translation of an experimental paper.

This investigation was carried out during the tenure of an Atomic Energy Commission Health Physics Fellowship administered by the Oak Ridge Institute of Nuclear Studies and held by one of the authors (HJH).

TABLE OF CONTENTS

	Page
ACKNOWLEDGEMENTS	ii
LIST OF FIGURES	vi
ABSTRACT	viii
Chapter	
I. INTRODUCTION	1
A. Bremsstrahlung	1
B. Cerenkov Radiation	5
C. Plasma Radiation	8
D. Transition Radiation	10
E. Scope of the Present Work	13
II. ELECTROMAGNETIC THEORY	15
A. Maxwell's Equations; Vector Potential	15
B. Hertz Vector; Wave Equation	16
C. Fourier Transformations	18
D. Rotation of Axes	20
E. Boundary Conditions	21
F. Form of Solution to Equation (2.18)	23
G. Saddle-Point Evaluation of Integral (2.34)	24
H. Transformation to Polar Coordinates	27

TABLE OF CONTENTS (Continued)

Page

I. Determination of the Field Vectors from $\vec{\Pi}(\vec{r}, t)$ 28

J. Poynting Flux and Number Distribution 29

K. Summary 32

III. TRANSITION RADIATION AND LOW-ENERGY BREMSSTRAHLUNG, ARBITRARY INCIDENCE 33

A. Current Density and Fourier Transform 34

B. Solutions to Wave Equations 39

C. Evaluation of the Constants in Equations (3.18) and (3.19). 41

D. Photon Number Distribution 43

E. Averaged Photon Number Distribution 47

1. Perpendicular Polarization
2. Parallel Polarization

F. Mean Square Scattering Angle Per Unit Length and Optical Constants 55

1. Mean Square Scattering Angle Per Unit Length

a. Lewis; Born Approximation
b. Nigam, Sundaresan, and Wu; 1st and 2nd Born Approximations
c. Integration Using Cross Sections of Lin

2. Optical Constants n and k

G. Summary 61

IV. RESULTS AND CONCLUSIONS 65

A. Results 65

TABLE OF CONTENTS (Continued)

Page

1. Normal Incidence

a. Copper
b. Silver
c. Gold

2. Arbitrary Incidence
3. Comparison with Experimental Results

B. Conclusions 91

APPENDIX I. DETERMINATION OF GREEN'S FUNCTION 93

APPENDIX II. STATISTICAL AVERAGES 96

LIST OF REFERENCES 104

LIST OF FIGURES

Figure		Page
1.	Rotation of Axes	20
2.	Transformation to Polar Coordinates	27
3.	Transformation to xyz Reference Frame	31
4.	Geometry - Transition Radiation and Low-Energy Bremsstrahlung, Arbitrary Incidence	33
5.	Mean Square Scattering Angle Per Unit Length - Gold	59
6.	Optical Constants - Copper	62
7.	Optical Constants - Silver	63
8.	Optical Constants - Gold	64
9.	Photon Intensity vs Wavelength - Copper, Normal Incidence	67
10.	Photon Intensity vs Electron Energy - Copper, Normal Incidence	68
11.	Photon Intensity vs Angle of Emission - Copper, Normal Incidence	69
12.	Photon Intensity vs Wavelength - Silver, Normal Incidence	72
13.	Photon Intensity vs Electron Energy - Silver, Normal Incidence	73
14.	Photon Intensity vs Angle of Emission - Silver, Normal Incidence	74
15.	Photon Intensity vs Wavelength - Gold, Normal Incidence	76
16.	Photon Intensity vs Electron Energy - Gold, Normal Incidence	77

LIST OF FIGURES (Continued)

Page

17. Photon Intensity vs Angle of Emission - Gold, Normal Incidence 78

18. Photon Intensity vs Wavelength - Silver, Arbitrary Incidence 82

19. Photon Intensity vs Electron Energy - Silver, Arbitrary Incidence 83

20. Photon Intensity vs Angle of Emission - Silver, Arbitrary Incidence 84

21. Photon Intensity vs Angle of Incidence - Silver, Arbitrary Incidence 85

22. Photon Intensity vs Angle of Azimuth - Silver, Arbitrary Incidence 86

23. Comparison of Photon Intensity vs Wavelength with Experiment - Silver, Arbitrary Incidence 90

ABSTRACT

A theoretical determination was made of the number distribution of photons emitted from a semi-infinite dielectric slab irradiated with electrons at an arbitrary angle of incidence. It was found that this quantity contains contributions from radiation generated by the induced electric polarization of the dielectric medium (transition radiation), and by multiple small-angle scattering of the electron on scattering centers assumed to be randomly distributed in the dielectric medium (bremsstrahlung). Interference effects between these two types of radiations are also exhibited.

Theoretical spectra were generated for plane foils of copper, silver, and gold irradiated by electrons at normal incidence and were compared with available experimental data. Good agreement was found at the higher electron energies ($\sim$100 keV), but the agreement was not as good at low electron energies ($\sim$25 keV). This discrepancy is felt to be partly due to uncertainties in the theoretical expression used for the mean square scattering angle and partly due to the fact that the foils used in obtaining the experimental results are too thick to satisfy the assumptions of the present theory.

Numerical theoretical results corresponding to the electron irradiation of plane foils of silver at various angles of electron incidence were also presented. An intense "peaking" of the emitted radiation around the wavelength

$\lambda = 3230$ Å was noted as the electron approached grazing incidence. The E^{-1} energy dependence of this radiation identified it as bremsstrahlung. Comparison of these results with recent experimental data shows fair agreement, but further work is necessary before conclusive interpretations can be made.

It is proposed that the irradiation of metals at oblique angles of incidence be studied thus providing a valuable means of studying optical bremsstrahlung generated near the surface of the irradiated medium. Data obtained in such experiments may yield results concerning the mean square scattering angle which could provide some insight on the effective electron-ion interaction potential in solids.

I. INTRODUCTION

The study of the emission of light from electron irradiated materials has long been of interest to physicists, having its origins in the early experimental investigations by Röntgen, Stokes, and Thomson[1] of the then unexplained cathode rays. Subsequent studies divided naturally into two general areas of investigation, one being concerned with the effects of cathode rays on certain materials and resulting in Röntgen's discovery of X rays in 1895, while the other was concerned with the intrinsic properties of the cathode rays leading directly to J. J. Thomson's discovery of the electron in 1897. The former area of interest—with certain aspects of which the present work is concerned—led to the now well-known phenomenon of bremsstrahlung, i.e., radiation emitted as a result of the "braking" of an electron by scattering in a medium.

A. Bremsstrahlung

In an excellent review of the early theoretical and experimental work dealing with the continuous X-ray spectrum, Webster[2] emphasizes the importance of the application of the then new quantum heat radiation theory of Planck to more general radiation problems as a possible means of explaining the observed continuous X-ray spectrum, and to thus demonstrate the validity of the new quantum theory. Kramers[3] used this method

to explain the absorption of X rays and the continuous X-ray spectrum by obtaining an approximate solution to the problem of the possible radiative processes which may occur when a free electron of given velocity approaches a positively charged nucleus. Later Mott[4] and Temple[5] extended Kramer's work by solving the wave equation for the scattering of charged particles by a Coulomb force and found that the quantum scattering cross section agreed exactly with the well-known Rutherford classical result for intermediate values of $Ze^2/\hbar v$. In 1931 Sommerfeld[6] presented the first complete quantum mechanical description of the bremsstrahlung process, a work which has since been extended by many writers, perhaps the best known treatment being that of Bethe and Heitler.[7] By combining the classical collision electrodynamics of a charged particle with a nucleus and the uncertainty principle of Heisenberg, one can obtain the Bethe-Heitler scattering cross section in a non-rigorous, semi-classical, but physically understandable manner.[8]

More recently Gluckstern, Hull, and Breit[9] derived expressions for the differential scattering cross section and its polarization dependence, working in the same approximation as did Bethe and Heitler; and Gluckstern and Hull[10] integrated this result over the direction of the scattered electron to obtain the photon angular and energy distributions. A generalization of Sommerfeld's earlier results to include relativistic effects has recently been given by Kulenkampf, Scheer, and Zeitler.[11] It must be pointed out, however, that almost all of the existing work has been devoted to the high

energy, i.e., X-ray end of the photon spectrum while very little attention has been devoted to the optical region which is of primary interest in the present work.

The effect of multiple scattering of electrons on isolated scattering centers in a medium has been considered by many writers with varying degrees of application. Bethe, Rose, and Smith[12] derived a Boltzmann diffusion equation describing the development in time of an initial electron configuration and obtained results for multiple scattering in thick plates in terms of the cross section for single scattering. Williams[13] considered the relativistic scattering of electrons and cosmic-ray particles including the important effects of the shielding of the nuclear charge by the atomic electrons and the finite size of the nucleus, but—as Goudsmit and Saunderson[14] point out—a comparison of his results with the experimental data indicates a consistent discrepancy. Goudsmit and Saunderson[14] employed certain properties of Legendre polynomials to present a theoretical treatment of multiple scattering which yields more nearly exact results and showed that the scattering depends in a sensitive way upon the atomic screening. Snyder and Scott[15] utilized a different approach to the multiple scattering problem, considered small-angle scattering by a screened potential field of the form $V(r) = (Ze^2/r)e^{-r/a}$ and showed the transition from the multiple scattering region to the long single scattering tail. Lewis[16] considered the multiple scattering problem in an infinite homogeneous medium and obtained results for the spatial and angular distribution, while still

another treatment is given by Molière[17,18] for the case of small angle multiple scattering in which the scattering is described in terms of a single scattering parameter x_α, which is characteristic of the scattering atom. The evaluation of this parameter is performed using Molière's earlier results[19] on the single scattering by a Fermi-Thomas potential in the second Born approximation. Nigam, Sundaresan, and Wu,[20] however, have argued that Molière's approach is incorrect and present expressions for multiple scattering in the second Born approximation by solving the Dalitz[21] relativistic formula for an electron interacting with a screened atomic field. Recent experimental results on multiple scattering of heavy ions[22] show agreement with the theory of Molière[17] as opposed to those of Nigam et al.[20] The author points out that previous results involving the multiple scattering of relativistic electrons and positrons for which the parameter $\alpha = (z_1 z_2)/137\beta$ never exceeds 0.6 are not adequate to allow a clear distinction to be made between the theories of Molière[17] and of Nigam et al.[20] but that for the heavy ions he has considered α ranges from 2.9 to 30.8, thus providing a check of the second Born approximation formulae. Reed and Nodvik[23] apply the Dalitz formula for the second Born approximation—following the method of Nigam et al.[20]—to the case of a potential involving the sum of three Yukawa-type potentials and obtain good agreement with the experimental results of Hanson, Lanzl, Lyman, and Scott.[24]

In contrast to the thorough investigation of bremsstrahlung from isolated scattering centers, very little work has been done in which the effects

of the medium upon the generated photons—i.e., refraction at the boundary, absorption by the medium, and coherency effects—have been considered. Gol'dman[25] and Andreev[26] give theoretical results for the electric field intensity of the photons generated by multiple scattering in the presence of a medium, i.e., including the effects of the boundary. A general consideration of the emitted radiation due to bremsstrahlung and transition radiation (discussed later in this chapter) by an electron penetrating a plane semi-infinite dielectric medium at normal incidence and experiencing scattering encounters on randomly distributed ion centers is presented by Ritchie, Ashley, and Emerson.[27] These results are contained as a special case of the present work. Numerical results pertaining to normally incident electrons will be presented.

In addition to bremsstrahlung, other possible radiation effects which must be considered in the present work are the radiation due to polarization effects of the electron on the dielectric medium, i.e., Cerenkov radiation, transition radiation, and plasmon radiation. One now reviews the major contributions to the understanding of these processes.

B. Cerenkov Radiation

It is now well known that a charged particle moving in a medium with a velocity greater than the phase velocity of light in that medium will be accompanied by an emission of radiation. Despite the fact that the theory of classical electrodynamics necessary for the explanation of such an effect

was known at the turn of the century—indeed, as is pointed out by Frank,[28] such eminent physicists as Kelvin (1901) and Sommerfeld (1904) had noted that electromagnetic radiation should be emitted by a charged particle moving with a velocity greater than that of light, but due to difficulties presented by the aether theory of that day and the later restriction of Einstein's relativity to velocities less than that of light, these ideas were abandoned—it was not until 1937 that Frank and Tamm[29] presented a satisfactory theoretical explanation of the weak radiation experimentally observed by Cerenkov[30] and which now bears his name. Actually, this weak radiation had previously been noticed by Madame Curie[31] in 1910 in the course of her researches with radioactivity, and had first been studied in a systematic manner by Mallet[32, 33, 34] who placed radioactive sources in or near transparent bodies and noted the emission of a faint bluish-white radiation. Mallet studied this phenomenon and was the first to discover that the radiation spectrum was continuous, thus lacking the characteristic line spectrum typical of "fluorescence", and hence was an entirely new phenomenon. However, Mallet attempted no explanation of the physical processes involved in this emission and for some unknown reason his experimental work was forgotten. It remained for Cerenkov[30] to rediscover this radiation during his experiments on the gamma-ray irradiation of pure liquids, and he also concluded that it represented a new phenomenon. Vavilov[35] proposed an explanation based on the process of bremsstrahlung but untenable difficulties soon became obvious. Cerenkov continued his experimental investigations and

concluded that the radiation was emitted by secondary electrons generated by the impinging gamma rays.[36] He later confirmed this view by means of electron irradiation[37] and also noted the now well-known asymmetry of the emitted intensity with respect to the incident particle direction.[38] The first mention of this new radiation in the American literature was in a letter by Cerenkov[39] which included the first photographs clearly illustrating the asymmetry of the emitted radiation. It was at this same time that Frank and Tamm[29] theoretically described this phenomenon by considering the classical electrodynamics of a uniformly moving electron in a dielectric medium and obtained the essential properties which are now called the Cerenkov relations, i.e., that a minimum velocity exists, $\beta_{min} = 1/n$, where n is the index of refraction of the medium, below which radiation is not possible, and that the radiation is emitted into a cone making an angle θ_c with the incident particle direction, θ_c being given by the well-known equation, $\cos\theta_c = 1/\beta n$. In addition, they derived an expression for the energy radiated per unit frequency interval per unit path length in the medium given by

$$\frac{d^2W}{d\omega\, dl} = \frac{e^2}{c^2}\,\omega\left(1 - \frac{1}{\beta^2 n^2}\right) . \tag{1.1}$$

Tamm[40] later presented a more general theoretical treatment in which he extended the previous work to consider certain aspects of the wave front and the time duration of the radiation pulse. Ginsburg[41] included the quantum mechanical effects of recoil due to photon emission by employing the

Schrödinger equation to obtain the quantum expression for the radiation output from a non-relativistic electron with no magnetic moment, and also employed the Dirac electron theory to obtain the exact relativistic result, including magnetic moment effects. As would be expected—since the Cerenkov effect occurs only for high energy particles and since the photons emitted are in the visible range, i.e., are of low energy—the quantum corrections are very small. Perhaps because of the weak intensity of the emitted radiation, it was not until after the perfection of the photomultiplier tube as a light detector that the Cerenkov effect experienced extensive application, especially in the field of high-energy physics.[42] It has been shown by Beck[43] and later by Garibian[44] that a general consideration of the radiation emitted by an electron in penetrating a dielectric medium will yield the contribution of Cerenkov radiation when the particle velocity is permitted to be greater than the phase velocity of light in the medium. Thus, further consideration of Cerenkov radiation in the present work is contained as a special case of the more general transition radiation which will be discussed shortly. One now presents a brief discussion of another type of radiation arising from polarization effects in the medium, i.e., the characteristic energy radiation due to collective plasma oscillations.

C. Plasma Radiation

In 1930 Rudberg[45] performed his pioneering experiments dealing with the characteristic energy loss spectra of electrons bombarding solid targets

and inspired renewed theoretical interest in an attempt to describe the physical processes involved. Rudberg and Slater[46] experienced some success by suggesting that the characteristic energy losses were due to discrete absorption of energy by the tightly bound core electrons of the bombarded medium through interband transitions. Bohm and Pines,[47, 48, 49, 50] in an extensive series of articles extending the earlier work by Bohm and Gross[51] on plasma oscillations, describe another means of characteristic energy absorption in which the conduction band electrons of a medium absorb energy through collective oscillations at a characteristic frequency ω_p which has come to be referred to as plasma oscillation at the plasma frequency. Ferrell[52] employed the Bohm-Pines theory to interpret the experimental results of Marton and Leder[53] on the scattering of electrons by a thin gold foil in which he (Ferrell) gives the angular dependence of characteristic electron energy losses. An excellent review of the progress toward an understanding of the characteristic electron energy loss spectra is given by Pines.[54]

In 1957 Ritchie[55] derived the angle-energy distribution of a fast electron traversing a thick metal foil and losing energy to the free conduction band electrons of the material. This distribution includes both the characteristics of the collective interactions described by Bohm, Pines, and Ferrell and the individual interaction of Rudberg and Slater, and in addition describes a short-lived loss at the frequency $\omega_p/\sqrt{2}$ which has come to be called the surface plasmon frequency. Ferrell[56] proposed a means of observing the plasma losses when he predicted that the conduction band electrons undergoing

collective oscillations should emit radiation at the plasma frequency ω_p. Ritchie and Eldridge[57] have since shown that the plasma theory of Ferrell[52] is contained in the more general transition radiation theory thus confirming the physical methods employed by Ferrell in deriving his distribution functions. One now presents a brief discussion of the main progress in developing the general transition radiation theory.

D. Transition Radiation

The phenomenon which has come to be referred to as transition radiation and which arises due to the induced electric polarization of a medium by an impinging charged particle was first described by Frank and Ginsburg[58] who considered the radiation emitted when a fast electron passes from a medium of dielectric properties given by ϵ_1 into a medium of different dielectric properties given by ϵ_2. They showed that this radiation was not a result of a change in the velocity of the electron but was due to induced polarization of the media. They further asserted that in the case of a fast electron moving from vacuum into a metal that the transition radiation intensity would be larger than the optical bremsstrahlung associated with the slowing down of the charge. It was also shown that in the special case of an electron moving into a perfect conductor the emitted radiation would be identical to that of the sudden collapse of a dipole, i.e., the annihilation of the electron and its image charge at the surface of the conductor. Since this early work of Frank and Ginsburg there has been an almost continual theoretical interest in this

phenomenon which has played an important role in the theory of metals. Beck[43] obtained the rigorous solution for the field of a point charge moving uniformly from a vacuum into a homogeneous dielectric medium. He found the characteristic transition radiation solution for large velocities and, in addition, found the characteristic Cerenkov cone for velocities greater than c/n, the phase velocity of light in the medium. This same connection between transition radiation and Cerenkov radiation was derived by Garibian[44] by considering the radiation emitted by a charged particle emerging from a dielectric medium into a vacuum. Askar'ian[59] proposed transition radiation as a method of generating millimeter length radiowaves by "bunches" of non-relativistic electrons impinging upon a metallic surface. Fainberg and Khizhniak[60] in considering the energy loss of a charged particle passing through a dielectric found that there is an increase in the intensity of the radiation when the dielectric is divided into layers. Garibian[61] analyzed the transition radiation emitted when a charged particle penetrates a large number of dielectric slabs separated by vacuum spaces and showed that the increased intensity could be peaked either in the forward or backward direction by a variation of the spacing of the dielectric slabs. He proposed this as a possible method of detecting relativistic particles. Pafomov[62] obtained the angular distributions of the transition radiation emitted by a charge moving normally into a finite slab from vacuum. He showed that in the case of an infinite slab his results reduced to those of Frank and Ginsburg.[58] Another consideration by Pafomov[63] of the transition radiation

emitted from an electron irradiated finite slab is given in which he considers both the case of the entering charge and the emerging charge and also takes into account the absorption of the medium. A similar consideration has also been given in a paper by Garibian and Chalikian.[64] Garibian[65] computed the energy loss by a charged particle traversing a finite slab and found that the energy loss due to transition radiation is important at high energies. In anticipation of the application of transition radiation as a fast particle detector and as a generator of short waves, Barsukov[66] derived the spectral and energy distribution of radiation produced in waveguides by ultra relativistic particles. Garibian[67] and Korkhmazyan[68] present results of their considerations of the transition radiation emitted by a charged particle incident on a dielectric slab at an arbitrary angle of incidence. Similar results are derived in the present work by a somewhat different method in Chapter 3. Garibian[69] has derived the spectral distribution of the radiation emitted by a charged particle moving through the interface of two media and has included the effect of multiple scattering; however, the effects of the boundary and of the medium on the multiple scattering have not been considered. Many other special aspects of transition radiation have been considered such as the radiation emitted by a moving charge in an inhomogeneous medium,[70] resonance effects in a laminar medium,[71] and the transition radiation in a plasma.[72] An excellent qualitative review of the properties of Cerenkov and transition radiation is given by Frank.[28] Ritchie and Eldridge[57] present a generalization of the theory of the transition

radiation emitted by a normally incident charged particle traversing a finite dielectric slab in which the wave properties of the incident charge are employed in the Born approximation. As was previously mentioned, these authors show that their result contains the plasma radiation results of Ferrell.[52] In addition they consider the case of the thick foil in which case their results reduce to the earlier Frank-Ginsburg[58] formulae, the thin foil, and a brief treatment of the effect of an oxide film which may be present on the dielectric surface. The most recent considerations are those of Ritchie, Ashley, and Emerson.[27, 73] In the first paper the radiation generated by bremsstrahlung and transition radiation produced by an electron traversing a semi-infinite dielectric medium at normal incidence is investigated from a macroscopic dielectric approach, a consideration which is contained in the present work for the special case of normal incidence. In the second paper the transition radiation is investigated from a microscopic approach which emphasized the individual events which occur when an energetic charged particle traverses a thin dielectric and obtained results consistent with those of the first paper.

E. Scope of the Present Work

In view of the valuable contribution of the theory of transition radiation to the explanation of the emitted radiation from electron irradiated metals and the comparatively recent theoretical considerations on the simultaneous generation of bremsstrahlung and transition radiation which have been

presented, it is of value to present in detail the general considerations involved in the determination of the photon yield from such physical processes—especially those in the visible region. The essential validity of a macroscopic dielectric approach which contains the contributions due to Cerenkov radiation, plasma radiation, and the radiation due to interband transitions of the tightly bound core electrons has been demonstrated. Therefore, for the purpose of the present work, one assumes that the properties of the irradiated dielectric material are adequately described in terms of a complex, frequency dependent dielectric constant of the form $\epsilon(\omega) = \epsilon_1(\omega) + i\epsilon_2(\omega)$. In Chapter II one employs this assumption to derive a general expression for the distribution of photons emitted by a charged particle passing from a vacuum into a medium of dielectric properties characterized by the dielectric constant $\epsilon(\omega)$. A particular physical situation is then considered which treats the passage of a charged particle at an arbitrary angle of incidence from vacuum into the dielectric medium and which includes the radiation due to polarization effects and due to bremsstrahlung caused by scattering on randomly distributed scattering centers. Numerical results are obtained by considering various values of the parameters involved and are compared with experimental results in Chapter IV.

II. ELECTROMAGNETIC THEORY

A model has been proposed by which one may calculate the photon yield in the far zone resulting from the passage of a charged particle through a vacuum into a medium described by a complex dielectric constant of the form $\epsilon(\omega) = \epsilon_1(\omega) + i\epsilon_2(\omega)$. It is the purpose of this chapter to develop the electromagnetic equations necessary to the determination of the photon number distribution $(d^2N)/(d\omega\, d\Omega)$ which represents the number of photons emitted per incident particle per unit frequency interval per unit solid angle in the direction specified by the angles Θ and Φ.

A. Maxwell's Equations; Vector Potential

The moving charged particle is described by charge and current densities $\rho(\vec{r}, t)$ and $\vec{J}(\vec{r}, t)$. Assuming homogeneous, isotropic, non-permeable media, one writes Maxwell's equations in the well-known form,

$$\nabla \times \vec{E}(\vec{r},t) = -\frac{1}{c}\frac{\partial \vec{B}(\vec{r},t)}{\partial t} \tag{2.1a}$$

$$\nabla \times \vec{H}(\vec{r},t) = \frac{4\pi}{c}\vec{J}(\vec{r},t) + \frac{1}{c}\frac{\partial \vec{D}(\vec{r},t)}{\partial t} \tag{2.1b}$$

$$\nabla \cdot \vec{D}(\vec{r},t) = 4\pi\rho(\vec{r},t) \tag{2.1c}$$

$$\nabla \cdot \vec{B}(\vec{r},t) = 0\,. \tag{2.1d}$$

One also has the constitutive relations between the field vectors (with $\mu = 1$

in non-permeable media).

$$\vec{D}(\vec{r},t) = \epsilon(\omega)\,\vec{E}(\vec{r},t) \tag{2.2a}$$

$$\vec{B}(\vec{r},t) = \vec{H}(\vec{r},t)\,. \tag{2.2b}$$

Contained, of course, in Equations (2.1) is the equation of continuity of charge,

$$\nabla\cdot\vec{J}(\vec{r},t) + \frac{\partial\rho(\vec{r},t)}{\partial t} = 0\,. \tag{2.3}$$

In the usual manner one defines the electromagnetic vector potential $\vec{A}(\vec{r}, t)$ with the equation,

$$\vec{B}(\vec{r},t) = \nabla\times\vec{A}(\vec{r},t)\,. \tag{2.4}$$

B. Hertz Vector: Wave Equation

Compact results can be obtained using the Hertz vector $\vec{\Pi}(\vec{r}, t)$ defined, in a manner similar to that given by Stratton,[74] by the equation,

$$\vec{A}(\vec{r},t) = \frac{\epsilon(\omega)}{c}\,\frac{\partial\vec{\Pi}(\vec{r},t)}{\partial t}\,. \tag{2.5}$$

Equation (2.4) becomes

$$\vec{B}(\vec{r},t) = \frac{\epsilon(\omega)}{c}\,\frac{\partial}{\partial t}\left[\nabla\times\vec{\Pi}(\vec{r},t)\right] \tag{2.6}$$

which when substituted into Equation (2.1a) yields the curl equation

$$\nabla\times\left[\vec{E}(\vec{r},t) + \frac{\epsilon(\omega)}{c^2}\,\frac{\partial^2\vec{\Pi}(\vec{r},t)}{\partial t^2}\right] = 0\,.$$

This equation is satisfied identically by the gradient of a scalar potential

$\phi(\vec{r}, t)$ defined through

$$\vec{E}(\vec{r},t) + \frac{\epsilon(\omega)}{c^2}\frac{\partial^2 \vec{\Pi}(\vec{r},t)}{\partial t^2} = -\nabla\phi(\vec{r},t) . \tag{2.7}$$

Further, since $\phi(\vec{r}, t)$ is arbitrary as long as it satisfies a homogeneous wave equation, one can write

$$\phi(\vec{r},t) = -\nabla\cdot\vec{\Pi}(\vec{r},t) . \tag{2.8}$$

Then, from Equations (2.7) and (2.8) one has the relationship between the electric field vector $\vec{E}(\vec{r}, t)$ and the Hertz vector $\vec{\Pi}(\vec{r}, t)$, i.e.,

$$\vec{E}(\vec{r},t) = \nabla[\nabla\cdot\vec{\Pi}(\vec{r},t)] - \frac{\epsilon(\omega)}{c^2}\frac{\partial^2 \vec{\Pi}(\vec{r},t)}{\partial t^2} . \tag{2.9}$$

One proceeds to derive the wave equation in the Hertz vector by employing the polarization vector $\vec{P}(\vec{r}, t)$ such that the equation of continuity (2.3) is satisfied identically, viz.,

$$\vec{J}(\vec{r},t) = \frac{\partial\vec{P}(\vec{r},t)}{\partial t} \tag{2.10}$$

$$\rho(\vec{r},t) = -\nabla\cdot\vec{P}(\vec{r},t) . \tag{2.11}$$

Then, using Equations (2.2a), (2.2b), (2.6), (2.9), and (2.10) in Maxwell's equation (2.1b), one obtains the non-homogeneous wave equation connecting the Hertz vector and the polarization of the medium:

$$\nabla\times[\nabla\times\vec{\Pi}(\vec{r},t)] - \nabla[\nabla\cdot\vec{\Pi}(\vec{r},t)] + \frac{\epsilon(\omega)}{c^2}\frac{\partial^2\vec{\Pi}(\vec{r},t)}{\partial t^2} = \frac{4\pi}{\epsilon(\omega)}\vec{P}(\vec{r},t) \tag{2.12}$$

which becomes, using the vector identity for the triple vector product in rectangular coordinates,

$$\nabla^2 \vec{\Pi}(\vec{r},t) - \frac{\epsilon(\omega)}{c^2}\frac{\partial^2 \vec{\Pi}(\vec{r},t)}{\partial t^2} = -\frac{4\pi}{\epsilon(\omega)}\vec{P}(\vec{r},t). \qquad (2.13)$$

C. Fourier Transformations

Employing the powerful methods of Fourier transformation, one can reduce Equations (2.6), (2.9), and (2.13) to ordinary differential equations involving only the z-coordinate dependence. One assumes conditions which allow transformation of all quantities according to the Fourier pair:

$$\vec{F}(\vec{r},t) = (2\pi)^{-3/2}\int_{-\infty}^{\infty} dk_x \int_{-\infty}^{\infty} dk_y \int_{-\infty}^{\infty} d\omega\, \vec{F}(\vec{k},\omega|z)\, e^{i(xk_x+yk_y-\omega t)} \qquad (2.14)$$

$$\vec{F}(\vec{k},\omega|z) = (2\pi)^{-3/2}\int_{-\infty}^{\infty} dx \int_{-\infty}^{\infty} dy \int_{-\infty}^{\infty} dt\, \vec{F}(\vec{r},t)\, e^{-i(xk_x+yk_y-\omega t)}. \qquad (2.15)$$

Equation (2.13), upon transformation, gives:

$$\nabla^2\left[\vec{\Pi}(\vec{k},\omega|z)\, e^{i(xk_x+yk_y-\omega t)}\right] - \frac{\epsilon(\omega)}{c^2}\frac{\partial^2}{\partial t^2}\left[\vec{\Pi}(\vec{k},\omega|z)\, e^{i(xk_x+yk_y-\omega t)}\right] +$$

$$+ \frac{4\pi}{\epsilon(\omega)}\vec{P}(\vec{k},\omega|z)\, e^{i(xk_x+yk_y-\omega t)} = 0. \qquad (2.16)$$

Similarly, Equation (2.10) becomes

$$\vec{J}(\vec{k},\omega|z)\, e^{i(xk_x+yk_y-\omega t)} - \frac{\partial}{\partial t}\left[\vec{P}(\vec{k},\omega|z)\, e^{i(xk_x+yk_y-\omega t)}\right] = 0. \qquad (2.17)$$

After performing the indicated operations in Equations (2.16) and (2.17), one combines the results to obtain the transformed wave equation,

$$\frac{d^2 \vec{\Pi}(\vec{k},\omega|z)}{dz^2} - \left(k_x^2 + k_y^2 - \epsilon(\omega)\frac{\omega^2}{c^2}\right)\vec{\Pi}(\vec{k},\omega|z) = -\frac{4\pi i}{\epsilon(\omega)\omega}\vec{J}(\vec{k},\omega|z). \quad (2.18)$$

One now transforms Equation (2.9) and obtains [with $\delta = (xk_x + yk_y - \omega t)$]

$$\vec{E}(\vec{k},\omega|z)e^{i\delta} - \nabla\left[\nabla\cdot\vec{\Pi}(\vec{k},\omega|z)\,e^{i\delta}\right] + \\ + \epsilon(\omega)\frac{\omega^2}{c^2}\frac{\partial^2}{\partial t^2}\left[\vec{\Pi}(\vec{k},\omega|z)\,e^{i\delta}\right] = 0. \quad (2.19)$$

Anticipating the application of boundary conditions, one finds it convenient to separate Equation (2.19) into component form. One writes

$$E_x(\vec{k},\omega|z)\,e^{i\delta} - \frac{\partial}{\partial x}\left\{\frac{\partial}{\partial x}\left[\Pi_x(\vec{k},\omega|z)e^{i\delta}\right] + \frac{\partial}{\partial y}\left[\Pi_y(\vec{k},\omega|z)e^{i\delta}\right] + \right. \\ \left. + \frac{\partial}{\partial z}\left[\Pi_z(\vec{k},\omega|z)\,e^{i\delta}\right]\right\} + \epsilon(\omega)\frac{\omega^2}{c^2}\frac{\partial^2}{\partial t^2}\left[\Pi_x(\vec{k},\omega|z)e^{i\delta}\right] = 0 \quad (2.20)$$

with similar expressions for the y and z components which, after one performs the indicated operations, become:

$$E_x = ik_x\left[ik_x\Pi_x + ik_y\Pi_y + \frac{\partial\Pi_z}{\partial z}\right] + \epsilon(\omega)\frac{\omega^2}{c^2}\Pi_x \quad (2.21a)$$

$$E_y = ik_y\left[ik_x\Pi_x + ik_y\Pi_y + \frac{\partial\Pi_z}{\partial z}\right] + \epsilon(\omega)\frac{\omega^2}{c^2}\Pi_y \quad (2.21b)$$

$$E_z = \frac{\partial}{\partial z}\left[ik_x\Pi_x + ik_y\Pi_y + \frac{\partial\Pi_z}{\partial z}\right] + \epsilon(\omega)\frac{\omega^2}{c^2}\Pi_z. \quad (2.21c)$$

Equation (2.6), using Equation (2.2b), is transformed and one has

$$\vec{H}(\vec{k},\omega|z)e^{i\delta} - \frac{\epsilon(\omega)}{c}\frac{\partial}{\partial t}\left[\nabla\times\vec{\Pi}(\vec{k},\omega|z)e^{i\delta}\right] = 0 \quad (2.22)$$

which, written in component form, is

$$H_x(\vec{k},\omega|z)\, e^{i\delta} = \frac{\epsilon(\omega)}{c}\frac{\partial}{\partial t}\left[\frac{\partial}{\partial y}\left(\Pi_z(\vec{k},\omega|z)e^{i\delta}\right) - \frac{\partial}{\partial z}\left(\Pi_y(\vec{k},\omega|z)e^{i\delta}\right)\right] \quad (2.23)$$

with similar expressions for the y and z components. Performing the differentiations, one finds:

$$H_x = -i\frac{\omega}{c}\epsilon\left[i k_y \Pi_z - \frac{\partial}{\partial z}\Pi_y\right] \quad (2.24a)$$

$$H_y = -i\frac{\omega}{c}\epsilon\left[\frac{\partial}{\partial z}\Pi_x - i k_x \Pi_z\right] \quad (2.24b)$$

$$H_z = -i\frac{\omega}{c}\epsilon\left[i k_x \Pi_y - i k_y \Pi_x\right] . \quad (2.24c)$$

D. Rotation of Axes

Now, to simplify the evaluation of conditions at the interface between two media, one chooses a coordinate system in which the x' axis coincides with the resultant of the J_x and J_y components. In this system $\vec{J}(\vec{r}, t)$—and therefore $\vec{\Pi}(\vec{r}, t)$—have only two components, the x' and z components. A simple rotation of axes in the xy plane yields the desired results with the transformation equations between the primed and unprimed systems being obtained from Figure 1.

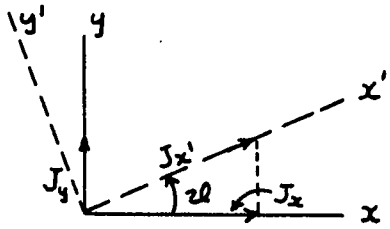

Fig. 1. - Rotation of Axes

$$x' = x\cos\theta + y\sin\theta \quad (2.25a)$$

$$y' = y\cos\theta - x\sin\theta \quad (2.25b)$$

$$k_{x'} = k_x\cos\theta + k_y\sin\theta \quad (2.26a)$$

$$k_{y'} = k_y\cos\theta - k_x\sin\theta \quad (2.26b)$$

Also from Figure 1 one has

$$J_x = J_{x'} \cos \vartheta \tag{2.27a}$$

$$J_y = J_{x'} \sin \vartheta \tag{2.27b}$$

$$\cos \vartheta = J_x (J_x^2 + J_y^2)^{-1/2} \tag{2.28a}$$

$$\sin \vartheta = J_y (J_x^2 + J_y^2)^{-1/2} . \tag{2.28b}$$

Then, employing Equations (2.25) and (2.26), one finds that $\exp i(xk_x + yk_y - \omega t) = \exp i(x'k_{x'} + y'k_{y'} - \omega t)$ and a Fourier transformation in the primed frame of Maxwell's equations in the primed frame yields results identical to those already derived (remembering that now $\Pi_{y'}(\vec{k}', \omega | z) = 0$).

E. Boundary Conditions

One applies the well-known conditions of continuity of the tangential components of the electric and magnetic field vectors at a boundary which require (in terms of the Fourier components):

$$E_{x'_1} = E_{x'_2} \tag{2.29a}$$

$$E_{y'_1} = E_{y'_2} \tag{2.29b}$$

$$H_{x'_1} = H_{x'_2} \tag{2.29c}$$

$$H_{y'_1} = H_{y'_2} \tag{2.29d}$$

where the subscripts 1 (2) refer to the medium below (above) the $z = 0$ plane. Using Equations (2.21) and (2.24) in the primed system and remembering

that $\Pi_{y'}(\vec{k}', \omega | z) = 0$, one writes (with $\epsilon_1 = 1$ for a vacuum):

$$i k_{x'}\left[i k_{x'} \Pi_{x'1} + \frac{\partial}{\partial z}\Pi_{z1}\right] + \frac{\omega^2}{c^2}\Pi_{x'1} = i k_{x'}\left[i k_{x'}\Pi_{x'2} + \frac{\partial}{\partial z}\Pi_{z2}\right] + \epsilon\frac{\omega^2}{c^2}\Pi_{x'2} \quad (2.30a)$$

$$i k_{y'}\left[i k_{x'}\Pi_{x'1} + \frac{\partial}{\partial z}\Pi_{z1}\right] = i k_{y'}\left[i k_{x'}\Pi_{x'2} + \frac{\partial}{\partial z}\Pi_{z2}\right] \quad (2.30b)$$

$$-i\frac{\omega}{c}\left(i k_{y'}\Pi_{z1}\right) = -i\epsilon\frac{\omega}{c}\left(i k_{y'}\Pi_{z2}\right) \quad (2.30c)$$

$$-i\frac{\omega}{c}\left[\frac{\partial}{\partial z}\Pi_{x'1} - i k_{x'}\Pi_{z1}\right] = -i\epsilon\frac{\omega}{c}\left[\frac{\partial}{\partial z}\Pi_{x'2} - i k_{x'}\Pi_{z2}\right]. \quad (2.30d)$$

Solution of this system of equations is straightforward and yields concise relations to be satisfied at the boundary. From Equation (2.30c) one finds

$$\Pi_{z1} = \epsilon\,\Pi_{z2}\,, \quad (2.31a)$$

which when substituted into Equation (2.30d) yields

$$\frac{\partial}{\partial z}\Pi_{x'1} = \epsilon\frac{\partial}{\partial z}\Pi_{x'2}\,. \quad (2.31b)$$

Equation (2.30b) is solved for $(\partial\Pi_{z2})/(\partial z)$ which is then substituted, along with Equation (2.31a) into Equation (2.30a), giving

$$\Pi_{x'1} = \epsilon\,\Pi_{x'2}\,. \quad (2.31c)$$

Then, rewriting Equation (2.30b), one has, in Equations (2.31), the four requirements on the Fourier components of the Hertz vector which must be satisfied at the z = 0 boundary.

$$i k_{x'}\Pi_{x'1} + \frac{\partial}{\partial z}\Pi_{z1} = i k_{x'}\Pi_{x'2} + \frac{\partial}{\partial z}\Pi_{z2}\,. \quad (2.31d)$$

F. Form of Solution to Equation (2.18)

One knows from classical electrodynamics that the radiation field behaves as an outgoing spherical wave; therefore, only that part of the general solution of Equation (2.18) which represents such a wave form is of interest in the present topic. However, the general solution of Equation (2.18) must still be found in order that the constants appearing in the homogeneous solution be evaluated. Further, since the radiation is to be observed in medium 1, that solution which applies to the lower ($z < 0$) half-space is of primary interest. Equation (2.18) in medium 1 is written

$$\frac{d^2 \vec{\Pi}_1(\vec{k}';\omega|z)}{dz^2} - \nu^2 \vec{\Pi}_1(\vec{k}';\omega|z) = -\frac{4\pi i}{\omega} \vec{J}_1(\vec{k}';\omega|z). \qquad (2.32)$$

Let us assume, for purposes of generality, that the transform of the desired radiation field solution of Equation (2.32) can be written in the simple form,

$$\vec{\Pi}_1(\vec{k}';\omega|z) = \hat{x}' A_{x'} e^{\nu z} + \hat{z} A_z e^{\nu z} \qquad (2.33)$$

where $\nu^2 = k_{x'}^2 + k_{y'}^2 - \omega^2/c^2$, $\hat{x}'$ is a unit vector along the x' axis, $\hat{z}$ is a unit vector along the z axis, and $A_{x'}$ and A_z are constants to be evaluated. According to Equation (2.14) in the primed reference frame, one writes

$$\vec{\Pi}(\vec{r}',t) = (2\pi)^{-3/2} \int_{-\infty}^{\infty}\int_{-\infty}^{\infty}\int_{-\infty}^{\infty} dk_{x'}\, dk_{y'}\, d\omega\, (\hat{x}' A_{x'} + \hat{z} A_z) \cdot$$

$$\cdot \exp[i(x'k_{x'} + y'k_{y'} - \omega t) + \nu z] \qquad (2.34)$$

the integration of which, applicable to the far zone, can be obtained by the "saddle-point" method described in the next section.

G. Saddle-Point Evaluation of Integral (2.34)

To apply the "saddle-point" method (method of steepest descents) described by Margenau and Murphy[75] and others,[76, 77] one writes the integrals over the k′ variables in the form

$$I = \int_{-\infty}^{\infty}\int_{-\infty}^{\infty} f(k_{x'}, k_{y'})\, e^{g(k_{x'}, k_{y'})} \frac{dk_{x'}}{k_{x'}} \frac{dk_{y'}}{k_{y'}} \tag{2.35}$$

where

$$f(k_{x'}, k_{y'}) = k_{x'} k_{y'} \left(\hat{x}' A_{x'} + \hat{z} A_z\right) \tag{2.36}$$

and

$$g(k_{x'}, k_{y'}) = i\left(x' k_{x'} + y' k_{y'}\right) + \left(k_{x'}^2 + k_{y'}^2 - \frac{\omega^2}{c^2}\right)^{1/2} z\,. \tag{2.37}$$

One sees that for large values of $|z|$ (corresponding to the far zone) the imaginary part of the exponent in Equation (2.35) causes rapid oscillations in the integrand which would be expected to contribute both positive and negative values to the integral. One finds that the major contribution to the integral under these conditions comes from the neighborhood of the point of stationary phase, the so-called "saddle-point", where the real part of $g(k_{k'}, k_{y'})$ is largest and the imaginary part is stationary. It is shown in Reference 75 that the Cauchy-Riemann equations locate this saddle-point $(k_{x'o}, k_{y'o})$ at the point where the first partial derivatives of $g(k_{x'}, k_{y'})$

vanish simultaneously, i.e.,

$$\frac{\partial g}{\partial k_{x'}}\Big|_{\substack{k_{x'o}\\k_{y'o}}} = 0 \quad , \qquad \frac{\partial g}{\partial k_{y'}}\Big|_{\substack{k_{x'o}\\k_{y'o}}} = 0 \ . \tag{2.38}$$

Having found the saddle-point, one expands $g(k_{x'}, k_{y'})$ about that point and evaluates the integral in the neighborhood of the saddle-point, thus

$$g(k_{x'},k_{y'}) = g(k_{x'o},k_{y'o}) + (k_{x'} - k_{x'o})\frac{\partial g}{\partial k_{x'}}\Big|_{\substack{k_{x'o}\\k_{y'o}}} + (k_{y'} - k_{y'o})\frac{\partial g}{\partial k_{y'}}\Big|_{\substack{k_{x'o}\\k_{y'o}}} +$$

$$+\frac{1}{2}\left\{(k_{x'} - k_{x'o})^2\frac{\partial^2 g}{\partial k_{x'}^2}\Big|_{\substack{k_{x'o}\\k_{y'o}}} + 2\,(k_{x'} - k_{x'o})(k_{y'} - k_{y'o})\frac{\partial^2 g}{\partial k_{x'}\partial k_{y'}}\Big|_{\substack{k_{x'o}\\k_{y'o}}} + (k_{y'} - k_{y'o})^2\frac{\partial^2 g}{\partial k_{y'}^2}\Big|_{\substack{k_{x'o}\\k_{y'o}}}\right\} \tag{2.39}$$

where terms in the small quantities $(k_{x'} - k_{x'o})$, $(k_{y'} - k_{y'o})$ of order higher than the second are neglected (Reference 77 shows that the exact result must be obtained by the inversion of series method, however for present purposes the above approximation suffices). By Equation (2.38) the second and third terms in Equation (2.39) vanish. One now makes the substitutions $k_{x'} = k_{x'o}e^{i\alpha}$, $k_{y'} = k_{y'o}e^{i\beta}$ where $-\Pi < \alpha < \Pi$ and $-\Pi < \beta < \Pi$, and expands the exponentials neglecting higher ordered terms in the small quantities α and β to obtain

$$(k_{x'} - k_{x'o}) = i\alpha\, k_{x'o} \tag{2.40a}$$

$$(k_{y'} - k_{y'o}) = i\beta\, k_{y'o} \ . \tag{2.40b}$$

Equation (2.39) becomes

$$g(k_{x'}, k_{y'}) = g(k_{x'o}, k_{y'o}) - \frac{1}{2}(A\alpha^2 + B\beta^2 + 2C\alpha\beta) \tag{2.41}$$

where

$$A = k_{x'o}^2 \frac{\partial^2 g}{\partial k_{x'}^2}\bigg|_{\substack{k_{x'o}\\ k_{y'o}}}, \qquad B = k_{y'o}^2 \frac{\partial^2 g}{\partial k_{y'}^2}\bigg|_{\substack{k_{x'o}\\ k_{y'o}}}, \qquad C = k_{x'o} k_{y'o} \frac{\partial^2 g}{\partial k_{x'} \partial k_{y'}}\bigg|_{\substack{k_{x'o}\\ k_{y'o}}}. \tag{2.42}$$

One also finds that $dk_{x'}/k_{x'} = id\alpha$ and $dk_{y'}/k_{y'} = id\beta$, therefore the integral becomes

$$I = \int_{-\infty}^{\infty}\int_{-\infty}^{\infty} f(k_{x'o}, k_{y'o})\, e^{g(k_{x'o}, k_{y'o})} \exp\left[-\tfrac{1}{2}\left(A\alpha^2 + B\beta^2 + 2C\alpha\beta\right)\right] i\,d\alpha\; i\,d\beta \tag{2.43}$$

where the function $f(k_{x'}, k_{y'})$ has been evaluated at the saddle-point and the limits $-\Pi$ to Π on α and β have been replaced by $-\infty$ to ∞ since α and β are small in the neighborhood of the saddle-point. The integrals over $d\alpha$ and $d\beta$ are of the form

$$\int_{-\infty}^{\infty} e^{-ax^2 \pm bx}\, dx = \left(\frac{\pi}{a}\right)^{1/2} e^{b^2/4a} \tag{2.44}$$

and Equation (2.43) is then given by

$$I = -k_{x'o} k_{y'o} \left(\hat{x}' A_{x'} + \hat{z} A_z\right) e^{g(k_{x'o}, k_{y'o})} (2\pi)(AB - C^2)^{-1/2} \tag{2.45}$$

where A, B, and C are given by Equation (2.42). Performing the operations required by Equations (2.38) and (2.42), one finds

$$k_{x'o} = \frac{\omega}{c} x' \left(x'^2 + y'^2 + z^2\right)^{-1/2} \tag{2.46a}$$

$$k_{y'o} = \frac{\omega}{c} y' \left(x'^2 + y'^2 + z^2\right)^{-1/2} \tag{2.46b}$$

$$A = k_{x'o}^2 \left(x'^2 + z^2\right)\left(i\frac{\omega}{c}\right)^{-1}\left(x'^2 + y'^2 + z^2\right)^{-1/2} \tag{2.46c}$$

$$B = k_{y'o}^2 \left(y'^2 + z^2\right)\left(i\frac{\omega}{c}\right)^{-1}\left(x'^2 + y'^2 + z^2\right)^{-1/2} \tag{2.46d}$$

$$C = k_{x'_0} k_{y'_0} x'y' \left(i\frac{\omega}{c}\right)^{-1} (x'^2 + y'^2 + z^2)^{-1/2} \tag{2.46e}$$

$$g(k_{x'_0}, k_{y'_0}) = i\frac{\omega}{c} (x'^2 + y'^2 + z^2)^{+1/2}. \tag{2.46f}$$

Substitution of the above values into Equation (2.45) yields

$$I = -i\frac{\omega}{c} z (x'^2+y'^2+z^2)^{-1/2} (2\pi)(\hat{x}' A_{x'} + \hat{z} A_z) \frac{\exp\left[i\frac{\omega}{c}(x'^2+y'^2+z^2)^{1/2}\right]}{(x'^2+y'^2+z^2)^{1/2}}. \tag{2.47}$$

The Hertz vector Equation (2.34) describing the far zone fields is

$$\vec{\Pi}_1(\vec{r}',t) = -\frac{iz(x'^2+y'^2+z^2)^{-1/2}}{(2\pi)^{1/2}(x'^2+y'^2+z^2)^{1/2}} \int_{-\infty}^{\infty} \frac{\omega}{c} (\hat{x}' A_{x'} + \hat{z} A_z) \exp\left[i\frac{\omega}{c}(x'^2+y'^2+z^2)^{1/2} - i\omega t\right]. \tag{2.48}$$

H. Transformation to Polar Coordinates

The form of Equation (2.48) immediately suggests the transformation to spherical polar coordinates which one now performs with the aid of Figure 2. Here Θ is the angle between the $-z$ axis and the observation direction $\hat{u}_R$, and Φ' is the azimuthal angle between the x' axis and $\hat{u}_R$.

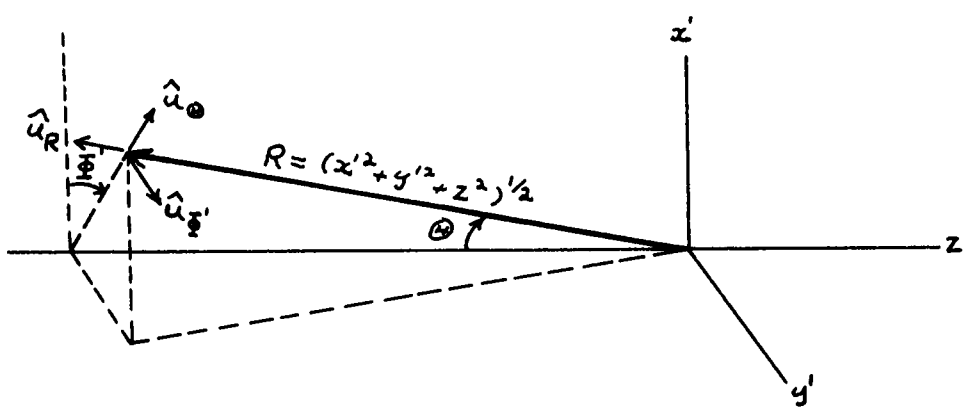

Fig. 2. - Transformation to Polar Coordinates

One has then:

$$\Pi_R = \Pi_{x'} \sin\Theta \cos\Phi' - \Pi_z \cos\Theta$$

$$\Pi_\Theta = \Pi_{x'} \cos\Theta \cos\Phi' + \Pi_z \sin\Theta$$

$$\Pi_{\Phi'} = - \Pi_{x'} \sin\Phi' .$$

Also, one writes:

$$\cos\Theta = z\,(x'^2 + y'^2 + z^2)^{-1/2}$$

$$R = (x'^2 + y'^2 + z^2)^{1/2} .$$

Hence, in component form, one obtains:

$$\Pi_R = -i \frac{\cos\Theta}{(2\pi)^{1/2}} \int_{-\infty}^{\infty} d\omega \, \frac{\omega}{c} (\sin\Theta \cos\Phi' A_{x'} - \cos\Theta A_z) \frac{\exp[i(\frac{\omega}{c}R - \omega t)]}{R} \tag{2.49a}$$

$$\Pi_\Theta = -i \frac{\cos\Theta}{(2\pi)^{1/2}} \int_{-\infty}^{\infty} d\omega \, \frac{\omega}{c} (\cos\Theta \cos\Phi' A_{x'} + \sin\Theta A_z) \frac{\exp[i(\frac{\omega}{c}R - \omega t)]}{R} \tag{2.49b}$$

$$\Pi_{\Phi'} = i \frac{\cos\Theta}{(2\pi)^{1/2}} \int_{-\infty}^{\infty} d\omega \, \frac{\omega}{c} \sin\Phi' A_{x'} \frac{\exp[i(\frac{\omega}{c}R - \omega t)]}{R} . \tag{2.49c}$$

One has, for the transformation of the k's

$$k_{x'} = \frac{\omega}{c} \sin\Theta \cos\Phi' \tag{2.50a}$$

$$k_{y'} = \frac{\omega}{c} \sin\Theta \sin\Phi' . \tag{2.50b}$$

I. Determination of the Field Vectors from $\vec{\Pi}(\vec{r}, t)$

One is interested in determining the number of photons emitted in the direction of observation defined by the angles Θ and Φ'. Therefore, considering

these quantities to be fixed, the components of the electric field that are of interest are found immediately from Equation (2.9), i.e.,

$$E_{\Theta} = \frac{\omega^2}{c^2} \Pi_{\Theta} \tag{2.51a}$$

$$E_{\Phi'} = \frac{\omega^2}{c^2} \Pi_{\Phi'} . \tag{2.51b}$$

Also, keeping only terms of order 1/R one finds (keeping the direction fixed)

$$H_{\Theta} = -\frac{\omega^2}{c^2} \Pi_{\Phi'} \tag{2.52a}$$

$$H_{\Phi'} = \frac{\omega^2}{c^2} \Pi_{\Theta} . \tag{2.52b}$$

Using Equations (2.49b) and (2.49c), one has the field components perpendicular to the photon propagation direction $\hat{u}_R$,

$$E_{\Theta} = H_{\Phi'} = \frac{-i \cos\Theta}{(2\pi)^{1/2} R} \int_{-\infty}^{\infty} d\omega \, \frac{\omega^3}{c^3} \left(A_{x'} \cos\Theta \cos\Phi' + A_z \sin\Theta \right) \cdot$$

$$\cdot \exp\left[i \left(\frac{\omega}{c} R - \omega t \right) \right] \tag{2.53a}$$

$$E_{\Phi'} = - H_{\Theta} = \frac{-i \cos\Theta}{(2\pi)^{1/2} R} \int_{-\infty}^{\infty} d\omega \, \frac{\omega^3}{c^3} A_{x'} \sin\Phi' \exp\left[i \left(\frac{\omega}{c} R - \omega t \right) \right] . \tag{2.53b}$$

J. Poynting Flux and Number Distribution

The energy flux, given by the Poynting vector, is

$$\vec{S}(\vec{r},t) = \frac{c}{4\pi} \vec{E}(\vec{r},t) \times \vec{H}(\vec{r},t) \tag{2.54}$$

from which one finds the radial component S_R:

$$S_R = \frac{c}{4\pi} \left(E_{\Theta} H_{\Phi'} - E_{\Phi'} H_{\Theta} \right) . \tag{2.55}$$

In the usual manner the energy radiated per unit solid angle is found to be

$$\frac{dW}{d\Omega} = \frac{c}{4\pi} R^2 \int_{-\infty}^{\infty} (E_\Theta H_{\Phi'} - E_{\Phi'} H_\Theta)\, dt \tag{2.56}$$

which becomes, using Equations (2. 51) and (2. 52)

$$\frac{dW}{d\Omega} = \frac{c}{4\pi} \int_{-\infty}^{\infty} d\omega \int_{-\infty}^{\infty} d\omega' \int_{-\infty}^{\infty} dt\, \frac{\omega^3}{c^3} \frac{\omega'^3}{c^3} \Big\{ \left| A_{x'} \cos\Theta \cos\Phi' + A_z \sin\Theta \right|^2 +$$

$$+ \left| A_{x'} \sin\Phi' \right|^2 \Big\} e^{i(\omega'-\omega)R/c} e^{i(\omega'-\omega)t} \cos^2\Theta \,. \tag{2.57}$$

Now, using the well-known Fourier representation of the Dirac delta function

$$2\pi\, \delta(\omega'-\omega) = \int_{-\infty}^{\infty} e^{i(\omega'-\omega)t}\, dt \,, \tag{2.58}$$

and the fact that $\Pi(-\omega) = \Pi^*(\omega)$ for the physical situation under consideration one finds for Equation (2. 57)

$$\frac{dW}{d\Omega} = \frac{c \cos^2\Theta}{2\pi} \int_0^{\infty} \frac{\omega^6}{c^6} \Big\{ \left| A_{x'} \cos\Theta \cos\Phi' + A_z \sin\Theta \right|^2 + \left| A_{x'} \sin\Phi' \right|^2 \Big\} d\omega. \tag{2.59}$$

The intensity distribution $[dI(\omega)]/d\Omega$, as usually defined,[8] is found from Equation (2. 59) to be

$$\frac{dI(\omega)}{d\Omega} = \frac{c \cos^2\Theta}{2\pi} \frac{\omega^6}{c^6} \Big\{ \left| A_{x'} \cos\Theta \cos\Phi' + A_z \sin\Theta \right|^2 + \left| A_{x'} \sin\Phi' \right|^2 \Big\} \tag{2.60}$$

which one divides by the photon energy $\hbar\omega$ to obtain the photon number distribution

$$\frac{d^2N}{d\omega\, d\Omega} = \frac{\cos^2\Theta}{2\pi\hbar} \frac{\omega^5}{c^5} \Big\{ \left| A_{x'} \cos\Theta \cos\Phi' + A_z \sin\Theta \right|^2 + \left| A_{x'} \sin\Phi' \right|^2 \Big\}. \tag{2.61}$$

Defining the plane of emission as that plane containing the normal to the dielectric medium (the z axis) and the direction of photon emission u_R, Equation (2.61) is divided (using Figure 2) into a number distribution of photons polarized parallel to $(d^2N_{\parallel})/(d\omega d\Omega)$ and perpendicular to $(d^2N_{\perp})/(d\omega d\Omega)$ the plane of emission. One has

$$\frac{d^2N_{\parallel}}{d\omega d\Omega} = \frac{\cos^2\Theta}{2\pi\hbar}\,\frac{\omega^5}{c^5}\left|A_{x'}\cos\Theta\cos\Phi' + A_z\sin\Theta\right|^2 \tag{2.62a}$$

$$\frac{d^2N_{\perp}}{d\omega d\Omega} = \frac{\cos^2\Theta}{2\pi\hbar}\,\frac{\omega^5}{c^5}\left|A_{x'}\sin\Phi'\right|^2 . \tag{2.62b}$$

Using Figure 3 one transforms back to the original xyz reference frame with the relations

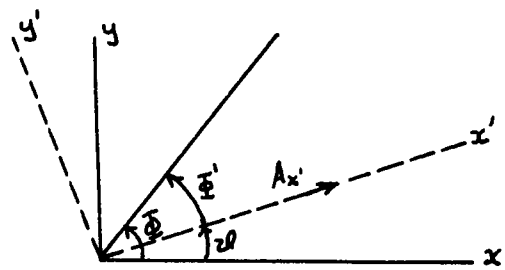

Fig. 3.-Transformation to xyz Reference Frame

$$A_{x'}\cos\Phi' = A_x\cos\Phi + A_y\sin\Phi \tag{2.63a}$$

$$A_{x'}\sin\Phi' = A_x\sin\Phi - A_y\cos\Phi . \tag{2.63b}$$

Then under this transformation Equations (2.62) become

$$\frac{d^2N_{\parallel}}{d\omega d\Omega} = \frac{\cos^2\Theta}{2\pi\hbar}\,\frac{\omega^5}{c^5}\left|\cos\Theta(A_x\cos\Phi + A_y\sin\Phi) + A_z\sin\Theta\right|^2 \tag{2.64a}$$

$$\frac{d^2N_\perp}{d\omega d\Omega} = \frac{\cos^2\Theta}{2\pi\hbar}\,\frac{\omega^5}{c^5}\left|A_x \sin\Phi - A_y \cos\Phi\right|^2. \tag{2.64b}$$

K. Summary

One has obtained the inhomogeneous wave equation connecting the Hertz vector with a source current density, has determined the boundary conditions on the components of this quantity, and finally has expressed the photon number distribution in terms of the constants appearing in the radiation solution to the wave equation in the Hertz vector. One now considers a particular physical situation under which a dielectric medium is irradiated by charged particles, and describes the resulting emitted radiation.

III. TRANSITION RADIATION AND LOW-ENERGY BREMSSTRAHLUNG, ARBITRARY INCIDENCE

One wishes to generalize the methods of Ritchie, Ashley, and Emerson[27] to include the case of non-normal incidence of the charged particle. One assumes a classical point mass of charge Ze traversing a space consisting of a vacuum ($\epsilon = 1$, $z < 0$) and a dielectric medium [$\epsilon(\omega)$, $z > 0$]. The charged particle moves with a velocity given by $\vec{v}(t)$ which is directed at an angle θ_i measured with respect to the normal to the dielectric medium (the z axis). It is further assumed that the particle is undeviated in the vacuum but experiences small angle scatters ($\langle \Theta^2 \rangle_\ell t \ll 1$) on randomly distributed scattering centers located in the semi-infinite dielectric (thickness $t \gg \lambda_{opt}$). The energy loss experienced by the particle as it traverses this space is assumed to be small compared to its initial energy. The geometry of the present situation is shown in Figure 4.

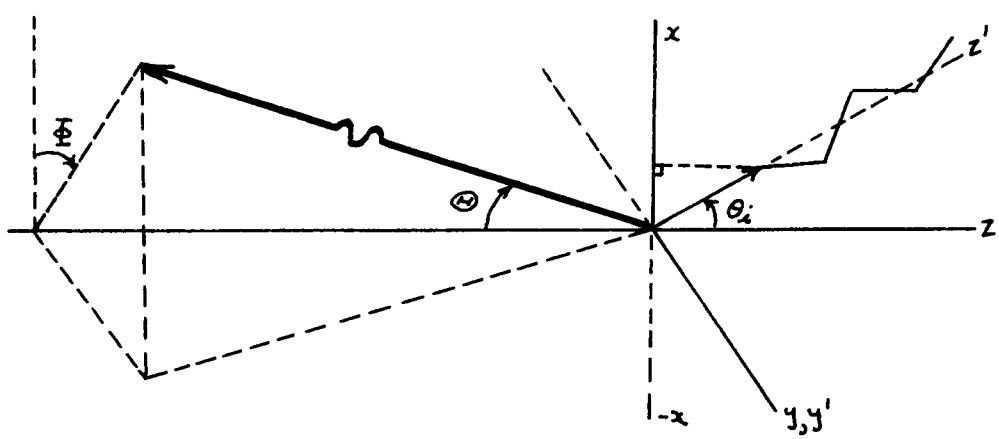

Fig. 4. - Geometry-Transition Radiation and Low-Energy Bremsstrahlung

The charged particle crosses into the dielectric at the origin with its velocity $\vec{v}(t)$ making an angle θ_i with the z axis. The projection of this velocity onto the plane vacuum-dielectric interface is taken to define the x axis. One must modify the approach of Ritchie, Ashley, and Emerson[27] somewhat in order to correctly match the field vectors at the z = 0 boundary. One assumes a current density $\vec{J}_o(\vec{r}_o, t)$ due to the passage of the charged particle—at some angle $\theta(t_o)$ with the z axis—through the $z = z_o$ plane. One then finds the Hertz vector $\vec{\Pi}_o(\vec{r}, t)$ resulting from the reaction of the medium to this current density, matches it at the z = 0 boundary to determine the arbitrary constants, and finally integrates (corresponding to a coherent sum) over the entire space $-\infty$ to ∞ to obtain the total radiation field specified by $\vec{\Pi}(\vec{r}, t)$. One then proceeds according to Chapter II to obtain the photon number distribution $(d^2N)/(d\omega\, d\Omega)$ for a particular scattering history and to average this quantity over all possible scattering configurations to obtain the quantity of interest $\langle (d^2N)/(d\omega\, d\Omega)\rangle$.

A. Current Density and Fourier Transform

One writes the current density in the form

$$\vec{J}_o(\vec{r}_o, t) = Ze\,\vec{v}(t)\,\delta\left(\vec{r}_o - \int_{-\infty}^{t} \vec{v}(t')\,dt'\right) \tag{3.1}$$

where Ze denotes the charge and $\vec{v}(t)$ the velocity of the particle, and $\vec{r}_o$ is the position at which the current density is to be determined. By using the assumption of small energy loss by the charged particle one considers the velocity of the particle to have a constant magnitude $v = |\vec{v}|$ and to be

directed along an instantaneous unit vector $\hat{u}(t)$. In the $x'y'z'$ reference frame—where the z' axis is the original undeviated direction of the charged particle—one writes the velocity as

$$\vec{v}(t) = v\left(\hat{x}' \sin\theta(t)\cos\phi(t) + \hat{y}' \sin\theta(t)\sin\phi(t) + \hat{z}' \cos\theta(t)\right) \tag{3.2}$$

where $\theta(t)$ and $\phi(t)$ are the instantaneous polar and azimuthal angles, respectively, of the particle. Then, in the xyz reference frame one has the expressions

$$v_x(t) = v\left(\sin\theta(t)\cos\phi(t)\cos\theta_i + \cos\theta(t)\sin\theta_i\right) \tag{3.3a}$$

$$v_y(t) = v \sin\theta(t)\sin\phi(t) \tag{3.3b}$$

$$v_z(t) = v\left(\cos\theta(t)\cos\theta_i - \sin\theta(t)\cos\phi(t)\sin\theta_i\right). \tag{3.3c}$$

Using the assumption of small angle scattering one writes $\sin\theta(t) \cong \theta(t)$ and $\cos\theta(t) \cong [1 - 1/2\,\theta^2(t)]$ in which case the velocity components are written

$$v_x(t) = v\left[\theta_x(t)\cos\theta_i + (1 - \tfrac{1}{2}\theta^2(t))\sin\theta_i\right] \tag{3.4a}$$

$$v_y(t) = v\,\theta_y(t) \tag{3.4b}$$

$$v_z(t) = v\left[(1 - \tfrac{1}{2}\theta^2(t))\cos\theta_i - \theta_x(t)\sin\theta_i\right] \tag{3.4c}$$

where one has used $\theta_x(t) \equiv \theta(t)\cos\phi(t)$, $\theta_y(t) \equiv \theta(t)\sin\phi(t)$, and $\theta^2(t) = \theta_x^2(t) + \theta_y^2(t)$ for convenience of notation. Writing Equation (3.1) in component form and performing the Fourier transformation prescribed by

Equation (2.15) one obtains—the integrations over dx and dy being simplified by the delta functions—

$$J_{ox}(\vec{k},\omega|z_o) = Ze\,(2\pi)^{-3/2}\int_{-\infty}^{\infty} u_x(t)\,\exp\left[-i\left(k_x v\int_{-\infty}^{t} u_x(t')dt' + k_y v\int_{-\infty}^{t} u_y(t')dt'\right)\right]\cdot$$

$$\cdot\,\delta\left(z_o - v\int_{-\infty}^{t} u_z(t')\,dt'\right)\,v\,dt \qquad (3.5)$$

with similar expressions for $J_{oy}(\vec{k},\omega|z_o)$ and $J_{oz}(\vec{k},\omega|z_o)$. The quantities $u_x(t)$, $u_y(t)$, and $u_z(t)$ are obtained from Equations (3.4). To solve this equation one must find the zero of the argument of the remaining delta function, i.e., using the expression for $u_z(t)$ one must solve the expression

P. 36 EQUATION (3.6) The integrand should be multiplied by $e^{i\omega t}$.

in an approximate manner by iteration. To do this one lets $z_o = vt\cos\theta_i$ and puts this result back into Equation (3.6) to obtain

P. 36 EQUATION (3.7) Sign of second term in square brackets in the integral should be positive.

$$-\infty$$

$$\cdot\; dz_o'/\cos\theta_i \;=\; 0 \qquad (3.7)$$

which yields the approximate zero for the d...

P. 36 EQUATION (3.8) The factor $(\cos\theta_i)^{-2}$ multiplying the integral should be changed to $(\cos\theta_i)^{-1}$, the sign of the second term in the square brackets in the integral should be positive and the following term should be added to the right hand side:

$$\left(k_x\sin\theta_i - \frac{\omega}{v}\right)\frac{\tan^2\theta_i}{v\cos\theta_i}\,\theta_x(z_o/v\cos\theta_i)\int_{-\infty}^{z_o/v\cos\theta_i}\theta_x(z_o'/v\cos\theta_i)\,dz_o'$$

z... ... simplifies the result to obtain

$$J_{ox}(\vec{k},\omega|z_o) = Ze\,(2\pi)^{-3/2}\left[\frac{\theta_x(t_1)\cos\theta_i + (1-\tfrac{1}{2}\theta^2(t_1))\sin\theta_i}{\cos\theta_i}\right]\cdot$$

$$\cdot\exp\left[i\left(\frac{\omega}{v} - k_x\sin\theta_i\right)\frac{z_o}{\cos\theta_i}\right]e^{-i\delta} \qquad (3.9a)$$

$$J_{oy}(\vec{k},\omega|z_o) = Ze\,(2\pi)^{-3/2}\,\frac{\theta_y(t_1)}{\cos\theta_i}\,\exp\left[i\left(\frac{\omega}{v} - k_x\sin\theta_i\right)\frac{z_o}{\cos\theta_i}\right]e^{-i\delta} \qquad (3.9b)$$

$$J_{oz}(\vec{k},\omega|z_o) = Ze\,(2\pi)^{-3/2}\left[\frac{(1-\tfrac{1}{2}\theta^2(t_1))\cos\theta_i - \theta_x(t_1)\sin\theta_i}{\cos\theta_i}\right]\cdot$$

$$\cdot\exp\left[i\left(\frac{\omega}{v} - k_x\sin\theta_i\right)\frac{z_o}{\cos\theta_i}\right]e^{-i\delta} \qquad (3.9c)$$

where

P. 37 EQUATION (3.10) Add the following to the expression for δ

$$(k_x\sin\theta_i - \omega/v)\tan^2\theta_i\,\theta_x(z_o/v\cos\theta_i)\int_{-\infty}^{z_o/v\cos\theta_i}\theta_x(z'_o/v\cos\theta_i\,\frac{dz'_o}{\cos\theta_i}$$

$$+ k_y\int_{-\infty}\theta_y(z'_o/v\cos\theta_i)\frac{dz'_o}{\cos\theta_i} - \frac{\omega\sin\theta_i}{v\cos^2\theta_i}\int_{-\infty}\theta_x(z'_o/v\cos\theta_i)\,dz'_o$$

$$-\frac{\omega}{2v\cos\theta_i}\int_{-\infty}^{z_o/v\cos\theta_i}\theta^2(z'_o/v\cos\theta_i)\,dz'_o + k_x\tan\theta_i\;\theta_x\int_{-\infty}^{z_o/v\cos\theta_i}\theta_x(z'_o/v\cos\theta_i)\,dz'_o$$

$$+ k_y\,\frac{\tan\theta_i}{\cos\theta_i}\;\theta_y\int_{-\infty}^{z_o/v\cos\theta_i}\theta_x(z'_o/v\cos\theta_i)\,dz'_o\,. \qquad (3.10)$$

In accordance with the assumption of small angle scattering one expands the quantity $e^{-i\delta}$ and keeps only terms such that $|\vec{J}|^2$ will contain terms no higher than second order in θ. One obtains

$$J_{ox}(\vec{k},\omega|z_o) = Ze\,(2\pi)^{-3/2}\,\frac{[\sin\theta_i + \rho(z_o/\cos\theta_i)]}{\cos\theta_i}\exp\left[+i\left(\frac{\omega}{v} - k_x\sin\theta_i\right)\frac{z_o}{\cos\theta_i}\right]$$

(3.11a)

$$J_{oy}(\vec{k},\omega|z_o) = Ze(2\pi)^{-3/2}\,\frac{\theta_y(z_o/\cos\theta_i)}{\cos\theta_i}\,\exp\left[+i\left(\frac{\omega}{v}-k_x\sin\theta_i\right)\frac{z_o}{\cos\theta_i}\right] \tag{3.11b}$$

$$J_{oz}(\vec{k},\omega|z_o) = Ze(2\pi)^{-3/2}\,\frac{\left[\cos\theta_i-\tau(z_o/\cos\theta_i)\right]}{\cos\theta_i}\,\exp\left[+i\left(\frac{\omega}{v}-k_x\sin\theta_i\right)\frac{z_o}{\cos\theta_i}\right] \tag{3.11c}$$

where

$$\rho(z_o/\cos\theta_i) = \theta_x(z_o/\cos\theta_i)\cos\theta_i - i\sin\theta_i\,A(\theta) - \frac{1}{2}\theta^2(z_o/\cos\theta_i)\sin\theta_i +$$

$$-i\sin\theta_i\,B(\theta^2) - \frac{1}{2}\sin\theta_i\,A^2(\theta) - i\theta_x(z_o/\cos\theta_i)\cos\theta_i\,A(\theta) \tag{3.12a}$$

$$\tau(z_o/\cos\theta_i) = \theta_x(z_o/\cos\theta_i)\sin\theta_i + i\cos\theta_i\,A(\theta) + \frac{1}{2}\theta^2(z_o/\cos\theta_i)\cos\theta_i +$$

$$+i\cos\theta_i\,B(\theta^2) + \frac{1}{2}\cos\theta_i\,A^2(\theta) - i\theta_x(z_o/\cos\theta_i)\sin\theta_i\,A(\theta) \tag{3.12b}$$

and

$$A(\theta) = k_x(\sin\theta_i\tan\theta_i+\cos\theta_i)\int_{-\infty}^{z_o/\cos\theta_i}\theta_x(z_o'/\cos\theta_i)\frac{dz_o'}{\cos\theta_i} + k_y\int_{-\infty}^{z_o/\cos\theta_i}\theta_y(z_o'/\cos\theta_i)\frac{dz_o'}{\cos\theta_i}$$

$$-\frac{\omega}{v}\tan\theta_i\int_{-\infty}^{z_o/\cos\theta_i}\theta_x(z_o'/\cos\theta_i)\frac{dz_o'}{\cos\theta_i} \tag{3.13a}$$

$$B(\theta^2) = k_x\sin\theta_i\,\theta_x(z_o/\cos\theta_i)\int_{-\infty}^{z_o/\cos\theta_i}\theta_x(z_o'/\cos\theta_i)\frac{dz_o'}{\cos\theta_i} + \frac{\omega}{2v}\int_{-\infty}^{z_o/\cos\theta_i}\theta^2(z_o'/\cos\theta_i)\frac{dz_o'}{\cos\theta_i}$$

P. 38 EQUATION (3.13b). Add the above term to the expression for $B(\theta^2)$.

One has considered the $\theta(z_o/v\cos\theta_i)$'s to be prescribed functions of z_o thus

P. 38 EQUATION ~~(3.36c)~~. Replace the third term inside braces, i.e., $\gamma\cos^2\theta_i$, by γ.

dropping the v dependence in the arguments. One may now use these expressions for the Fourier components of the current density to obtain the field $\vec{\Pi}_o(\vec{k}, \omega|z)$ resulting from the charged particle's motion through the $z = z_o$ plane. For simplicity of notation one writes

$$\vec{J}_o(\vec{k},\omega|z_o) = \left[\hat{u}_\perp J_{os}(\vec{k},\omega|z_o) + \hat{u}_{\parallel} J_{op}(\vec{k},\omega|z_o)\right]\delta(z-z_o) \tag{3.14}$$

where $J_{os}(\vec{k}, \omega|z_o)$ is the component of $\vec{J}_o$ in the xy plane, i.e., the resultant of $J_{ox}(\vec{k}, \omega|z_o)$ and $J_{oy}(\vec{k}, \omega|z_o)$, and $J_{op}(\vec{k}, \omega|z_o)$ is the component along the z axis where $\hat{u}_\perp$ and $\hat{u}_\parallel$ are unit vectors along these directions.

B. Solutions to Wave Equations

The wave equations connecting $\vec{\Pi}_o(\vec{k}, \omega|z)$ and $\vec{J}_o(\vec{k}, \omega|z_o)$ in both media are found from Equation (2.18) to be

$$\frac{d^2\vec{\Pi}_{o1}}{dz^2} - \nu^2\vec{\Pi}_{o1} = -\Lambda\left[\hat{u}_\perp J_{os_1} + \hat{u}_{\parallel} J_{op_1}\right]\delta(z-z_o) \tag{3.15a}$$

$$\frac{d^2\vec{\Pi}_{o2}}{dz^2} - \nu'^2\vec{\Pi}_{o2} = -\frac{\Lambda}{\epsilon}\left[\hat{u}_\perp J_{os_2} + \hat{u}_{\parallel} J_{op_2}\right]\delta(z-z_o) \tag{3.15b}$$

where the subscript 1 (2) refers to the vacuum (dielectric) and where

$$\nu^2 = k_x^2 + k_y^2 - \frac{\omega^2}{c^2} \tag{3.16a}$$

$$\nu'^2 = k_x^2 + k_y^2 - \epsilon\frac{\omega^2}{c^2} \tag{3.16b}$$

and

$$\Lambda = \frac{4\pi i}{\omega} \tag{3.17}$$

One must solve Equations (3.15), apply the required boundary conditions obtained from the continuity requirement on the electric and magnetic field vectors, and integrate over all space to obtain the Fourier component of the total radiation field. One notes that while the charged particle is moving in medium one, i.e., $z_o < 0$, there is no source present in medium two and the right side of Equation (3.15b) is zero. A particular solution to Equation (3.15a) is found by the Green's function method described in Appendix I. Hence one writes the general solutions to Equations (3.15) when $z_o < 0$—as

$$\vec{\Pi}_{o1}(\vec{k},\omega|z) = \hat{u}_\perp\left[\tilde{A}_{\perp_1}e^{\nu z} + \frac{\Lambda}{2\nu} J_{os_1}e^{-\nu|z-z_o|}\right] + \hat{u}_{\parallel}\left[\tilde{A}_{\parallel_1} + \frac{\Lambda}{2\nu} J_{op_1}e^{-\nu|z-z_o|}\right] \quad (3.18a)$$

$$\vec{\Pi}_{o2}(\vec{k},\omega|z) = \hat{u}_\perp \tilde{B}_{\perp_1}e^{-\nu' z} + \hat{u}_{\parallel}\tilde{B}_{\parallel_1}e^{-\nu' z}. \quad (3.18b)$$

In the same manner one notes that while the charged particle is moving in medium two, i.e., $z_o > 0$, there is no source present in medium one and hence the right side of Equation (3.15a) is zero. The particular solution to Equation (3.15b) is found in the same manner as before and one has—for $z_o > 0$—

$$\vec{\Pi}_{o1}(\vec{k},\omega|z) = \hat{u}_\perp \tilde{A}_{\perp_2}e^{\nu z} + \hat{u}_{\parallel}\tilde{A}_{\parallel_2}e^{\nu z} \quad (3.19a)$$

$$\vec{\Pi}_{o2}(\vec{k},\omega|z) = \hat{u}_\perp\left[\tilde{B}_{\perp_2}e^{-\nu' z} + \frac{\Lambda}{2\nu\epsilon} J_{os_2}e^{-\nu'|z-z_o|}\right] + \hat{u}_{\parallel}\left[\tilde{B}_{\parallel_2}e^{-\nu' z} + \frac{\Lambda}{2\nu\epsilon} J_{op_2}e^{-\nu'|z-z_o|}\right] \quad (3.19b)$$

The tilde is used over these constants to differentiate them from the A's appearing in the radiation solution of Chapter II since now one finds that

integration of the particular solution in Equation (3.18a) will yield a radiation term (see Appendix I).

C. Evaluation of the Constants in Equations (3.18) and (3.19)

One must now apply the requirements imposed by the boundary conditions, given by Equations (2.31), to Equations (3.18) and (3.19) in order to evaluate the constants in these equations. The constants obtained from Equations (3.18) will be employed in the integration of $\vec{\Pi}_{o1}$ while the charge is in medium one, i.e., when integrating from $-\infty$ to 0, and the constants obtained from Equations (3.19) will be used in the integration of $\vec{\Pi}_{o1}$ while the charge is in medium two, i.e., when integrating from 0 to ∞. From Equations (3.18) and (2.31) one obtains

$$\tilde{A}_{\perp_1} + \frac{\Lambda}{2\nu} J_{os_1} e^{\nu z_o} = \epsilon \tilde{B}_{\perp_1} \tag{3.20a}$$

$$\nu \tilde{A}_{\perp_1} - \frac{\Lambda}{2} J_{os_1} e^{\nu z_o} = -\nu' \epsilon \tilde{B}_{\perp_1} \tag{3.20b}$$

$$\tilde{A}_{//_1} + \frac{\Lambda}{2\nu} J_{op_1} e^{\nu z_o} = \epsilon \tilde{B}_{//_1} \tag{3.20c}$$

$$\nu \tilde{A}_{//_1} - \frac{\Lambda}{2} J_{op_1} e^{\nu z_o} = -\nu' \tilde{B}_{//_1} + i k_x \left[\tilde{B}_{\perp_1} - \tilde{A}_{\perp_1} - \frac{\Lambda}{2\nu} J_{os_1} e^{\nu z_o}\right]. \tag{3.20d}$$

Using Equations (3.19) and (2.31) one has the results

$$\tilde{A}_{\perp_2} = \epsilon \left[\tilde{B}_{\perp_2} + \frac{\Lambda}{2\nu'\epsilon} J_{os_2} e^{-\nu' z_o}\right] \tag{3.21a}$$

$$\nu \tilde{A}_{\perp_2} = \epsilon \left[-\nu' \tilde{B}_{\perp_2} + \frac{\Lambda}{2\epsilon} J_{os_2} e^{-\nu' z_o}\right] \tag{3.21b}$$

$$\tilde{A}_{\parallel 2} = \epsilon \left[\tilde{B}_{\parallel 2} + \frac{\Lambda}{2\nu'\epsilon} J_{op_2} e^{-\nu' z_o} \right] \tag{3.21c}$$

$$\nu \tilde{A}_{\parallel 2} + i k_x \tilde{A}_{\perp 2} = i k_x \left[\tilde{B}_{\perp 2} + \frac{\Lambda}{2\nu'\epsilon} J_{os_2} e^{-\nu' z_o} \right] + \left[-\nu' \tilde{B}_{\perp 2} + \frac{\Lambda}{2\epsilon} J_{op_2} e^{-\nu' z_o} \right]. \tag{3.21d}$$

These two sets of equations are solved in a straightforward manner to yield the constants

$$\tilde{A}_{\perp 1} = \frac{\Lambda}{2\nu} \frac{(\nu - \nu')}{(\nu + \nu')} J_{os_1} e^{\nu z_o} \tag{3.22a}$$

$$\tilde{A}_{\parallel 1} = \frac{\Lambda}{(\nu\epsilon + \nu')} \left[\frac{(\nu\epsilon - \nu')}{2\nu} J_{op_1} + \frac{i k_x (1-\epsilon)}{(\nu + \nu')} J_{os_2} \right] e^{\nu z_o} \tag{3.22b}$$

when $z_o < 0$, and

$$\tilde{A}_{\perp 2} = \frac{\Lambda}{(\nu + \nu')} J_{os_2} e^{-\nu' z_o} \tag{3.23a}$$

$$\tilde{A}_{\parallel 2} = \frac{\Lambda}{(\nu\epsilon + \nu')} \left[J_{op_2} + \frac{i k_x (1-\epsilon)}{(\nu + \nu')} J_{os_2} \right] e^{-\nu' z_o} \tag{3.23b}$$

when $z_o > o$. Only those constants applicable to the vacuum solution, i.e., $\vec{\Pi}_1(\vec{k}, \omega | z)$, are given since one is concerned with the photon yield observed in the vacuum. It is now an easy matter for one to use these constants in Equations (3.18) and (3.19) and to integrate over dz_o to obtain the Fourier components of the total radiation field. One obtains the results

$$\Pi_{s1} = \left\{ \frac{\Lambda}{2\nu} \left[\int_{-\infty}^{o} \frac{(\nu - \nu')}{(\nu + \nu')} J_{os_1} e^{(\nu \cos\theta_i + \alpha)\frac{z_o}{\cos\theta_i}} dz_o - \frac{J_{os_1} \cos\theta_i}{(\nu \cos\theta_i - \alpha)} \right] + \right.$$

$$\left. + \frac{\Lambda}{(\nu + \nu')} \int_{o}^{\infty} J_{os_2} e^{-(\nu' \cos\theta_i - \alpha)\frac{z_o}{\cos\theta_i}} dz_o \right\} e^{\nu z} \tag{3.24a}$$

$$\Pi_{P1} = \left\{ \frac{\Lambda}{(\nu\epsilon+\nu')} \left[\int_{-\infty}^{0} \frac{(\nu\epsilon-\nu')}{2\nu} J_{op_1} e^{(\nu\cos\theta_i+\alpha)\frac{z_0}{\cos\theta_i}} dz_0 - \frac{(\nu\epsilon+\nu')}{2\nu} \frac{J_{op_1}\cos\theta_i}{(\nu\cos\theta_i-\alpha)} \right.\right.$$

$$+ \int_{-\infty}^{0} \frac{i k_x (1-\epsilon)}{(\nu+\nu')} J_{os_1} e^{(\nu\cos\theta_i+\alpha)\frac{z_0}{\cos\theta_i}} dz_0 + \int_{0}^{\infty} J_{op_2} e^{-(\nu'\cos\theta_i-\alpha)\frac{z_0}{\cos\theta_i}} dz_0$$

$$\left.\left. + \int_{0}^{\infty} \frac{i k_x (1-\epsilon)}{(\nu+\nu')} J_{os_2} e^{-(\nu'\cos\theta_i-\alpha)\frac{z_0}{\cos\theta_i}} dz_0 \right] \right\} e^{\nu z} \qquad (3.24b)$$

where one has incorporated the exponential dependence of the $\vec{J}_o$ components given in Equations (3.11) in the quantity $\alpha = i(\omega/v - k_x \sin\theta_i)$ and the quantities J_{os1}, J_{os2}, J_{op1}, and J_{op2} are now the coefficients of this exponential in Equations (3.11). The second term in the brackets in Equation (3.24a) comes from that part of the integral over the particular solution $\Lambda/2\nu J_o e^{-\nu|z-z_o|}$ which represents the transform of an outgoing spherical wave and hence contributes to the total radiation field (see Appendix I). The second term inside the brackets of Equation (3.24b) arises from the same considerations in the z component.

D. Photon Number Distribution

Equations (3.24) represent those parts of the Hertz vector solution which, when Fourier transformed to obtain $\vec{\Pi}_1(\vec{r}, t)$, have the characteristics of the radiation field. Hence the considerations employed in Chapter II can be used to obtain the photon number distribution for a particular scattering history by identifying the quantities inside the braces in Equations (3.24a) and (3.24b) with the constants A_x, and A_z, respectively, appearing in

Equation (2.33), i.e., one now has

$$A_{x'} = \{\text{Term inside braces, Equation (3.24a)}\} \tag{3.25a}$$

and

$$A_z = \{\text{Term inside braces, Equation (3.24b)}\} \tag{3.25b}$$

One substitutes these values into Equations (2.62) to obtain the photon number distributions

$$\frac{d^2N_\perp}{d\omega\Omega} = \frac{\mu^2\omega^5}{2\pi\hbar c^5}\left|\left\{\frac{\Lambda}{2\nu}\left[\frac{(\nu-\nu')}{(\nu+\nu')}\int_{-\infty}^{0} J_{os_1}\sin\Phi' e^{(\nu\cos\theta_i+\alpha)\frac{z_0}{\cos\theta_i}}dz_0 - \frac{J_{os_1}\cos\theta_i\sin\Phi'}{(\nu\cos\theta_i-\alpha)}\right] + \frac{\Lambda}{(\nu+\nu')}\int_0^{\infty} J_{os_2}\sin\Phi' e^{-(\nu'\cos\theta_i-\alpha)\frac{z_0}{\cos\theta_i}}dz_0\right\}\right|^2 \tag{3.26a}$$

and

$$\begin{aligned}\frac{d^2N_\parallel}{d\omega d\Omega} = \frac{\mu^2\omega^5}{2\pi\hbar c^5}\Bigg|&\cos\Theta\left\{\frac{\Lambda}{2\nu}\left[\frac{(\nu-\nu')}{(\nu+\nu')}\int_{-\infty}^{0} J_{os_1}\cos\Phi' e^{(\nu\cos\theta_i+\alpha)\frac{z_0}{\cos\theta_i}}dz_0 + \right.\right.\\ &\left.\left. - \frac{J_{os_1}\cos\theta_i\cos\Phi'}{(\nu\cos\theta_i-\alpha)}\right] + \frac{\Lambda}{(\nu+\nu')}\int_0^{\infty} J_{os_2}\cos\Phi' e^{-(\nu'\cos\theta_i-\alpha)\frac{z_0}{\cos\theta_i}}dz_0\right\}\\ &+\sin\Theta\left\{\frac{\Lambda}{(\nu\epsilon+\nu')}\left[\int_{-\infty}^{0}\frac{(\nu\epsilon+\nu')}{2\nu}J_{op_1}e^{(\nu\cos\theta_i+\alpha)\frac{z_0}{\cos\theta_i}}dz_0 - \frac{(\nu\epsilon+\nu')J_{op_1}\cos\theta_i}{2\nu(\nu\cos\theta_i-\alpha)}\right.\right.\\ &+\frac{ik_x(1-\epsilon)}{(\nu+\nu')}\int_{-\infty}^{0} J_{os_1}e^{(\nu\cos\theta_i+\alpha)\frac{z_0}{\cos\theta_i}}dz_0 + \int_0^{\infty} J_{op_2}e^{-(\nu'\cos\theta_i-\alpha)\frac{z_0}{\cos\theta_i}}dz_0\\ &\left.\left.+\frac{ik_x(1-\epsilon)}{(\nu+\nu')}\int_0^{\infty} J_{os_2}e^{-(\nu'\cos\theta_i-\alpha)\frac{z_0}{\cos\theta_i}}dz_0\right]\right\}\Bigg|^2\end{aligned} \tag{3.26b}$$

where the variousparameters entering these equations must have their respective values in spherical polar coordinates. Using Figure 3 on page one obtains

$$J_{os_i} \cos\Phi' = J_{ox_i} \cos\Phi + J_{oy_i} \sin\Phi \quad , \quad i = 1,2. \tag{3.27a}$$

$$J_{os_i} \sin\Phi' = J_{ox_i} \sin\Phi - J_{oy_i} \cos\Phi \quad , \quad i = 1,2. \tag{3.27b}$$

Since there is no scattering in medium one, $\theta(z_o/\cos\theta_i) = 0$ and J_{ox1}, J_{oy1}, and J_{oz1} are obtained from the coefficients of the exponential term in Equations (3.11). The integrals over medium one, i.e., from $-\infty$ to 0 can be performed easily since they are of zeroth order in $\theta(z_o/\cos\theta_i)$. Then using the coefficients for J_{ox2}, J_{oy2}, and J_{oz2} obtained from Equations (3.11) with $\theta(z_o/\cos\theta_i) \neq 0$, performing the integrations involving zeroth ordered terms in $\theta(z_o/\cos\theta_i)$, and collecting terms one obtains

$$\frac{d^2 N_\perp}{d\omega\, d\Omega} = \frac{\mu^2 \omega^5}{2\pi \hbar c^5} \left| \frac{\Lambda Z e (2\pi)^{-3/2}}{(\nu+\nu')} \left\{ \left[\frac{\nu' \cos\theta_i + \alpha}{\alpha^2 - \nu^2 \cos^2\theta_i} + \frac{1}{\nu' \cos\theta_i - \alpha} \right] \sin\theta_i \sin\Phi + \right.\right.$$

$$+ \int_0^\infty \frac{(\theta_x \cos\theta_i \sin\Phi - \theta_y \cos\Phi)}{(\nu' \cos\theta_i - \alpha)} e^{-\gamma' \frac{z_o}{\cos\theta_i}} \frac{\gamma' dz_o}{\cos\theta_i} +$$

$$\left.\left. + T_{11}(z_o/\cos\theta_i) + T_{21}(z_o/\cos\theta_i) \right\} \right|^2 \tag{3.28a}$$

In the same manner the integrations in the parallel component are performed and one has

$$\frac{d^2 N_{\parallel}}{d\omega\, d\Omega} = \frac{\mu^2 \omega^5}{2\pi \hbar c^5} \left| \frac{\Lambda Z e}{(2\pi)^{3/2}} \left\{ \left[\frac{(\nu' \cos\theta_i + \alpha)\mu}{\alpha^2 - \nu^2 \cos^2\theta_i} + \frac{\mu}{\nu' \cos\theta_i - \alpha} + \frac{(-i\frac{\omega}{c})(\epsilon - 1)(1-\mu^2)}{(\nu\epsilon + \nu')} \cdot \right.\right.\right.$$

$$\cdot \left(\frac{1}{\nu \cos\theta_i + \alpha} + \frac{1}{\nu' \cos\theta_i - \alpha} \right) \Bigg] \frac{\sin\theta_i \cos\Phi}{(\nu + \nu')} + \left[\frac{\nu' \cos\theta_i + \alpha\epsilon}{\alpha^2 - \nu^2 \cos^2\theta_i} + \frac{1}{\nu' \cos\theta_i - \alpha} \right] \cdot$$

$$\cdot \frac{\cos\theta_i \sin\Theta}{(\nu\epsilon + \nu')} + \left[\frac{\mu}{\nu + \nu'} + \frac{(-i\frac{\omega}{c})(\epsilon - 1)(1-\mu^2)}{(\nu + \nu')(\nu\epsilon + \nu')} \right] \int_0^\infty \frac{(\theta_x \cos\theta_i \cos\Phi + \theta_y \sin\Phi)}{(\nu' \cos\theta_i - \alpha)} \cdot$$

$$\left. \cdot\, e^{-\zeta' \frac{z_0}{\cos\theta_i}} \frac{\zeta' dz_0}{\cos\theta_i} + T_{12}(z_0/\cos\theta_i) + T_{22}(z_0/\cos\theta_i) \right\} \Bigg|^2 \qquad (3.28b)$$

where

$$T_{\parallel} = -\frac{\sin\theta_i \sin\Phi}{\nu' \cos\theta_i - \alpha} \int_0^\infty i\, A(\Theta)\, e^{-\zeta' \frac{z_0}{\cos\theta_i}} \frac{\zeta' dz_0}{\cos\theta_i} \qquad (3.29a)$$

$$T_{21} = -\frac{\sin\theta_i \sin\Phi}{\nu' \cos\theta_i - \alpha} \int_0^\infty \left(\frac{1}{2}\theta^2(z_0/\cos\theta_i) + i\, B(\theta^2) + \frac{1}{2} A^2(\Theta) + \frac{i\, \theta_x(z_0/\cos\theta_i) A(\Theta)}{\tan\theta_i} \right) \cdot$$

$$\cdot\, e^{-\zeta' \frac{z_0}{\cos\theta_i}} \frac{\zeta' dz_0}{\cos\theta_i} \qquad (3.29b)$$

$$T_{12} = -\left[\left(\frac{\mu}{\nu + \nu'} + \frac{(-i\frac{\omega}{c})(\epsilon - 1)(1-\mu^2)}{(\nu + \nu')(\nu\epsilon + \nu')} \right) \sin\theta_i \cos\Phi + \frac{\cos\theta_i \sin\Theta}{(\nu\epsilon + \nu')} \right] \int_0^\infty i\, A(\Theta) \cdot$$

$$\cdot \frac{e^{-\zeta' \frac{z_0}{\cos\theta_i}}}{(\nu' \cos\theta_i - \alpha)} \frac{\zeta' dz_0}{\cos\theta_i} - \frac{\sin\theta_i \sin\Theta}{(\nu\epsilon + \nu')(\nu' \cos\theta_i - \alpha)} \int_0^\infty \theta_x(z_0/\cos\theta_i)\, e^{-\zeta' \frac{z_0}{\cos\theta_i}} \frac{\zeta' dz_0}{\cos\theta_i}$$

(3.29c)

$$T_{22} = -\left[\left(\frac{\mu}{\nu+\nu'} + \frac{(-i\frac{\omega}{c})(\epsilon-1)(1-\mu^2)}{(\nu+\nu')(\nu\epsilon+\nu')}\right)\sin\theta_i \cos\Phi + \frac{\cos\theta_i \sin\Theta}{(\nu\epsilon+\nu')}\right]\int_0^\infty \left(\frac{1}{2}\theta^2(z_0/\cos\theta_i) + i\,B(\theta^2) + \right.$$

$$\left. + \frac{1}{2}A^2(\theta)\right)\frac{e^{-\zeta'\frac{z_0}{\cos\theta_i}}\,\zeta' dz_0}{(\nu'\cos\theta_i - \alpha)\cos\theta_i} + \left[\left(\frac{\mu}{\nu+\nu'} + \frac{(-i\frac{\omega}{c})(\epsilon-1)(1-\mu^2)}{(\nu+\nu')(\nu\epsilon+\nu')}\right)\sin\theta_i \cos\Phi + \right.$$

$$\left. - \frac{\sin^2\theta_i \sin\Theta}{\cos\theta_i\,(\nu\epsilon+\nu')}\right]\int_0^\infty \frac{i\,\theta_x(z_0/\cos\theta_i)\,A(\theta)\,e^{-\zeta'\frac{z_0}{\cos\theta_i}}}{\tan\theta_i\,(\nu'\cos\theta_i - \alpha)}\,\frac{\zeta' dz_0}{\cos\theta_i} \tag{3.29d}$$

and where $A(\theta)$ and $B(\theta^2)$ are given by Equations (3.13). Equations (3.28) are written in the above form to illustrate the fact that the photon yield consists of terms which are independent of $\theta(z_o/\cos\theta_i)$ and which represent transition radiation contributions, terms involving simple integrations of $\theta(z_o/\cos\theta_i)$ which represent the contributions due to bremsstrahlung, and finally terms T_{11}, T_{21}, T_{12}, and T_{22} which arise from the expansion of the exponential in the current density given by Equations (3.9), and which represent interference between the two types of radiations.

E. Averaged Photon Number Distribution

The analysis of Equations (3.28) is performed by converting to integrations over the particle's initial direction, i.e., along the z' axis where one considers the scattering law to be sufficiently peaked in the forward direction to enable one to treat the deflection $\theta(z')$ as a two dimensional vector at right angles to the z' axis. Employing these considerations one

evaluates the absolute squares of the magnitudes given in Equations (3.28) and keeps only those terms of order $\theta^2(z')$ or less to obtain the photon yield for a particular scattering history. This quantity must be averaged over all possible statistically independent scattering histories to obtain the averaged photon yield $\langle (d^2N)/(d\omega\, d\Omega)\rangle$. One performs this average in the following manner.

The charged particle is assumed to travel undeviated in vacuum along the z' axis, to penetrate the dielectric to a distance z_1' where it experiences its first scattering encounter after which it is deviated into the direction specified by the angles θ_1 and ϕ_1, to proceed along this new direction to a depth z_2' where it experiences its second scattering event after which its direction is spcified by the angles θ_2 and ϕ_2, and so on through the semi-infinite dielectric medium. It is further assumed that the path of the charged particle between successive scattering events is a straight line. The trajectory of the charged particle during such a scattering history may be described by the set

$$\begin{matrix} z_1', & \theta_1, & \phi_1 \\ z_2', & \theta_2, & \phi_2 \\ \vdots & \vdots & \vdots \\ z_k, & \theta_k, & \phi_k \end{matrix} \tag{3.30}$$

where z_k' is the z' coordinate of the particle at the instant it experiences its kth scattering, θ_k is its polar angle <u>after</u> the kth scatter, and ϕ_k is its azimuthal angle <u>after</u> the kth scatter.

Now, one lets γ represent the probability of a scattering event per unit length in the dielectric, i.e., γ is the inverse mean free path length of the charged particle in the dielectric medium and is written

$$\gamma = N \int \sigma(\theta)\, d\Omega \tag{3.31}$$

In Equation (3.31) N is the number of scattering centers per unit volume and $\sigma(\theta)$ is the differential cross section for single scattering—assumed to be strongly peaked in the forward direction allowing one to consider $\theta(z')$ to be a two dimensional vector $\vec{\theta}(z')$ perpendicular to the z' axis. The probability of a scatter into the solid angle $d\Omega$ about θ is then given by

$$p(\theta)\, d\Omega = N\, \sigma(\theta)\, \gamma^{-1} \tag{3.32}$$

One writes the probability for occurrence of the scattering history specified by the set (3.30) in the form

$$P(z', \theta, \phi)\, dz'\, d\Omega = \prod_{k=1}^{\infty} e^{-\gamma(z'_k - z'_{k-1})} \gamma\, dz_k\; p(|\vec{\theta}_k - \vec{\theta}_{k-1}|)\, d\vec{\theta}_k \tag{3.33}$$

where $|\vec{\theta}_k - \vec{\theta}_{k-1}|^2 = \theta_k^2 + \theta_{k-1}^2 - 2\,\theta_k\,\theta_{k-1}\cos(\phi_k - \phi_{k-1})$. The terms in this infinite product have their usual interpretations, i.e., $e^{-\gamma(z'_k - z'_{k-1})}$ is the probability that the charged particle will traverse the distance $(z'_k - z'_{k-1})$ without scattering, $\gamma\, dz'_k$ is the probability that a scatter will occur within dz'_k about z'_k, and $p(|\vec{\theta}_k - \vec{\theta}_{k-1}|)\, d\vec{\theta}_k$ is the probability of scattering into the angle $d\vec{\theta}_k$ about $\vec{\theta}_k - \vec{\theta}_{k-1}$. In order to consider all possible statistically

independent scattering histories one integrates this probability, i.e., one performs the operation

$$\left\langle \frac{d^2N}{d\omega d\Omega} \right\rangle = \prod_{k=1}^{\infty} \int_{z'_{k-1}}^{\infty} e^{-\gamma(z'_k - z'_{k-1})} \gamma\, dz_k \int p(|\vec{\theta}_k - \vec{\theta}_{k-1}|) d\vec{\theta}_k \frac{d^2N}{d\omega d\Omega} \tag{3.34}$$

The analysis of Equation (3.34)—using Equations (3.28) converted to integration over dz'_k—is a lengthy process with the major steps being given in Appendix II. One writes the following results:

1. Perpendicular Polarization $\langle (d^2N_\perp)/(d\omega\, d\Omega) \rangle$

$$\left\langle \frac{d^2N_\perp}{d\omega d\Omega} \right\rangle = \frac{Z^2 \alpha \beta^2 \mu^2}{\pi^2 \omega |\mu+\sigma|^2} \left\{ |T_{01}|^2 + \frac{T_{11} \langle \Theta^2 \rangle_\ell}{|\gamma + \beta\sigma\cos\theta_i|^2\, 4\, \mathrm{Re}\left[-i \frac{\omega}{c} \sigma \cos\theta_i\right]} + \right.$$

$$\left. - \mathrm{Re}\left[T_{01}^* T_{21}\right] \right\} \tag{3.35}$$

where

$$T_{01} = \left[\frac{\beta\sigma\cos\theta_i - \gamma}{\gamma^2 - \beta^2\mu^2\cos^2\theta_i} + \frac{1}{\gamma + \beta\sigma\cos\theta_i} \right] \sin\theta_i \sin\Phi \tag{3.36a}$$

$$T_{11} = \left\{ 1 + \frac{\sin^2\theta_i \sin^2\Phi}{|\gamma + \beta\sigma\cos\theta_i|^2} \left[(\gamma \sin\theta_i \cos\Phi - \beta \sin\Theta)^2 + \gamma^2 \sin^2\theta_i \sin^2\Phi \right] \right\} \tag{3.36b}$$

$$T_{21} = \frac{\langle \Theta^2 \rangle_\ell \sin\theta_i \sin\Phi}{\zeta' (\gamma + \beta\sigma\cos\theta_i)^2} \left[2 + \beta\sigma\cos\theta_i + \gamma\cos^2\theta_i - \frac{\beta \sin\Theta \cos\Phi\, (1 + \sin^2\theta_i)}{\sin\theta_i} + \right.$$

$$\left. - \frac{(\gamma \sin\theta_i \cos\Phi - \beta\sin\Theta)^2 + \gamma^2 \sin^2\theta_i \sin^2\Phi}{(\gamma + \beta\sigma\cos\theta_i)} \right] \tag{3.36c}$$

and where $\zeta' = -i\,\omega/c\beta(\beta\sigma\cos\theta_i + \gamma)$, $\gamma = (1 - \beta\sin\Theta\cos\Phi\sin\theta_i)$, $\alpha = e^2/\hbar c$,

$\beta = v/c$, $\mu = \cos\Theta$, $\sigma = (\epsilon - 1 + \mu^2)^{1/2}$, with $\epsilon(\omega)$ being the complex frequency-dependent dielectric constant of the semi-infinite medium through which the charged particle moves, and $\langle\Theta^2\rangle_\ell$ is the mean square scattering angle per unit length in the medium. The terms in Equation (3.35) have straightforward interpretations with the first term inside the braces representing those transition radiation photons having their electric vectors polarized in a plane perpendicular to the plane of emission (defined by the z axis and the direction of photon emission), the second term inside the braces containing those bremsstrahlung photons having this polarization as well as interference terms between the two radiations arising from first order terms in $\theta(z')$, and the last term inside the braces representing interference terms from second order terms in $\theta(z')$. One can show that the transition radiation term in Equation (3.35) is identical with that of the same polarization obtained by Korkhmazyan[68] by a somewhat different approach, and also that for normal-incidence ($\theta_i = 0$) Equation (3.35) reduces to the previously derived result of Ritchie, Ashley, and Emerson.[27] One further notes that in the case where the plane of incidence (defined by the velocity vector of the charged particle and the z axis) and the plane of emission coincide ($\Phi = 0$, $\Phi = 180°$) there are no perpendicularly polarized transition radiation photons and thus no interference terms. In this case $T_{o1} = 0$, $T_{11} = 1$ and one notes that the bremsstrahlung radiation shows roughly a $(\cos\theta_i)^{-1}$ dependence on the angle of incidence and hence increases rapidly as one approaches grazing incidence ($\theta_i \sim 80°$). This is easily understood since more

scatters will occur within the observable distance λ_{opt} than in the case of normal incidence, resulting in a larger photon yield.

In the special case of non-relativistic electron velocities one has $\beta \ll 1$, $\gamma = 1$, and Equation (3.35) reduces to

$$\left\langle \frac{d^2 N_\perp}{d\omega d\Omega} \right\rangle^{N.R.} = \frac{Z^2 \alpha \beta^2 \mu^2 \left(1 + \sin^4\theta_i \sin^2\Phi\right) \langle \Theta^2 \rangle_\ell}{\pi^2 \omega \, |\mu + \sigma|^2 \, 4 \, \mathrm{Re}\left[-i \frac{\omega}{c} \sigma \cos\theta_i\right]} \tag{3.37}$$

where the various quantities in the above equation have the values given after Equations (3.36). One notes that the transition radiation component is unimportant for low electron velocities and that the perpendicular polarization component consists entirely of bremsstrahlung with a $(\cos\theta_i)^{-1}$ dependence on the angle of incidence.

2. Parallel Polarization $\langle (d^2 N_{\parallel})/(d\omega \, d\Omega) \rangle$

$$\left\langle \frac{d^2 N_{\parallel}}{d\omega d\Omega} \right\rangle = \frac{Z^2 \alpha \beta^2 \mu^2}{\pi^2 \omega} \left\{ |T_{02}|^2 + \frac{T_{12} \langle \Theta^2 \rangle_\ell}{|\gamma + \beta\sigma\cos\theta_i|^2 \, 4 \, \mathrm{Re}\left[-i \frac{\omega}{c} \sigma \cos\theta_i\right]} + \right.$$

$$\left. - \mathrm{Re}\left[T_{02}^* T_{22}\right] \right\} \tag{3.38}$$

where

$$T_{02} = \left\{ \left[\frac{(\beta\sigma\cos\theta_i - \gamma)\mu}{\gamma^2 - \beta^2\mu^2\cos^2\theta_i} + \frac{\mu}{\gamma + \beta\sigma\cos\theta_i} + \frac{(\epsilon - 1)(1 - \mu^2)}{(\mu\epsilon + \sigma)} \left(\frac{1}{\beta\mu\cos\theta_i - \gamma} + \frac{1}{\gamma + \beta\sigma\cos\theta_i} \right) \right] \cdot \right.$$

$$\left. \cdot \frac{\sin\theta_i \cos\Phi}{(\mu + \sigma)} + \left[\frac{\beta\sigma\cos\theta_i - \epsilon\gamma}{\gamma^2 - \beta^2\mu^2\cos^2\theta_i} + \frac{1}{\gamma + \beta\sigma\cos\theta_i} \right] \frac{\cos\theta_i \sin\Phi}{(\mu\epsilon + \sigma)} \right\} \tag{3.39a}$$

$$T_{12} = \Bigg\{ \Bigg| \Bigg[\left(\frac{\mu}{\mu+\sigma} + \frac{(\epsilon-1)(1-\mu^2)}{(\mu+\sigma)(\mu\epsilon+\sigma)} \right) \left(1 + \frac{\beta \sin\Theta \cos\Phi \sin\theta_i}{\gamma+\beta\sigma\cos\theta_i} \right) + \frac{\beta\cos\theta_i\,(1-\mu^2)}{(\mu\epsilon+\sigma)(\gamma+\beta\sigma\cos\theta_i)} \Bigg] \Bigg|^2 +$$

$$+ \Bigg| \Bigg[\left(\frac{\mu}{\mu+\sigma} + \frac{(\epsilon-1)(1-\mu^2)}{(\mu+\sigma)(\mu\epsilon-\sigma)} \right) \gamma \sin^2\theta_i \cos\Phi + \frac{(2\gamma+\beta\sigma\cos\theta_i)\sin\theta_i\cos\theta_i\sin\Theta}{(\mu\epsilon+\sigma)} \Bigg] \cdot$$

$$\cdot \frac{1}{\gamma+\beta\sigma\cos\theta_i} \Bigg|^2 + 2\,\mathrm{Re}\Bigg[\left(\left\{ \frac{\mu}{\mu+\sigma} + \frac{(\epsilon-1)(1-\mu^2)}{(\mu+\sigma)(\mu\epsilon+\sigma)} \right\} \left\{ 1 + \frac{\beta\sin\Theta\cos\Phi\sin\theta_i}{\gamma+\beta\sigma\cos\theta_i} \right\} \right.$$

$$\left. + \frac{\beta\cos^2\theta_i\,(1-\mu^2)}{(\mu\epsilon+\sigma)(\gamma+\beta\sigma\cos\theta_i)} \right)^* \left(\left\{ \frac{\mu}{\mu+\sigma} + \frac{(\epsilon-1)(1-\mu^2)}{(\mu+\sigma)(\mu\epsilon+\sigma)} \right\} \gamma \sin^2\theta_i \cos\Phi + \right.$$

$$\left. + \frac{(2\gamma+\beta\sigma\cos\theta_i)\sin\theta_i\cos\theta_i\sin\Theta}{(\mu\epsilon+\sigma)} \right) \frac{\cos\Phi}{\gamma+\beta\sigma\cos\theta_i} \Bigg] \Bigg\} \tag{3.39b}$$

$$T_{22} = \Bigg\{ \frac{\langle\Theta^2\rangle_1}{\zeta'(\gamma+\beta\sigma\cos\theta_i)^2} \Bigg[\left(\left\{ \frac{\mu}{\mu+\sigma} + \frac{(\epsilon-1)(1-\mu^2)}{(\mu+\sigma)(\mu\epsilon+\sigma)} \right\} \sin\theta_i \cos\Phi + \frac{\cos\theta_i \sin\Theta}{(\mu\epsilon+\sigma)} \right) \Big(2 +$$

$$+ \beta\sigma\cos\theta_i - 2\beta\sin\Theta\cos\Phi\sin\theta_i - \frac{\{[\gamma\sin\theta_i\cos\Phi - \beta\sin\Theta]^2 + \gamma^2\sin^2\theta_i\sin^2\Phi\}}{(\gamma+\beta\sigma\cos\theta_i)} \Big) +$$

[illegible]

P. 53 EQUATION (3.39c). Replace last term of equation, i.e.,

$\gamma \cos^2 \theta_i$, by γ .

The various quantities entering these equations have the same values as given after Equations (3.36). Now, the terms in Equation (3.38) have the interpretations under which the first term inside the braces represents those transition radiation photons having their electric vectors polarized in the plane of emission, the second term represents bremsstrahlung photons and

first order interference terms, and the last term represents interference between the transition radiation and bremsstrahlung arising from second order terms in $\theta(z')$. Again one can show that the transition radiation term in Equation (3.38) is identical with that of the same polarization obtained by Korkhmazyan[68] and that at normal incidence ($\theta_i = 0$) Equation (3.38) reduces to the previously derived result of Ritchie, Ashley, and Emerson[27] which contains the earlier results of Frank and Ginsburg.[58] One notes that the bremsstrahlung radiation term again shows the approximately $(\cos\theta_i)^{-1}$ dependence on the angle of incidence.

Again, for the special case of non-relativistic electrons one has $\beta \ll 1$, $\gamma = 1$, and Equation (3.38) reduces to

$$\left\langle \frac{d^2 N_{\parallel}}{d\omega\, d\Omega} \right\rangle^{N.R.} = \frac{Z^2 \alpha \beta^2 \mu^2}{\pi^2 \omega} \left\{ \left| T_{02} \right|^2 + \frac{T_{12} \langle \Theta^2 \rangle_\ell}{4\, \mathrm{Re}\{-i \frac{\omega}{c} \sigma \cos\theta_i\}} - \mathrm{Re}\left[T_{02}^* T_{22} \right] \right\} \tag{3.40}$$

where

$$T_{02} = \frac{(1-\epsilon)}{(\mu\epsilon+\sigma)} \cos\theta_i \sin\Theta \tag{3.41a}$$

$$T_{12} = \left\{ \left| \frac{\mu}{\mu+\sigma} + \frac{(\epsilon-1)(1-\mu^2)}{(\mu+\sigma)(\mu\epsilon+\sigma)} \right|^2 + \left| \left[\frac{\mu}{\mu+\sigma} + \frac{(\epsilon-1)(1-\mu^2)}{(\mu+\sigma)(\mu\epsilon+\sigma)} \right] \sin^2\theta_i \cos\Phi + \right.\right.$$

$$\left. + 2 \sin\theta_i \cos\theta_i \sin\Theta \right|^2 + 2\, \mathrm{Re} \left[\left(\frac{\mu}{\mu+\sigma} + \frac{(\epsilon-1)(1-\mu^2)}{(\mu+\sigma)(\mu\epsilon+\sigma)} \right)^* \left(\left\{ \frac{\mu}{\mu+\sigma} + \right.\right.\right.$$

$$\left.\left.\left. + \frac{(\epsilon-1)(1-\mu^2)}{(\mu+\sigma)(\mu\epsilon+\sigma)} \right\} \left\{ \sin^2\theta_i \cos^2\Phi + \frac{2 \sin\theta_i \cos\theta_i \sin\Theta \cos\Phi}{(\mu\epsilon+\sigma)} \right\} \right] \right\} \tag{3.41b}$$

$$T_{22} = \frac{\langle \Theta^2 \rangle_\ell}{(-i\frac{\omega}{c}\sigma\cos\theta_i)} \left\{ \left[\left(\frac{\mu}{\mu+\sigma} + \frac{(\epsilon-1)(1-\mu^2)}{(\mu+\sigma)(\mu\epsilon+\sigma)} \right) \sin\theta_i \cos\Phi + \frac{\cos\theta_i \sin\Theta}{(\mu\epsilon+\sigma)} \right] \left[2 + \right.\right.$$

$$\left. - \sin^2\theta_i \right] + \left[\left(\frac{\mu}{\mu+\sigma} + \frac{(\epsilon-1)(1-\mu^2)}{(\mu+\sigma)(\mu\epsilon+\sigma)} \right) \cos\Phi - \frac{\sin\Theta}{\cos\theta_i(\mu\epsilon+\sigma)} \right] \cdot$$

P. 55 EQUATION (3.41c). Delete $\cos^2 \theta_i$ in the last line of the equation.

which again shows that the parallel polarization component consists of transition radiation (with a $\cos^2 \theta_i$ dependence on the angle of incidence), bremsstrahlung (with a $[\cos\theta_i]^{-1}$ dependence), and interference effects between these two types of radiation.

F. Mean Square Scattering Angle Per Unit Length and Optical Constants

In order to generate theoretical spectra from Equations (3.35) and (3.38), one must determine the quantities $\langle \Theta^2 \rangle_\ell$ and $\epsilon(\omega)$ for use as input data. One now briefly discusses the values employed for these quantities in the numerical analysis which is to follow.

1. Mean Square Scattering Angle Per Unit Length

As was pointed out in Chapter I, there are many theories concerning the multiple scattering of electrons from which one may deduce the quantity of interest to the present work. One has chosen to briefly discuss three theories appropriate to the present work in order to illustrate the choice of the final expression employed in Chapter IV.

a. Lewis; Born Approximation. - Lewis[16] has considered the multiple scattering problem in an infinite, homogeneous medium by expressing the solution to the diffusion equation—electrons diffusing through some medium with boundary conditions corresponding to a single electron moving in the + z direction and incident at the origin—in terms of an expansion in spherical harmonics. In the small angle approximation his results yield

$$\langle \Theta^2 \rangle = \frac{4 \int k_\ell \, ds}{\ell(\ell+1)} \tag{3.42}$$

where k_ℓ is determined from the spherical harmonic solution of the diffusion equation. In the special case of the Born approximation, i.e., a potential $V(r) = (Ze^2/r)\, e^{-r/a}$, one uses Lewis' expression (15′) for k_ℓ with $\ell = 2$ to obtain

$$\langle \Theta^2 \rangle_\ell = \frac{8\pi N Z^2 r_0^2 (1-\beta^2)}{\beta^4} \left\{ \ln \left[\frac{2\beta}{Z^{1/3} \alpha (1-\beta^2)^{1/2}} \right] - 1 \right\} \tag{3.43}$$

where N is the density of scattering centers, Z is the atomic number of the scatterer, r_o is the classical electron radius, $\beta = v/c$, and $\alpha = e^2/\hbar c \simeq 1/137$ is the fine structure constant. As expected the scattering is more important for high Z materials and for low electron energies.

b. Nigam, Sundaresan, and Wu; 1st and 2nd Born Approximations. - Nigam, Sundaresan, and Wu[20] have given a derivation of multiple scattering in which they have combined the exact theory of Goudsmit and Saunderson[14] with the single scattering cross section of Dalitz[21] for electrons scattered by a screened atomic field. Their results, accurate to the 2nd Born

approximation, can be used to obtain the quantity $\langle \Theta^2 \rangle_\ell$. Ritchie, Ashley, and Emerson[27] give, in the small-angle approximation,

$$\langle \Theta^2 \rangle_\ell = \frac{2 Q_2}{3t} \tag{3.44}$$

where Q_2 is given by Equation (56a) of Nigam et al.[20] One finds

$$\langle \Theta^2 \rangle_\ell = \frac{8\pi N Z(Z+1) r_0^2 (1-\beta^2)}{\beta^4} \Bigg\{ \ln\left[\frac{1.77\,\beta}{\mu Z^{1/3} \alpha_0 (1-\beta^2)^{1/2}}\right] - 1 - \frac{\beta^2}{4} + \frac{5\pi\alpha\beta}{12} +$$

$$- \frac{\alpha}{\beta}\left[\frac{\mu Z^{1/3}\alpha_0 (1-\beta^2)^{3/2}}{0.885\,\beta}\right] - \frac{1}{2}\ln\Bigg[1 + 4\alpha\left(\frac{\mu Z^{1/3}\alpha_0 (1-\beta^2)^{1/2}}{0.885\,\beta}\right)\Bigg(1.448\beta +$$

$$+ \frac{(1-\beta^2)}{\beta}\ln\left\{\frac{\mu Z^{1/3}(1-\beta^2)^{1/2}\alpha_0}{0.885\,\beta}\right\} + \frac{0.231}{\beta}\Bigg)\Bigg]\Bigg\} \tag{3.45}$$

where again N is the density of scattering centers, Z is the atomic number of the scatterer, r_0 the classical electron radius, $\alpha_0 = e^2/\hbar c \simeq 1/137$ is the fine structure constant, $\beta = v/c$, $\alpha = Z\alpha_0$, and $\mu = 0(1)$ is a parameter of order one (1) arising from the screening in the Dalitz[21] cross section and is to be chosen such that the exponentially screened field is the closest approximation to the actual field V(r). In the present comparison for gold we have used $\mu = 1.8$ in accordance with the agreement with experiment cited by Nigam et al.[20] In the first Born approximation one neglects terms in (3.45) containing the parameter $\alpha = Ze^2/\hbar c$ to obtain

$$\langle \Theta^2 \rangle_\ell = \frac{8\pi N Z(Z+1) r_0^2 (1-\beta^2)}{\beta^4} \left\{ \ln\left[\frac{1.77\,\beta}{\mu Z^{1/3}\alpha_0 (1-\beta^2)^{1/2}}\right] - 1 - \frac{\beta^2}{4} \right\} \tag{3.46}$$

which differs only slightly from the results obtained from Lewis.[16] The factor Z^2 in Equation (3.43) is now replaced by $Z(Z+1)$ since scattering off atomically bound electrons is included in (3.46), the differences in the slowly varying logarithmic terms of (3.43) and (3.46) are minor and finally the term involving β^2 in (3.46) will be negligible at low electron energies.

c. Integration Using Cross Sections of Lin. - The exact definition of the mean square scattering angle per unit length is given by

$$\langle \Theta^2 \rangle_\ell = N \int \theta^2 \frac{d\sigma}{d\Omega} \, d\Omega \tag{3.47}$$

where N is the density of scattering centers, θ is the angle of scatter in a single event, and $d\sigma/d\Omega$ is the differential scattering cross section for single scattering of electrons. The theoretically determined cross sections for gold (Z = 79) of Lin,[78] calculated from the Hartree potential for mercury (Z = 80) fitted by Byatt,[79] were used to perform a numerical integration of Equation (3.47) for various energies. This integration was performed through the Romberg integration method described by Bauer, Rutishauser, and Stiefel[80] which applies a linear transformation to the trapezoidal rule to obtain a rapidly convergent series of approximations.

The above mentioned theories have been evaluated numerically for gold at energies of 50, 100, 120, 188, 200, and 400 keV (since Lin's cross sections were quoted for these energies) and are represented graphically in Figure 5. One observes at low electron energies ($T < 200$ keV) that the results obtained by integration of Equation (3.47) are approximately a factor of 2 greater than

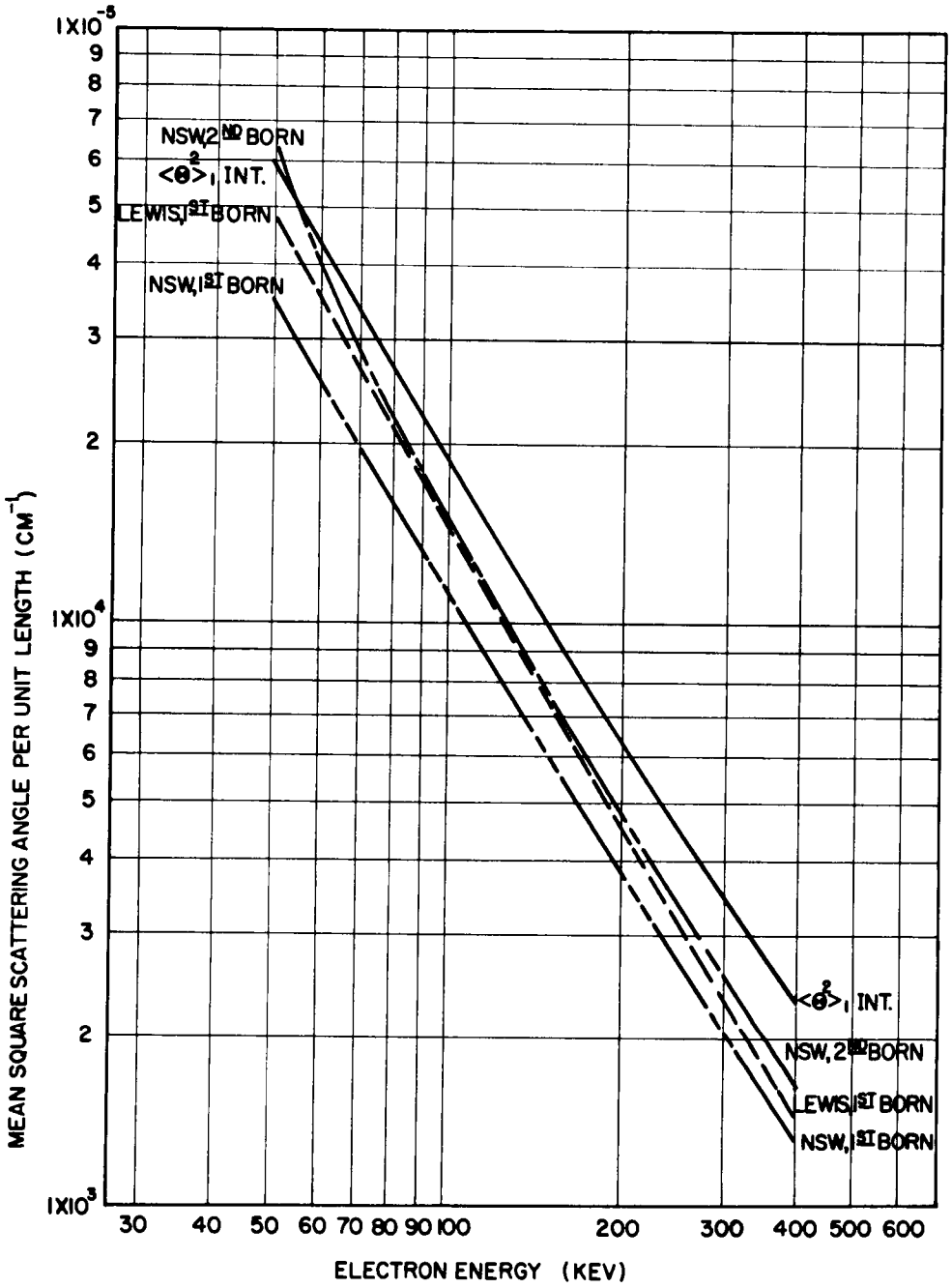

Fig. 5. - Mean Square Scattering Angle Per Unit Length - Gold

the results of the 1st Born approximation of Nigam et al.,[20] Equation (3.46), while the results from Lewis,[16] Equation (3.43), are approximately mid-way between these two extremes. One further notes that the results in the 2nd Born approximation of Nigam et al.[20] are appreciably higher (factor of ~ 2) at low energy than their 1st Born approximation indicating that higher Born approximations are indeed important for low energy electron scattering. Because it yields results differing only slightly from those obtained from the cross sections of Lin, the expression (3.43) was used for the numerical evaluations which follow in Chapter IV.

2. Optical Constants n and k

The dielectric constant $\epsilon = \epsilon(\omega)$ must be determined for the several materials of interest in order to generate theoretical spectra from Equations (3.35) and (3.38). One has chosen to employ experimentally determined values of the reflectances r_s and r_p—the reflectance of light of wavelength λ with the electric vector normal to and parallel with, respectively, the plane of incidence. From Fresnel's equations the relationships between n, the refractive index, k, the extinction coefficient, and the reflectances r_s and r_p are given by[81]

$$r_s = \left| \frac{[(n+ik)^2 - \sin^2\varphi] - \cos\varphi}{[(n+ik)^2 - \sin^2\varphi] + \cos\varphi} \right|^2 \tag{3.48a}$$

$$r_p = \left| \frac{[(n+ik)^2 - \sin^2\varphi] - (n+ik)^2\cos\varphi}{[(n+ik)^2 - \sin^2\varphi] + (n+ik)^2\cos\varphi} \right|^2 \tag{3.48b}$$

where φ is the angle of incidence of the light measured with respect to the normal to the plane reflecting material. Hence, the experimental determination of r_s or r_p or a combination of both (unpolarized light) enables one to calculate the optical constants n and k. From these data the dielectric constant can be computed using the well-known relationship

$$\epsilon(\omega) = \left[n(\omega) + i\,k(\omega)\right]^2 \tag{3.49}$$

Reflectances determined experimentally by Ehrenreich and Phillip[82] for silver, by Minor[83] for copper, and by Philip[84] for gold have been used to obtain the optical constants n and k for input data in the present work. These values are shown graphically in Figures 6, 7, and 8.

G. Summary

The photon yield from a dielectric medium through which a charged particle has penetrated has been determined in terms of the angle of particle incidence θ_i, the geometry of observation (angles Θ and Φ), the scattering properties of the medium $\langle\Theta^2\rangle_\ell$, and the optical properties of the medium $\epsilon(\omega)$. One now generates theoretical spectra for various materials and compares the numerical results with available experimental data.

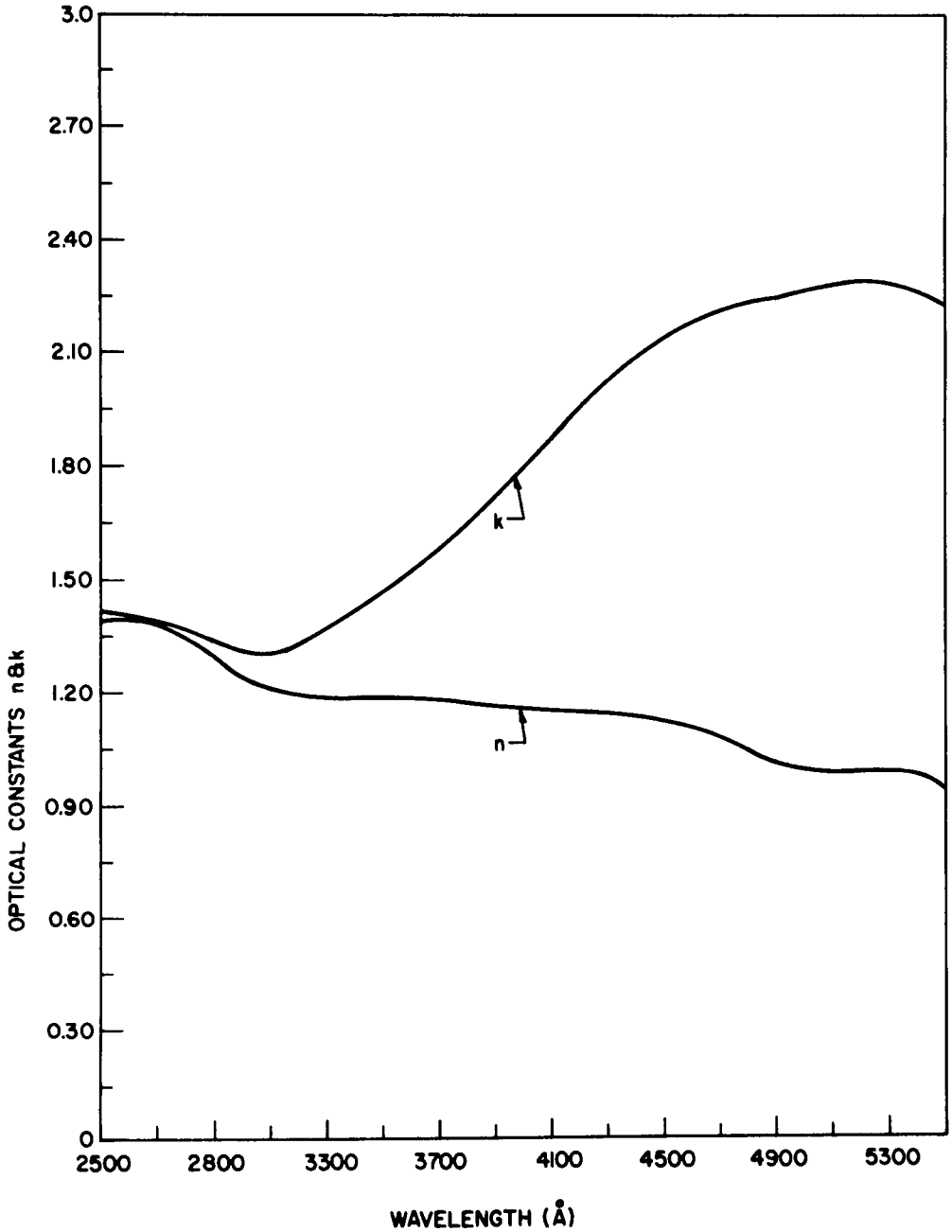

Fig. 6. - Optical Constants - Copper

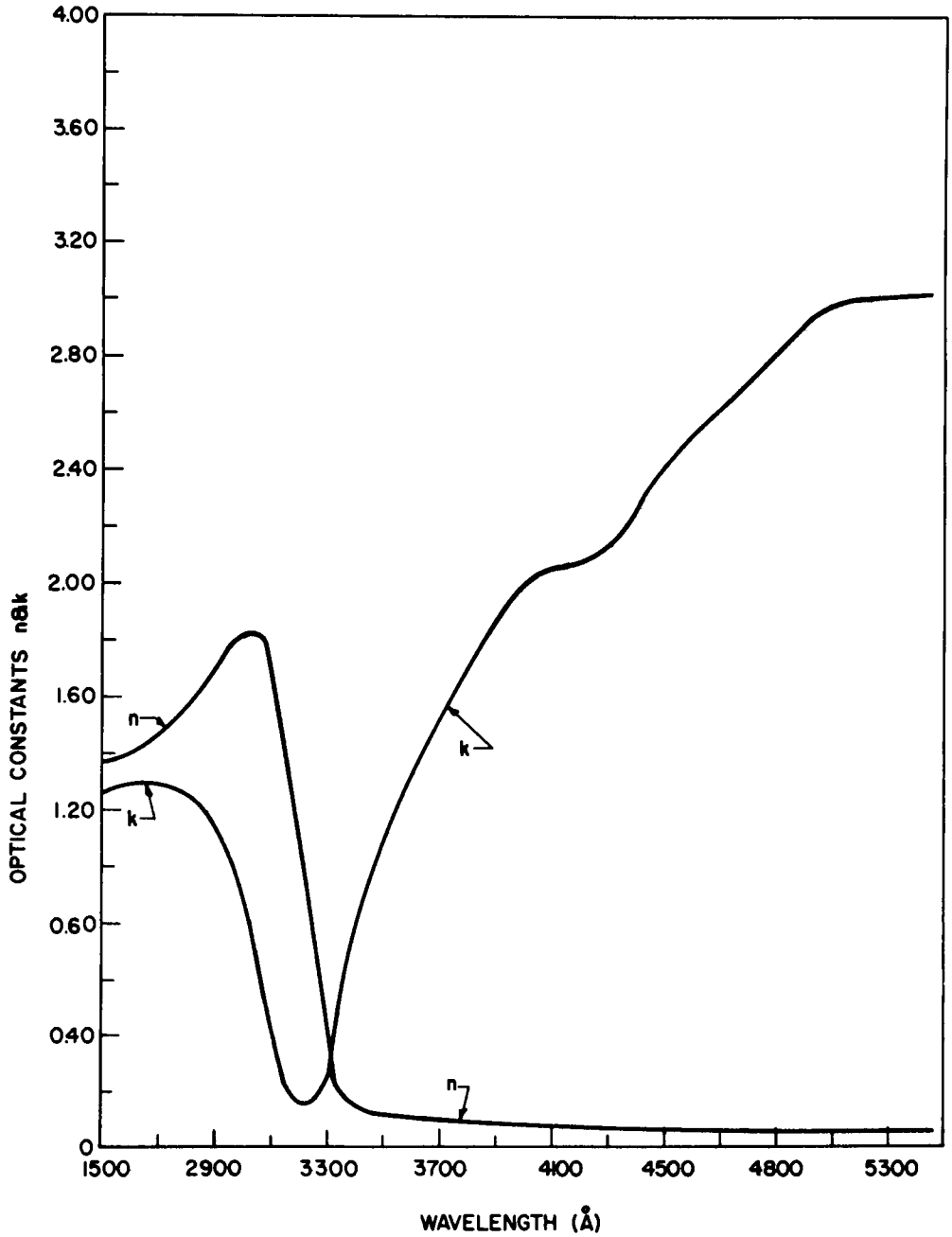

Fig. 7. Optical Constants - Silver

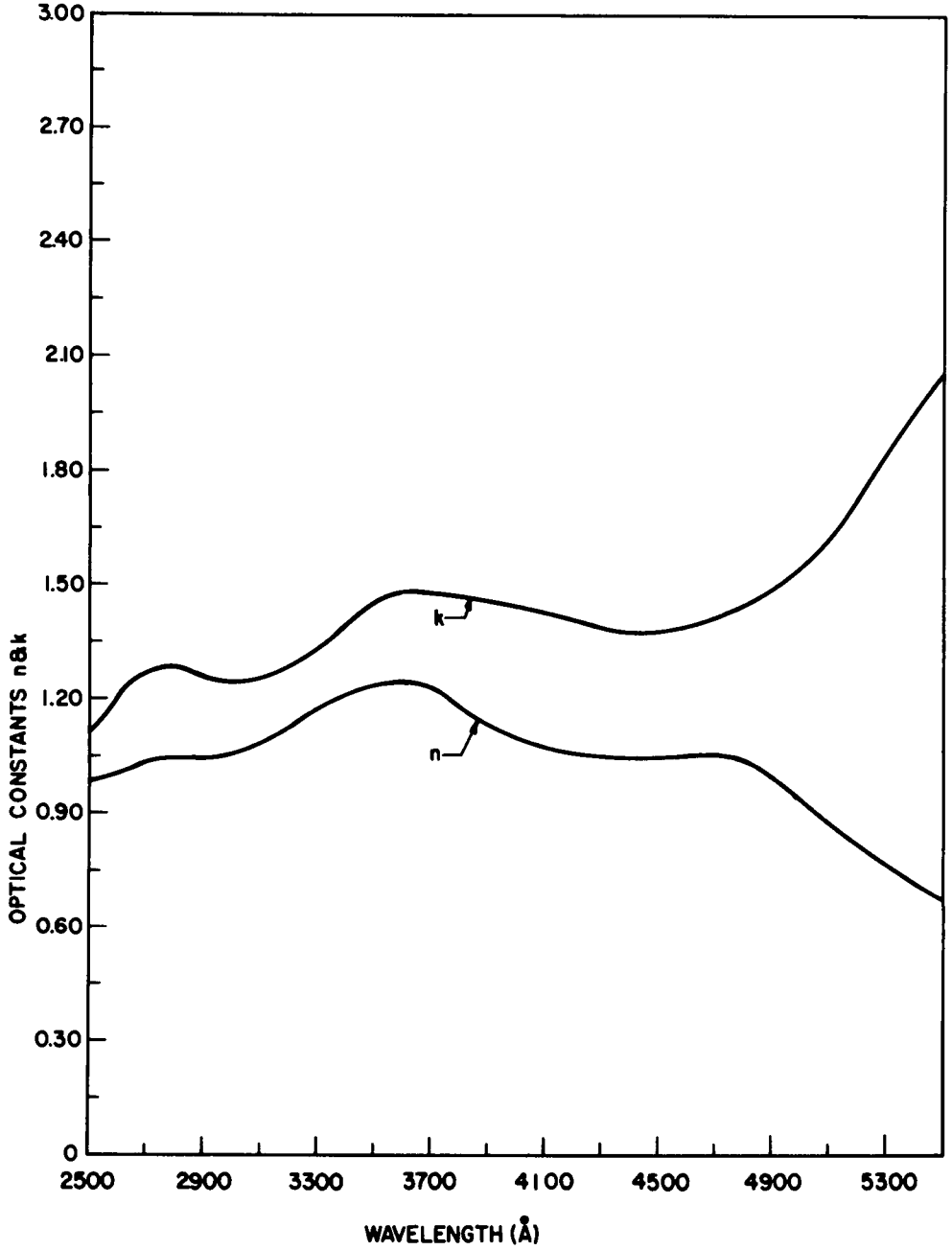

Fig. 8. - Optical Constants - Gold

IV. RESULTS AND CONCLUSIONS

To better facilitate the comparison of numerical results obtained from the present theory with experimental results, the general expressions for the photon number distributions $\langle (d^2N)/(d\omega\, d\Omega)\rangle_{\perp,\parallel}$ given by Equations (3.35) and (3.38) with Z = -1 for electrons have been converted to photon intensity distributions $\langle (d^2W)/(d\lambda\, d\Omega)\rangle_{\perp,\parallel}$. Explicitly one has performed the transformation (using the chain rule of differential calculus)

$$\left\langle \frac{d^2W}{d\lambda\, d\Omega} \right\rangle_{\perp,\parallel} = \frac{(2\pi c)^2(\hbar)}{\lambda^3} \left\langle \frac{d^2N}{d\omega\, d\Omega} \right\rangle_{\perp,\parallel} \tag{4.1}$$

and where now the quantity ω in Equations (3.35) and (3.38) must be replaced by its equivalent, $2\pi c/\lambda$. The use of the theoretical expression of Lewis[16] for the mean square scattering angle $\langle \Theta^2 \rangle$, and of the experimentally determined reflectances r_s and r_p from which the optical constants for the various materials were obtained—as discussed in Chapter III and illustrated graphically in Figures 5, 6, 7, and 8—enable one to generate theoretical spectra which can be compared with experimental values. All numerical calculations were obtained using the Control Data Corporation 1604A digital computer.

A. Results

After performing the transformation to a wavelength dependent photon

intensity given by Equation (4.1) the resulting forms of Equations (3.35) and (3.38) for a given material of dielectric constant $\epsilon(\lambda)$ and scattering properties $\langle\Theta^2\rangle_\ell$ are functions of wavelength λ, angle of electron incidence θ_i, angle of photon emission Θ, angle of azimuth Φ, and electron kinetic energy T. The numerical analysis is broken up into two groups of data the first being obtained for normal electron incidence, $\theta_i = 0$, and the last for non-normal incidence, $\theta_i \neq 0$.

1. Normal Incidence

In the case of normal incidence the azimuthal dependence goes out and one obtains the various distributions of the photon intensities $\langle(d^2W)/(d\lambda\, d\Omega)\rangle_{\perp,\parallel}$ by varying one of the remaining parameters λ, T, or Θ while keeping the other two fixed. This has been done for various materials in the wavelength region $\lambda = 2500$ to $\lambda = 5500$ and the results are given below for copper, silver, and gold.

a. Copper. - Using the optical constants for copper from Figure 6 the theoretical spectral distribution, angular distribution, and energy dependence of the emitted radiation from an electron bombarded copper slab have been determined and are shown in Figures 9, 10, and 11. In each case, figures labelled (a) show the photon intensity due to parallel polarized photons while figures labelled (b) show the intensity due to perpendicularly polarized photons. In Figure 9 one notes that the perpendicular component of the photon intensity which is entirely due to bremsstrahlung (9b) is several orders of

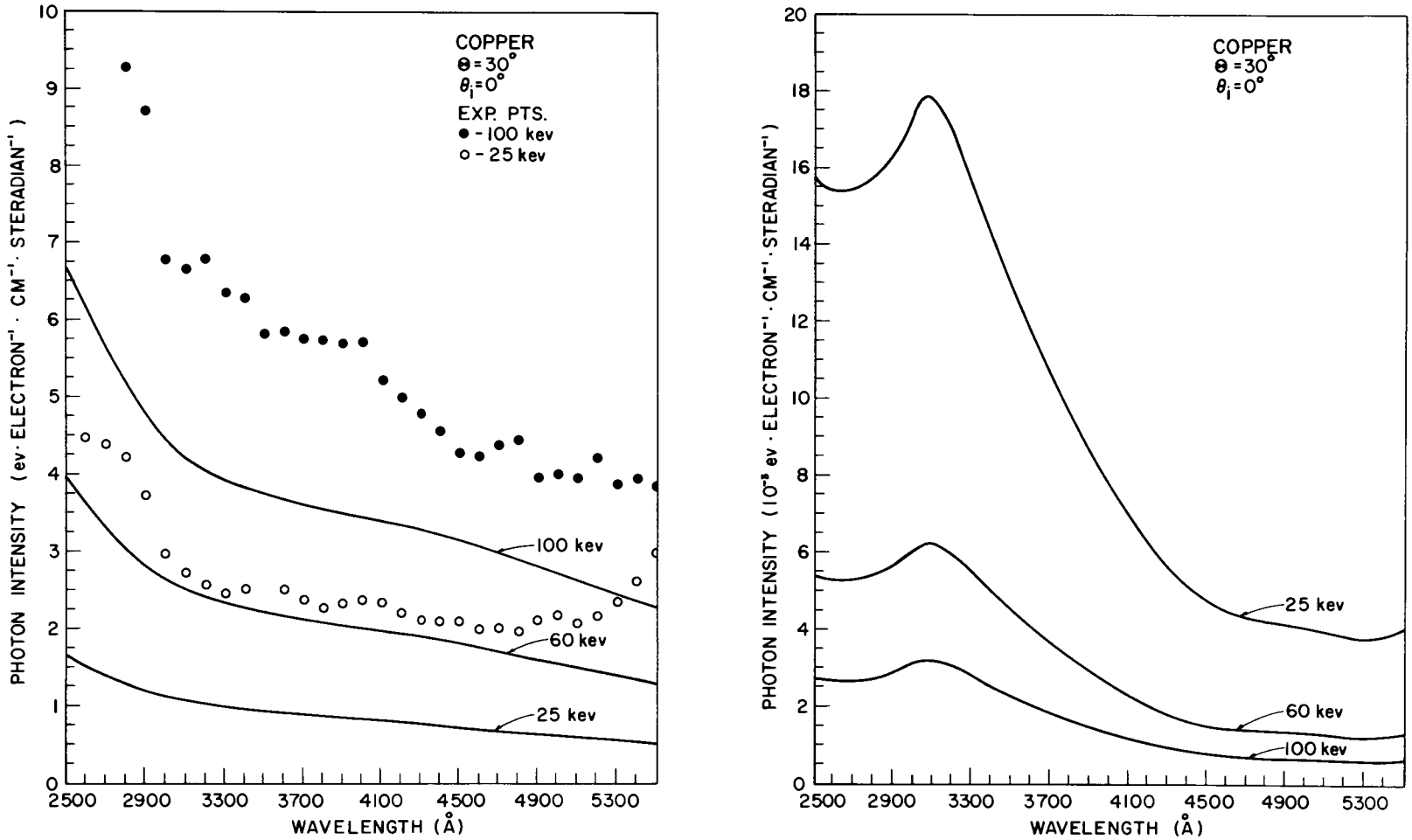

(a) Parallel Polarization

(b) Perpendicular Polarization

Fig. 9. - Photon Intensity vs Wavelength - Copper, Normal Incidence

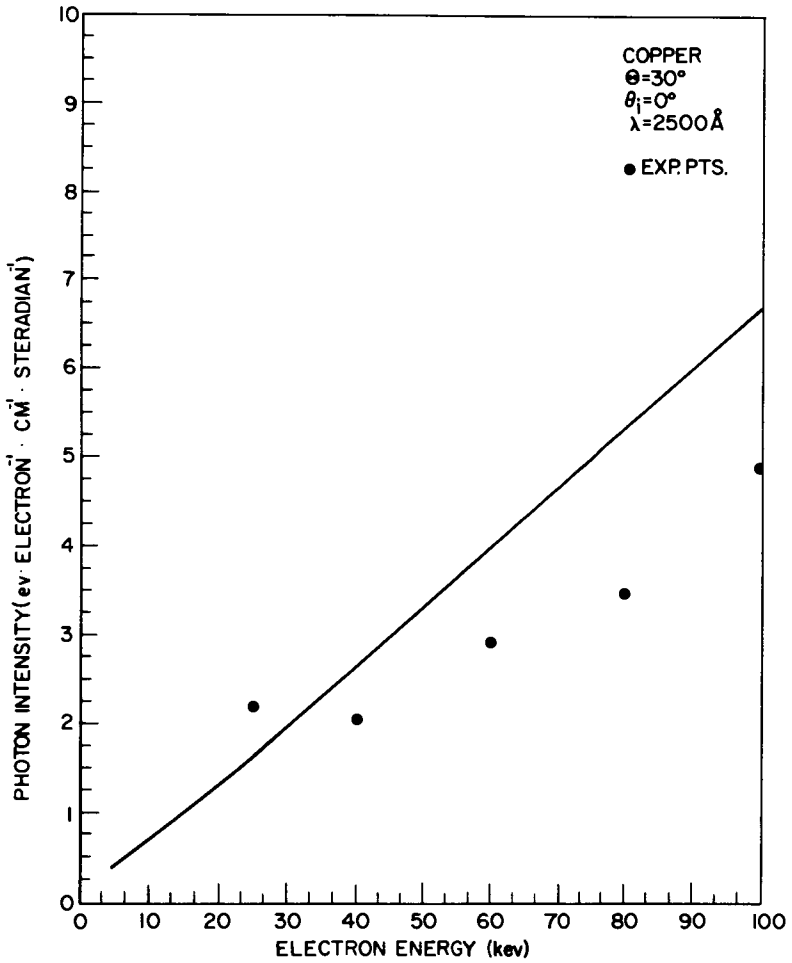

(a) Parallel Polarization

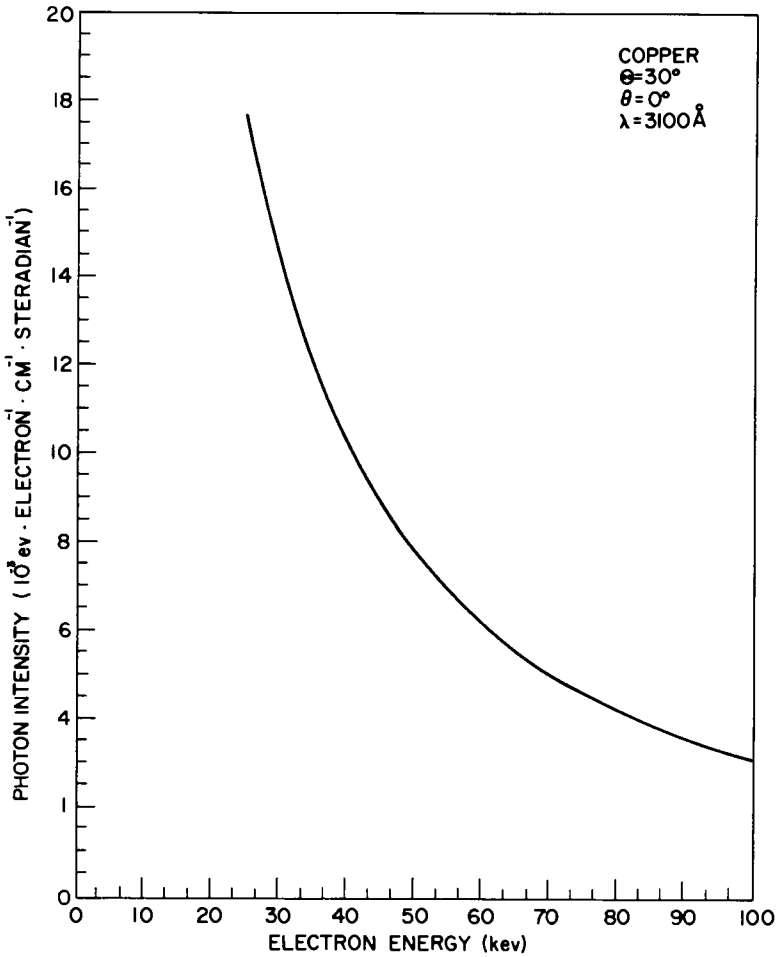

(b) Perpendicular Polarization

Fig. 10. - Photon Intensity vs Electron Energy - Copper, Normal Incidence

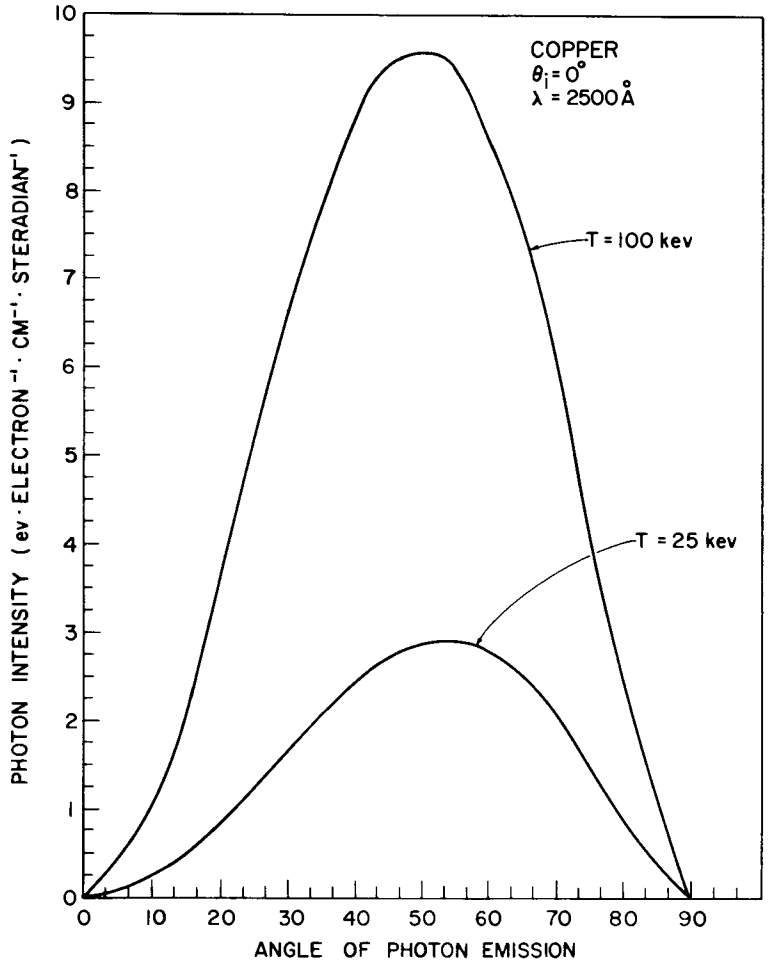

(a) Parallel Polarization

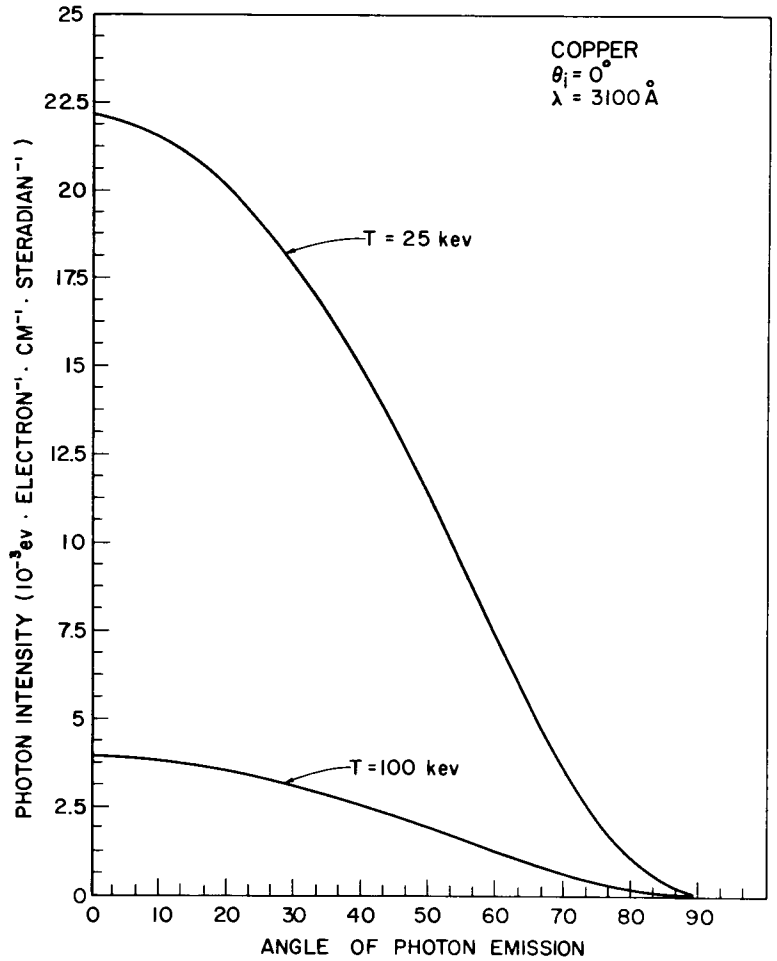

(b) Perpendicular Polarization

Fig. 11. - Photon Intensity vs Angle of Emission - Copper, Normal Incidence

magnitude lower than that shown for the parallel component (9a) which contains contributions from both transition radiation and bremsstrahlung. An investigation of the energy dependence shown by Figure 10 shows that the parallel component of the photon intensity has the linear dependence upon electron energy T characteristic of the transition radiation (except for a slight deviation at energies $T < 25$ keV where an upward trend can be noted due to low energy bremsstrahlung) while the perpendicular component shows the 1/T dependence expected of bremsstrahlung. Figure 9b also shows the effect of the absorption of the medium upon bremsstrahlung photons where the departure of the spectrum from the usual continuum in the vicinity of 3100 Å can be seen to correspond to a decrease in the extinction coefficient k in Figure 6. Experimentally determined points by Emerson et al.[85] are shown for the parallel component and one sees that the theoretical values are lower by approximately a factor of 2.5 at T = 25 keV (open circles) and a factor of 1.5 at T = 100 keV (closed circles). One must note, however, that these experimental points were obtained from transmission experiments using a copper foil of thickness 1270 Å and as such does not strictly conform with the theoretical approximations of a semi-infinite medium. The effect of back scattered electrons due to large angle scatters and the reflection of photons from the second foil surface would be expected to contribute radiation which may account for some of the discrepancy. The angular distribution of the emitted radiation is shown in Figure 11 where one notes that the parallel component (transition radiation) shows a maximum at the

emission angle of approximately 50° while the bremsstrahlung component is strongest in the backward direction $\Theta = 0$. No experimental values are available at present for comparison of the angular distributions or the perpendicular components. Summarizing, one finds that the spectral distribution for copper in the range $\lambda = 2500$ to 5500 Å and for electron energies from T = 25 to 100 keV consists of two distinct components, one (perpendicularly polarized) due to low energy bremsstrahlung and the other (parallel polarization) primarily due to transition radiation, the interpretation of the parallel component being accomplished with the aid of the angular distribution and the energy dependence of the emitted radiation.

b. Silver. - The optical constants from Figure 7 were used to obtain the theoretical spectral, energy, and angular distributions of silver which are shown in Figures 12, 13, and 14, respectively. The spectral distribution differs from that of copper in that for the parallel component (Figure 12a) one now observes a rapid decrease in photon intensity to a minimum at $\sim$3200 Å followed by a sharp peak at $\sim$3320 Å which "tails off" into the typical $1/\lambda$ continuum. The effect of the absorption of the medium upon the bremsstrahlung photons is more apparent in the perpendicular component (Figure 12b) where one now notes a sharp peak in the neighborhood of 3270 Å (the extinction coefficient k is seen from Figure 7 to have a small value in the region 3100 to 3300 Å). Again the agreement between the theoretical spectrum and the experimentally determined points of Emerson et al.[85] is poor for low energy T = 25 keV but within a factor of 1.5 at an energy of T = 100 keV. The

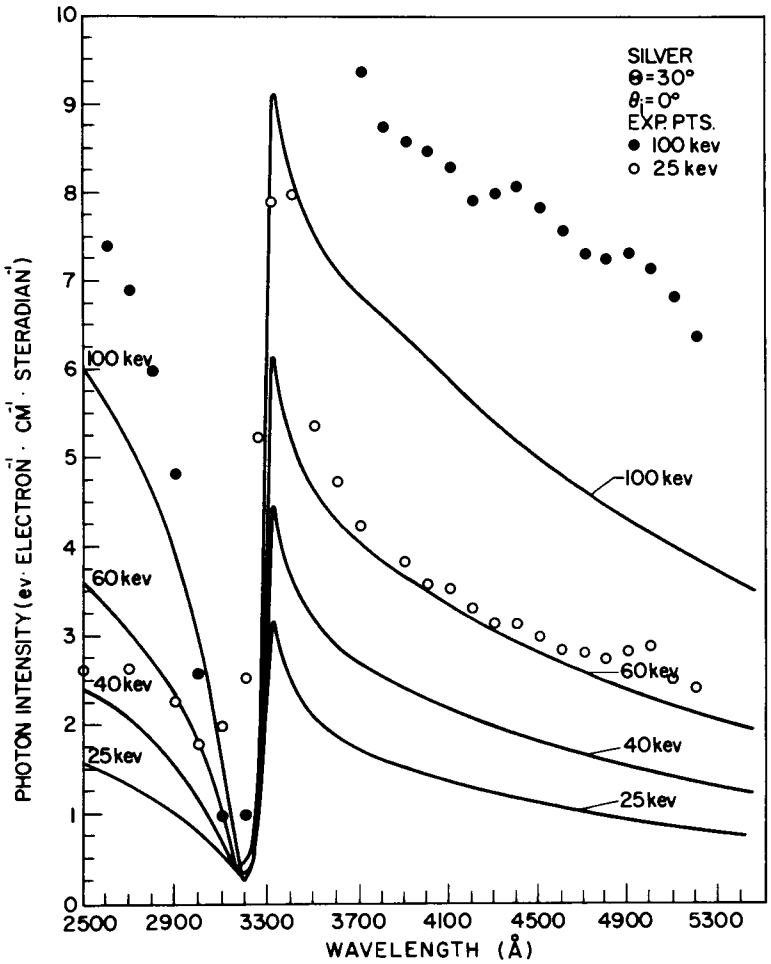

(a) Parallel Polarization

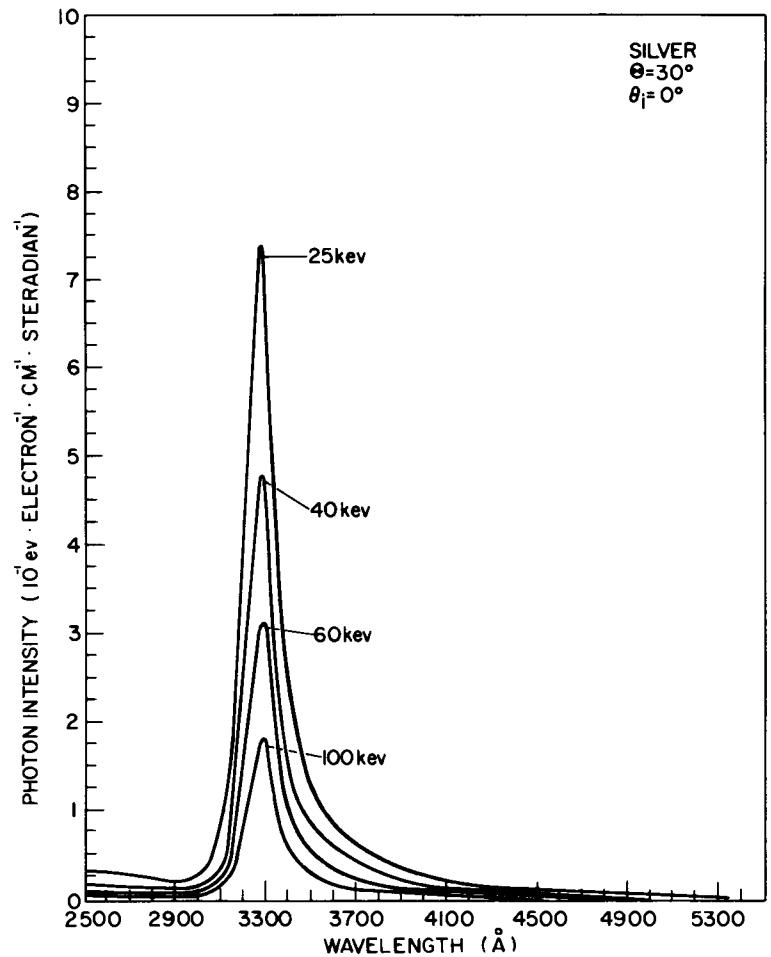

(b) Perpendicular Polarization

Fig. 12. - Photon Intensity vs Wavelength - Silver, Normal Incidence

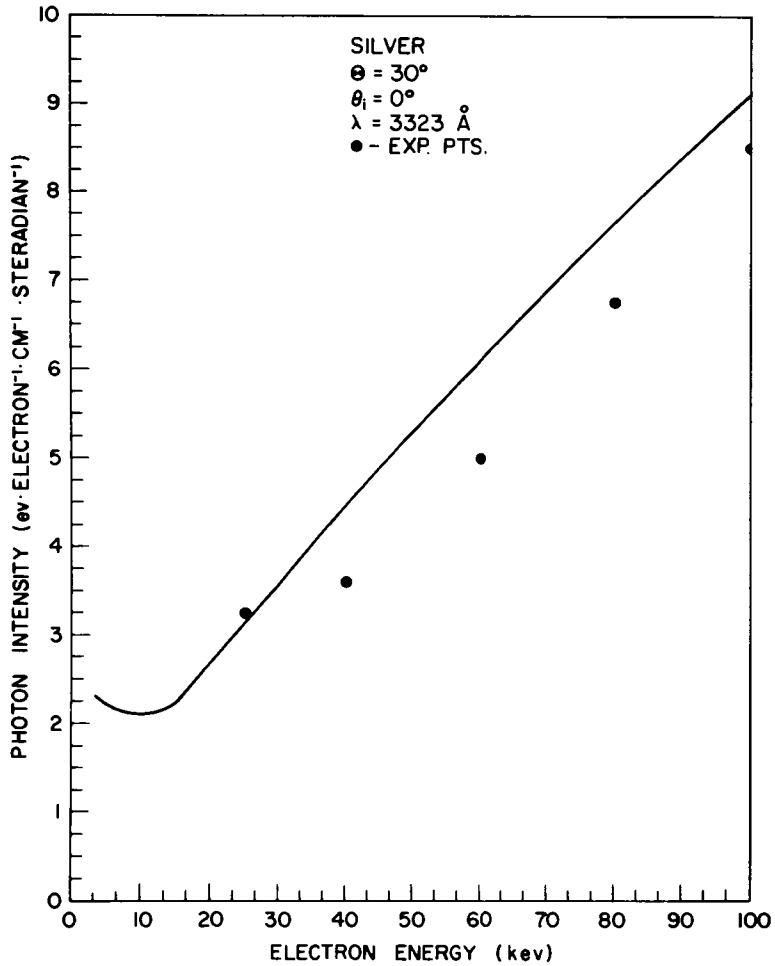

(a) Parallel Polarization

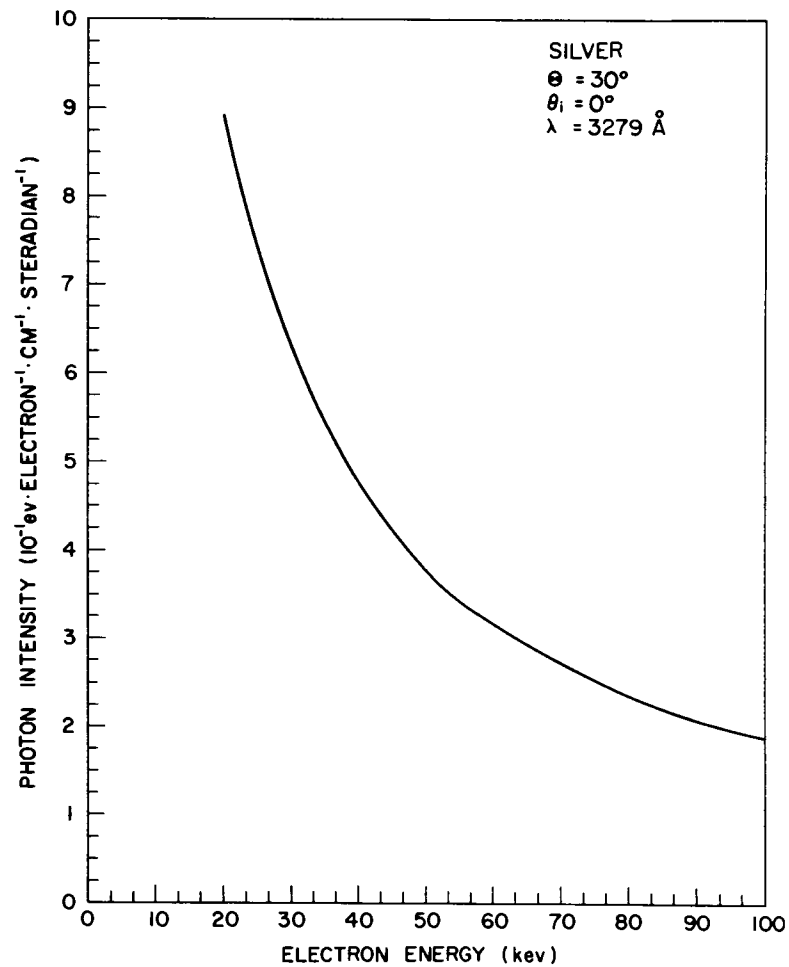

(b) Perpendicular Polarization

Fig. 13. - Photon Intensity vs Electron Energy - Silver, Normal Incidence

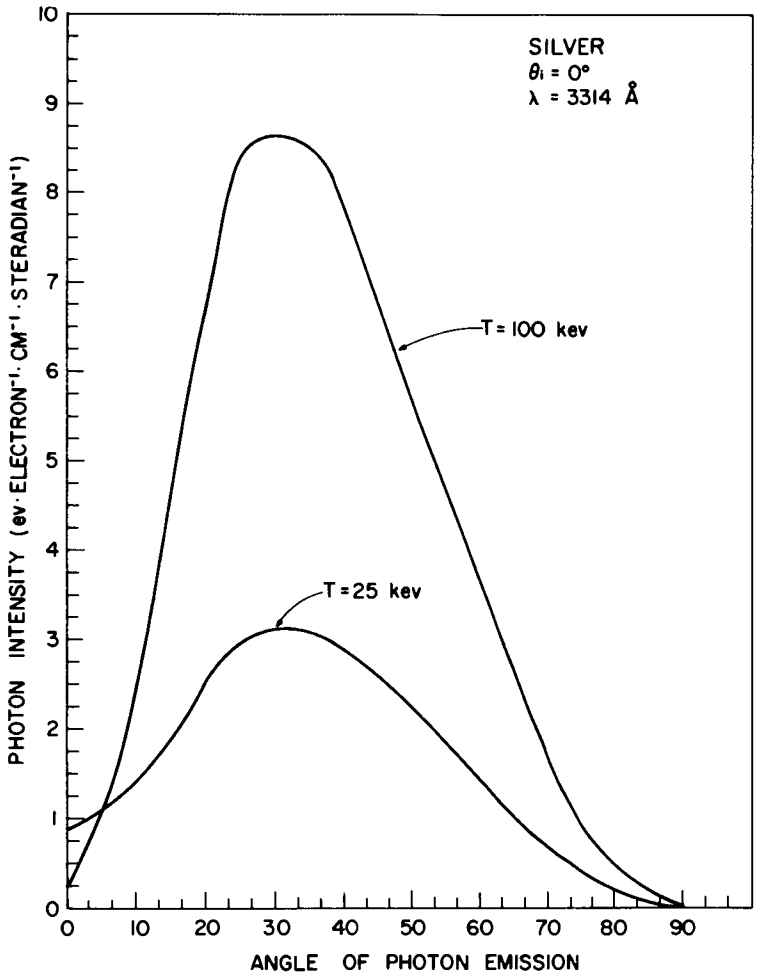

(a) Parallel Polarization

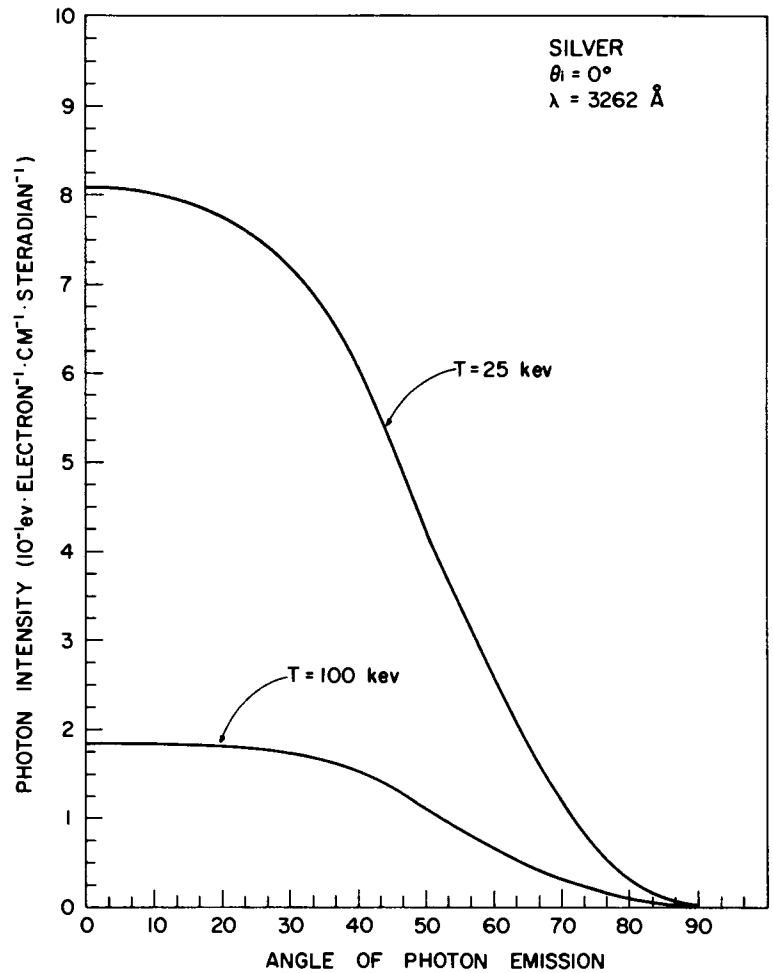

(b) Perpendicular Polarization

Fig. 14. - Photon Intensity vs Angle of Emission - Silver, Normal Incidence

experimental points were obtained from transmission experiments using a thin silver foil of 710 Å thickness. The energy dependence of the photon intensity, shown in Figure 13, again shows the almost linear dependence of the parallel component (where now the 1/T dependence of the parallel polarized bremsstrahlung is more apparent below T = 20 keV than in the case of copper; this is to be expected since silver has a higher Z value than copper) for energies greater than 20 keV again identifying this component as primarily transition radiation, while the perpendicular component (Figure 13b) again shows the typical 1/T bremsstrahlung characteristics. The angular distributions of the emitted radiation shown in Figure 14 are very similar to those of copper except that the peak emission of the parallel component for silver is in the neighborhood of $\Theta = 30°$. One also notes that for small angles $\Theta < 5°$ the photon intensity decreases with increasing energy leading to the conclusion that for observation in this area the parallel component of bremsstrahlung competes with transition radiation. The angular distribution of the perpendicular component is seen to be similar to that of copper.

c. Gold. - The theoretical spectral, energy, and angular distributions for a thick gold slab—using the optical constants from Figure 8—are given in Figures 15, 16, and 17, respectively. One notes the typical $1/\lambda$ "tailing off" of the spectrum in Figure 15 with a few humps in those areas corresponding to a decrease in the extinction coefficient k of Figure 8. The intensity of the parallel component is again larger than that of the perpendicular component by at least an order of magnitude. The linear energy dependence of the

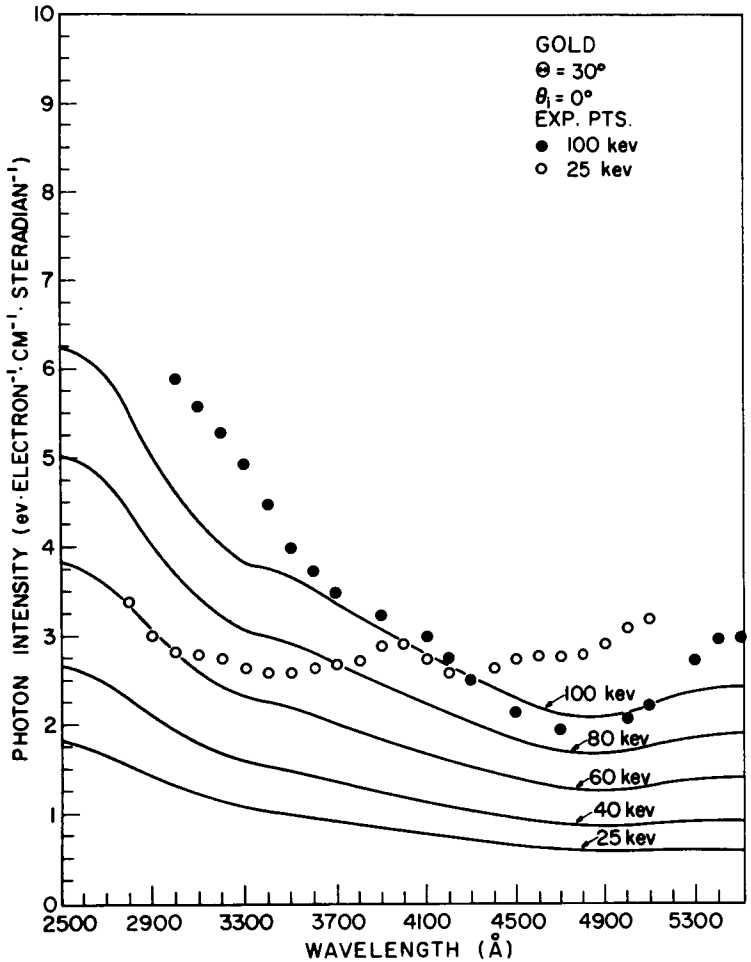

(a) Parallel Polarization

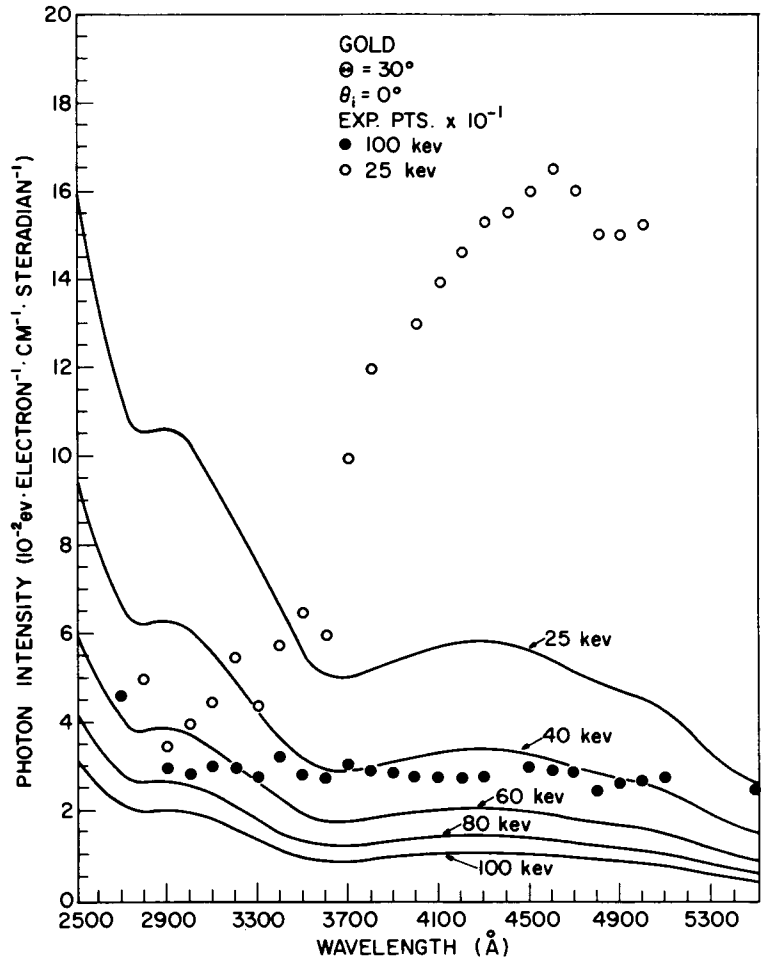

(b) Perpendicular Polarization

Fig. 15. - Photon Intensity vs Wavelength - Gold, Normal Incidence

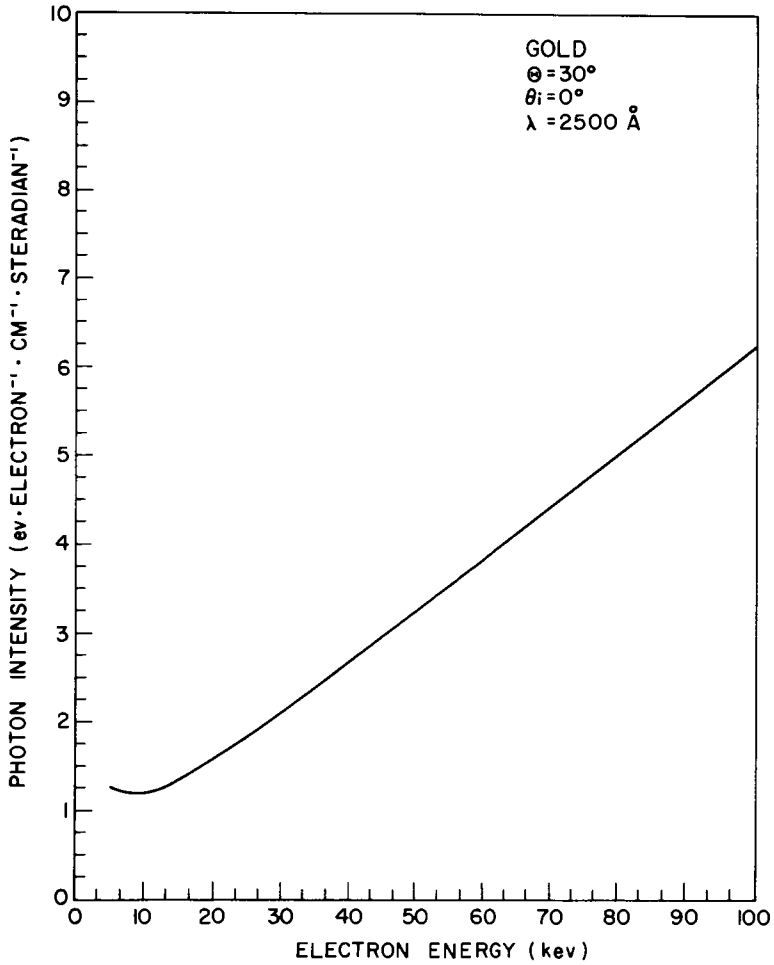

(a) Parallel Polarization

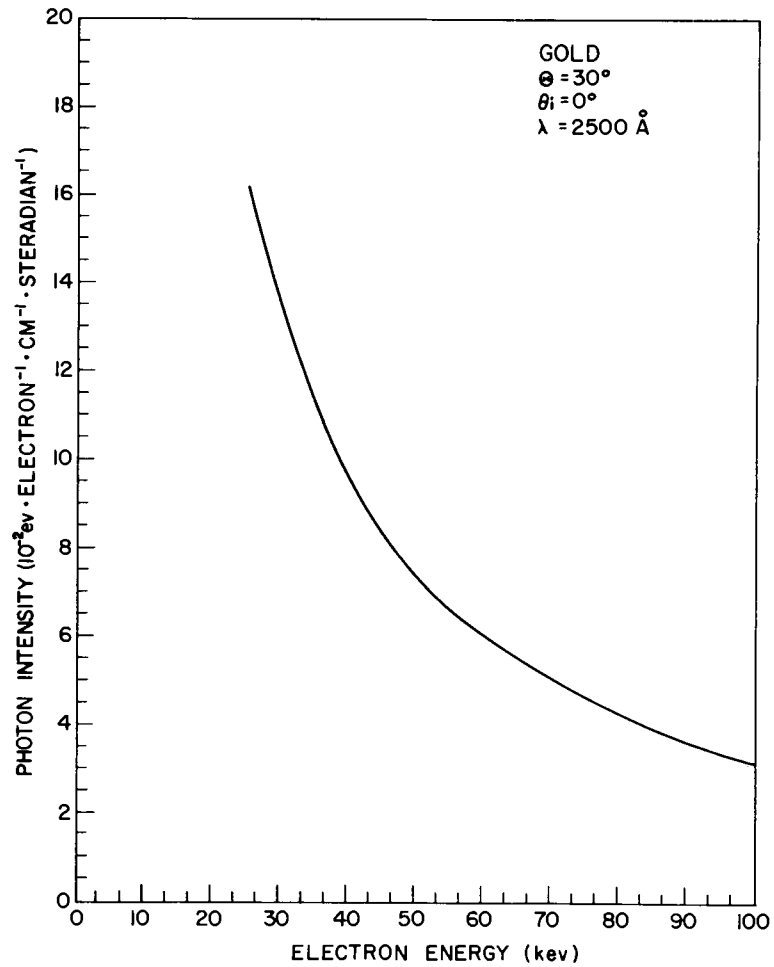

(b) Perpendicular Polarization

Fig. 16. - Photon Intensity vs Electron Energy - Gold, Normal Incidence

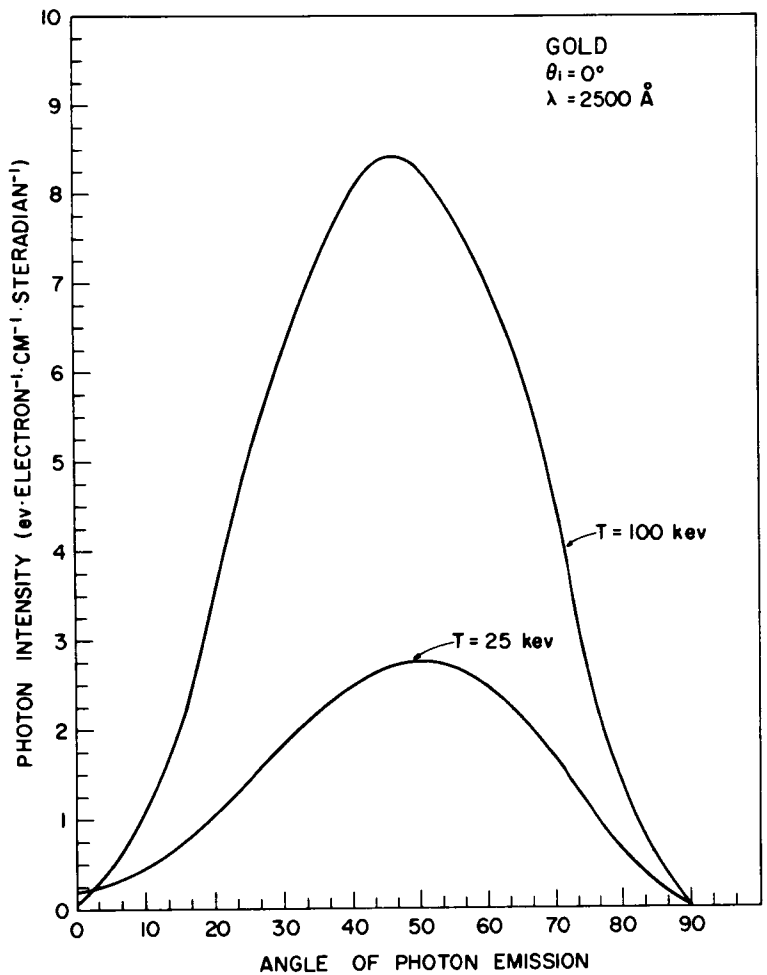

(a) Parallel Polarization

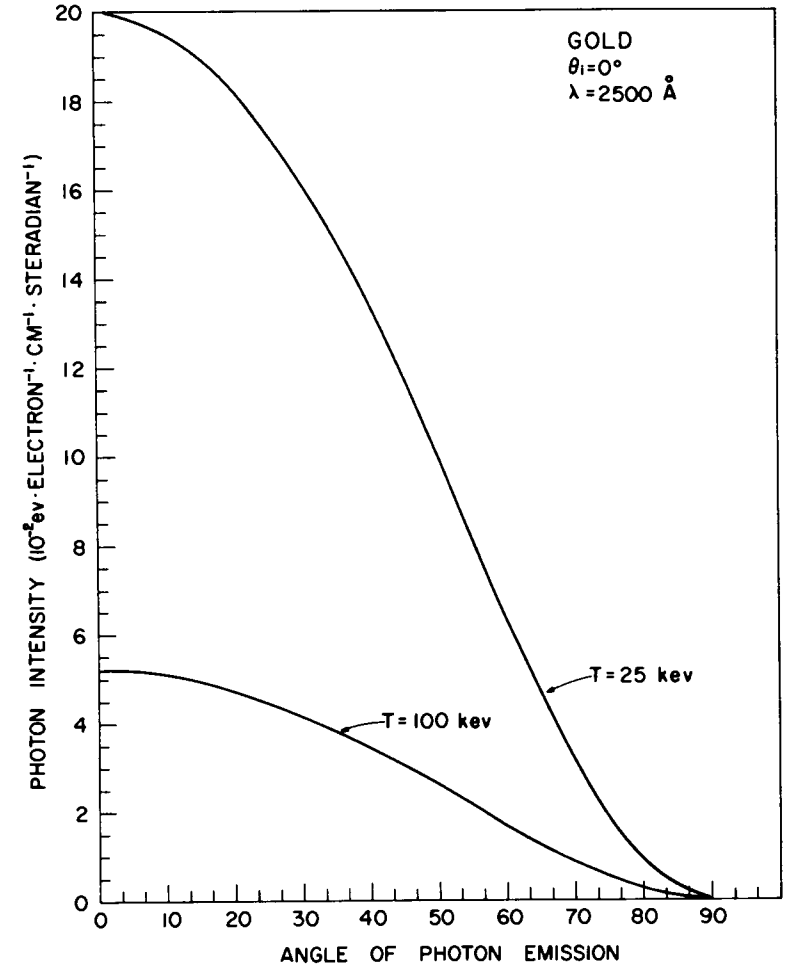

(b) Perpendicular Polarization

Fig. 17. - Photon Intensity vs Angle of Emission - Gold, Normal Incidence

parallel photon intensity shown in Figure 16a again leads one to associate this component with transition radiation while the perpendicular component is caused by bremsstrahlung. The deviation of the energy dependence shown in Figure 16a from a linear dependence emphasizes the greater contribution of the parallel component of bremsstrahlung at low electron energies. The angular distributions, Figure 17, of the polarization components of the emitted radiation are very much like those of copper with the parallel photon intensity being greatest for $\Theta \sim 45^\circ$ to 50° and the perpendicular component being greatest in the $\Theta = 0^\circ$, i.e., the backward, direction. The comparison of the spectral distributions in Figure 15 with the experimental data of Hammer *et al.*[86] for a 530-Å gold foil again shows the poor agreement at low electron energies (T = 25 keV) where one would expect scattering of the electron beam to be important, while the agreement at higher energies (T = 100 keV)—where the transition radiation is more dominant—is excellent. The discrepancy at low electron energies is more evident in the perpendicular component where the experimental values of Hammer *et al.*[86] have been scaled down by a factor of 10 for purposes of comparison. This of course distorts the comparison of the relative shape of the curves but is used to illustrate the fact that there is an order of magnitude discrepancy between the theoretical and experimental spectral distribution of the perpendicular components. The explanation of this discrepancy must necessarily await further experimental data with slabs of material which more nearly satisfy the approximations incorporated in the theoretical evaluation of the small angle

scattering.

Summarizing the numerical results for the three materials copper, silver, and gold—representing low, intermediate, and high Z materials—one finds that the parallel polarized component of the photon intensity is larger than the perpendicularly polarized component by at least an order of magnitude and because of its approximately linear dependence on energy (for $T > 20$ keV) is interpreted as radiation due to polarization of the dielectric medium (transition radiation). The 1/T energy dependence of the perpendicular component clearly labels the source of this radiation as being due to bremsstrahlung from electron scattering on randomly distributed nuclei in the dielectric. The spectrum of silver differs in that there is a sharp rise in the intensity of the parallel component in the area of 3300 Å which has been attributed to an interband transition between the d-band electrons.[87] The angular and energy distributions are similar for all three materials with the only differences being the angle of photon emission for maximum intensity. One now considers numerical results obtained for angles of electron incidence other than zero.

2. Arbitrary Incidence

In the case of an arbitrary angle of electron incidence ($\theta_i \neq 0$) the photon intensities $\langle (d^2W)/(d\lambda\, d\Omega)\rangle_{\perp,\parallel}$ are functions of five variables in addition to the optical properties of the medium [through $\epsilon(\lambda)$, assumed here to be known from experiment] and the scattering properties (through $\langle \Theta^2 \rangle$, assumed

here to be described by the theoretical results of Lewis[16]). Hence the dependence of the photon intensities upon these variables can be determined by holding four fixed while one is varied until all possible combinations are included. This was easily accomplished on the computer and the numerical results obtained for silver Z = 47 are presented in Figures 18 through 22. As before, the figure labelled (a) refers to the parallel polarization component of the intensity while the (b) has reference to the perpendicular component. The dependence of the parallel polarized photon intensity upon the azimuthal angle Φ, given in Figure 22a, shows a maximum in the $\Phi = 0$ direction corresponding to emission in the forward direction of the electron's motion. This is to be expected due to the assumption of small angle electron scattering about the incident electron's motion as well as relativistic effects. Because of this maximum and because observation in the plane of incidence is the most common experimental procedure, the remaining dependences of the photon intensity have been presented with the azimuthal angle fixed at $\Phi = 0$. The spectral distribution of the emitted radiation is shown in Figure 18 for various angles of incidence θ_i. One notes that as the electron incidence approaches grazing angles ($\theta_i > 80^\circ$) there is a strong peaking of the photon intensity at approximately $\lambda = 3230$ Å which is attributed to the $(\cos \theta_i)^{-1}$ dependence of the bremsstrahlung terms in Equations (3.35) and (3.38), and is due to the fact that more scatters per incident electron occur within the observable distance λ_{opt} than at smaller angles, hence giving rise to more photons. Both polarization components (18a and 18b) show this strong peaking, however

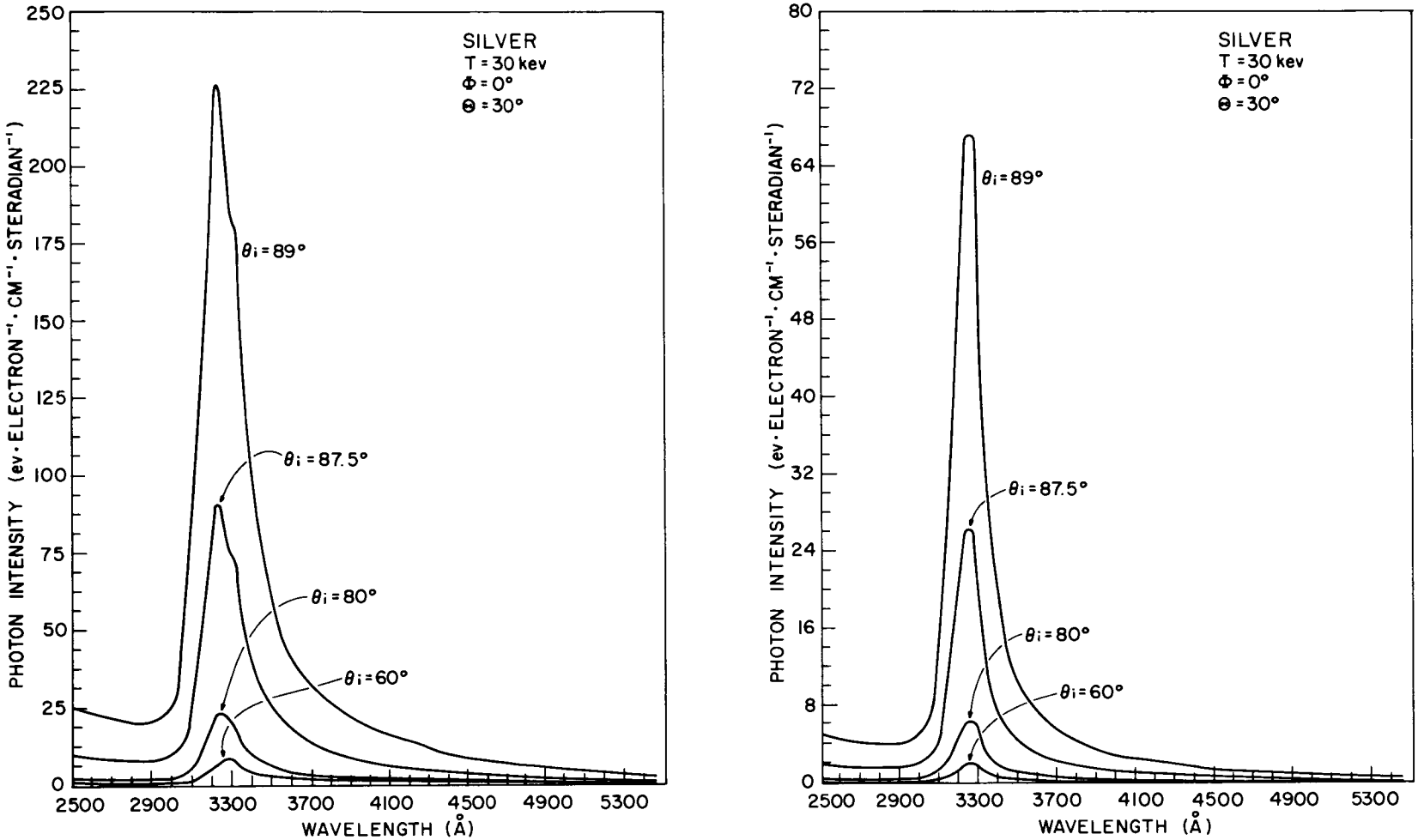

(a) Parallel Polarization

(b) Perpendicular Polarization

Fig. 18. - Photon Intensity vs Wavelength - Silver, Arbitrary Incidence

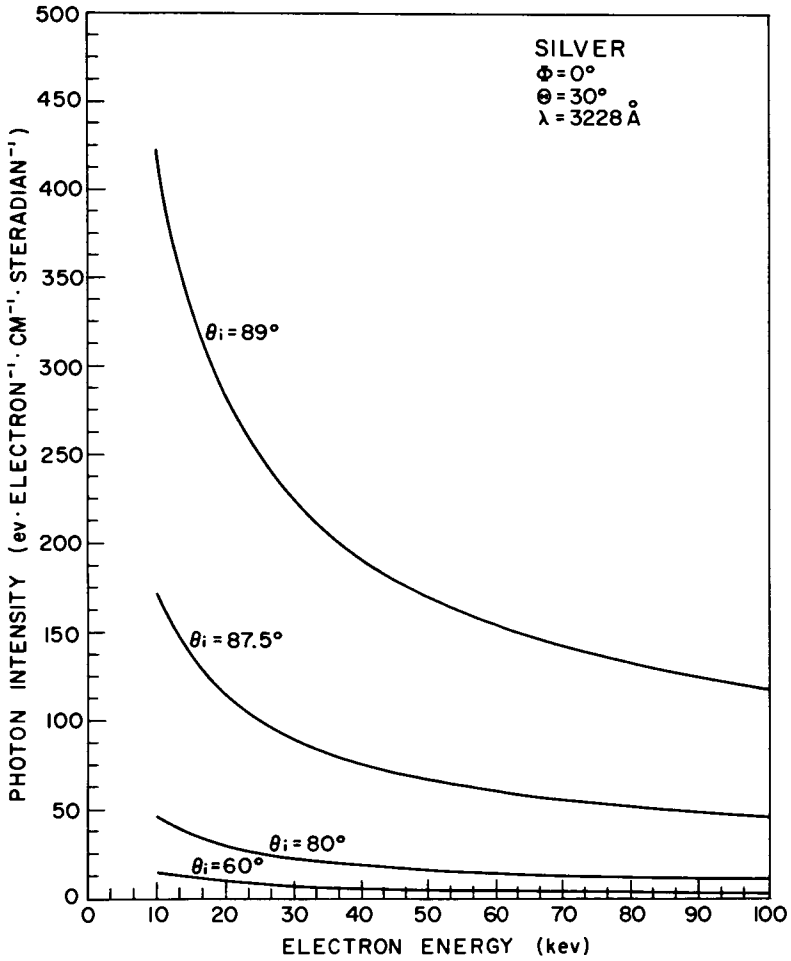

(a) Parallel Polarization

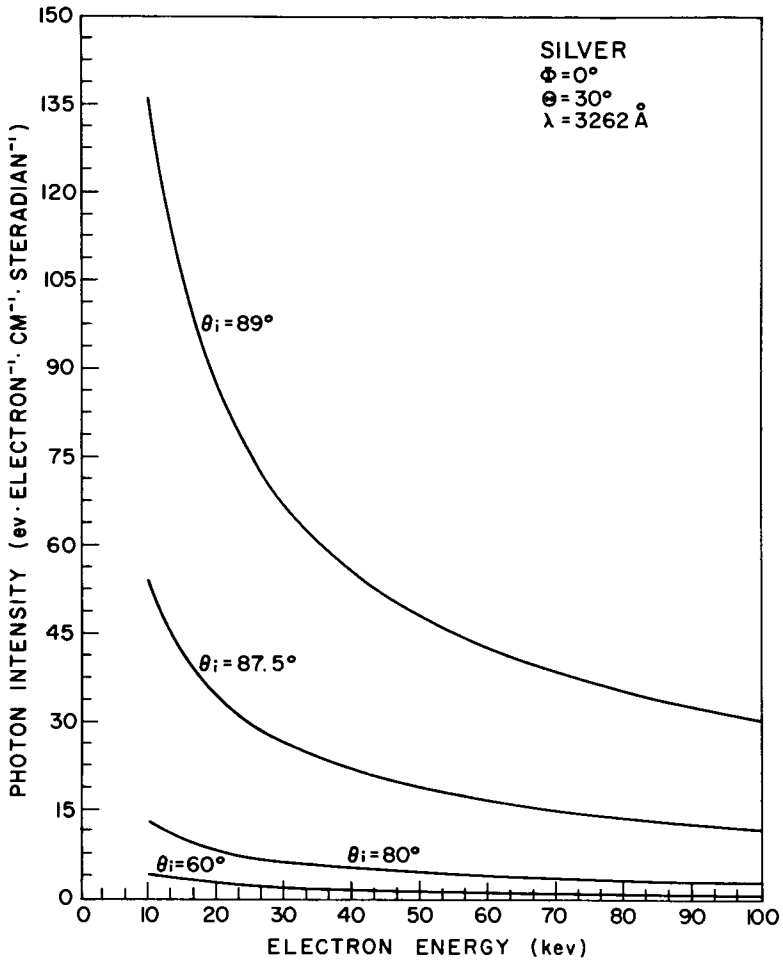

(b) Perpendicular Polarization

Fig. 19. - Photon Intensity vs Electron Energy - Silver, Arbitrary Incidence

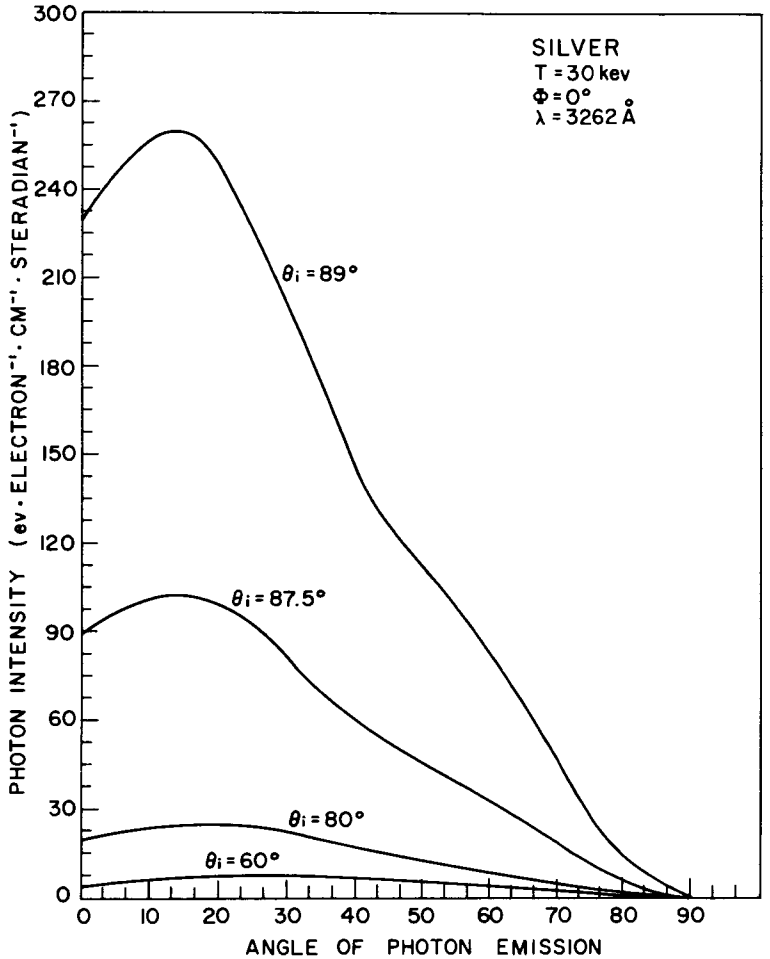

(a) Parallel Polarization

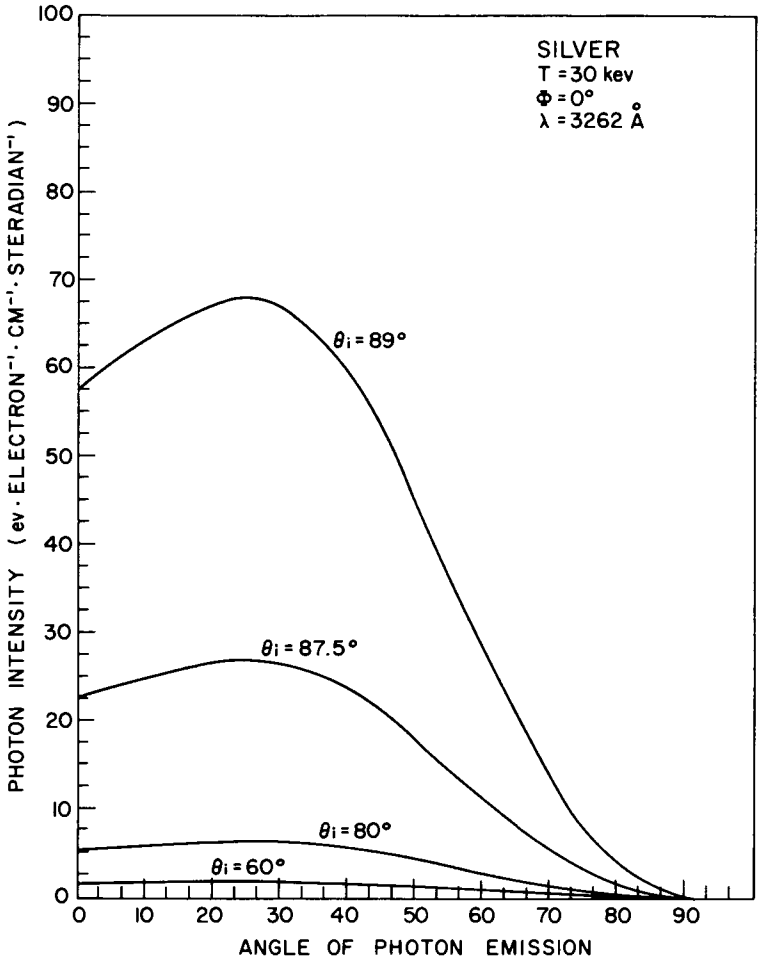

(b) Perpendicular Polarization

Fig. 20. - Photon Intensity vs Angle of Emission - Silver, Arbitrary Incidence

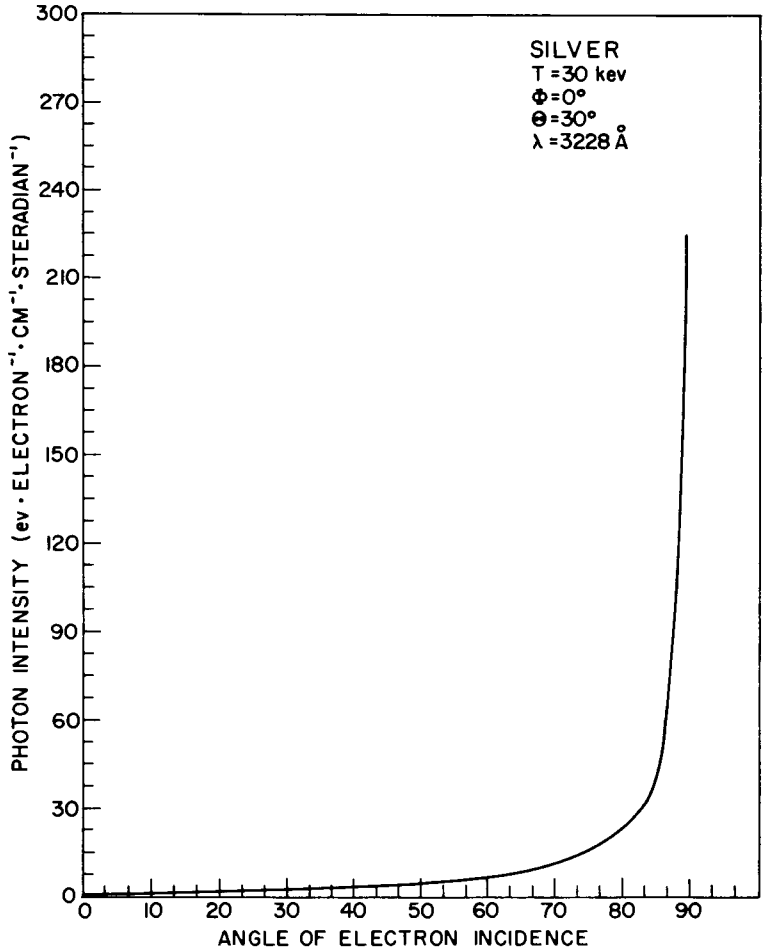

(a) Parallel Polarization

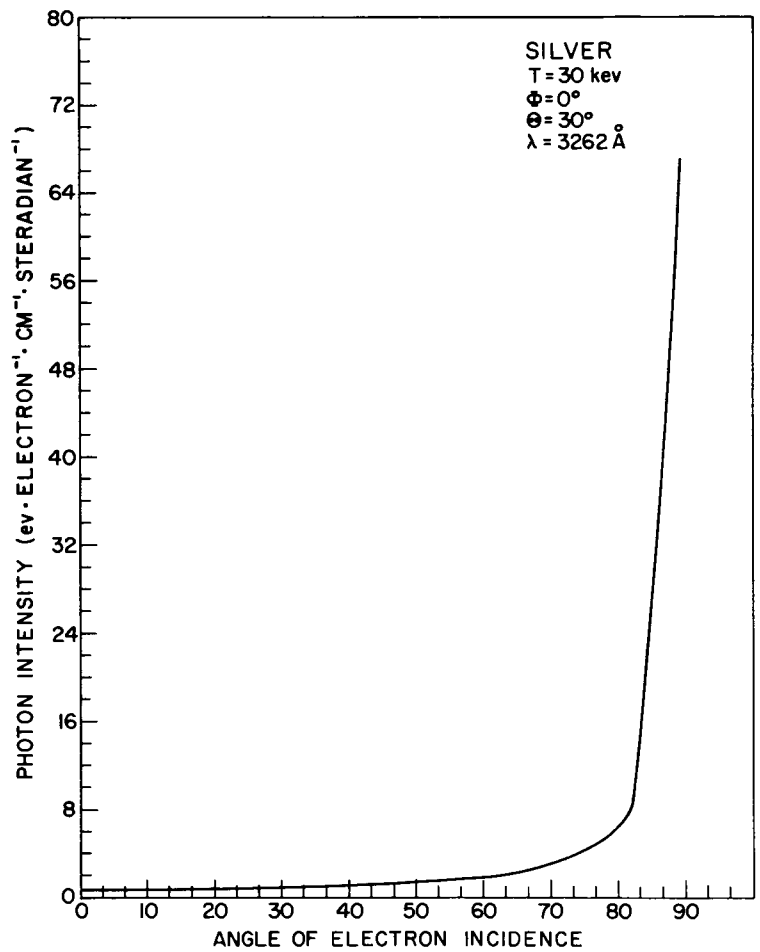

(b) Perpendicular Polarization

Fig. 21. - Photon Intensity vs Angle of Incidence - Silver, Arbitrary Incidence

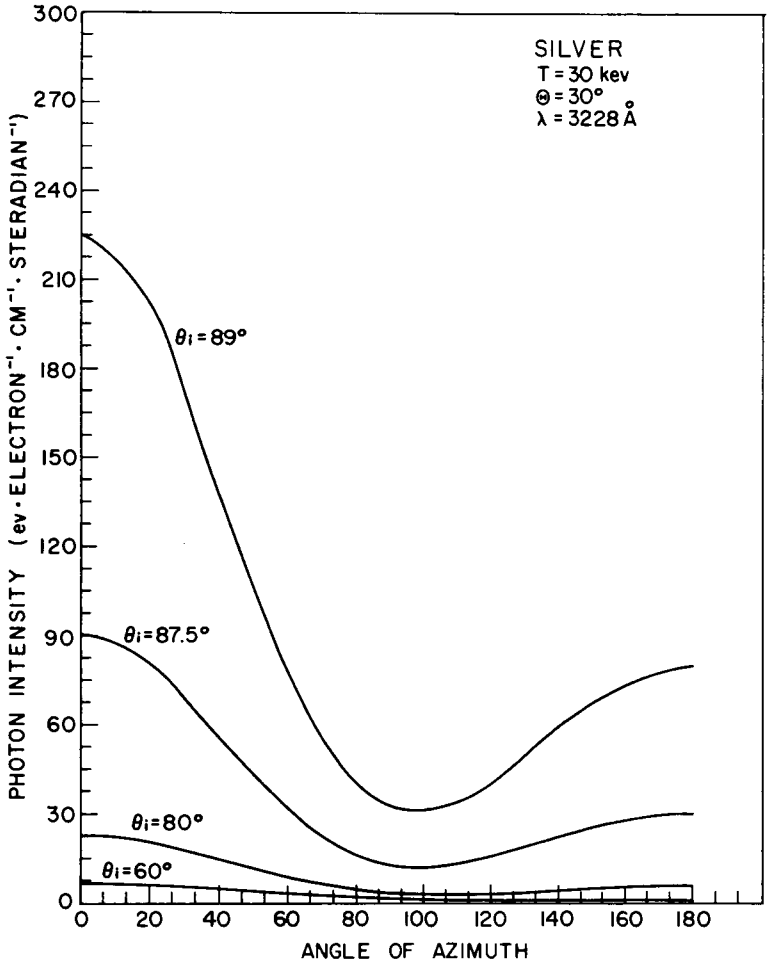

(a) Parallel Polarization

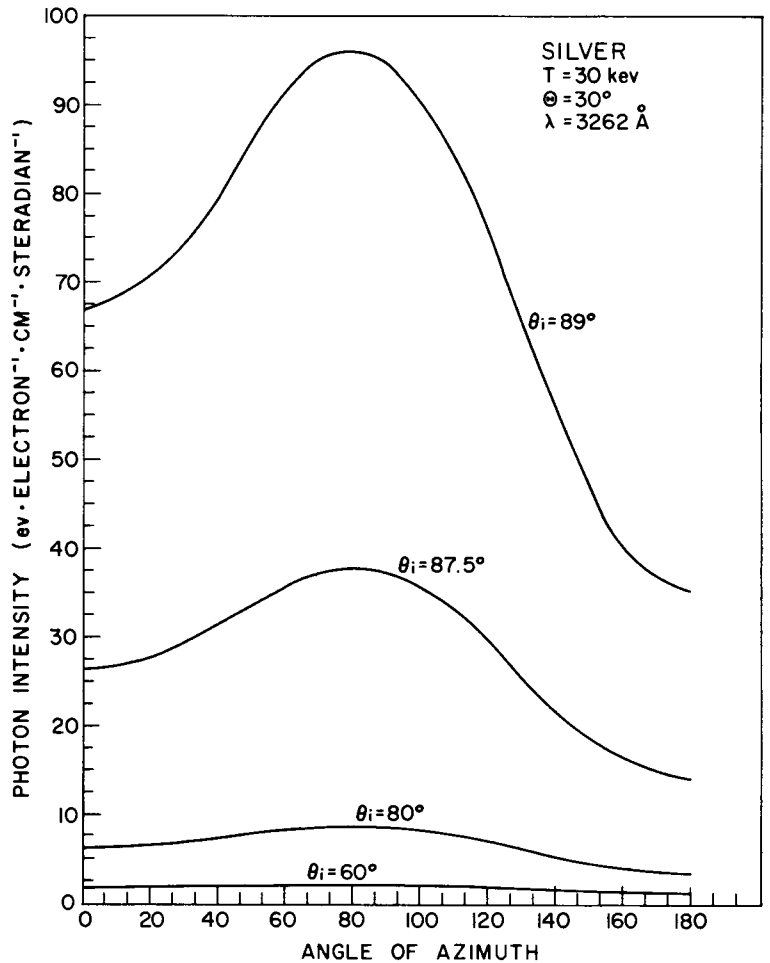

(b) Perpendicular Polarization

Fig. 22. - Photon Intensity vs Angle of Azimuth - Silver, Arbitrary Incidence

a slight "hump" is detectable in the parallel component at approximately 3314 Å which corresponds to the wavelength at the peak of the transition radiation and hence is attributed to this phenomenon and to constructive interference between the bremsstrahlung and the transition radiation. This was determined by making a separate evaluation of a first order approximation to the bremsstrahlung spectrum in which case this "hump" is no longer evident. The intensity of the parallel component is approximately a factor of 3.5 greater than the perpendicular component, which is attributed to the polarization effect on the bremsstrahlung photons by transmission into the vacuum at the boundary. The energy distributions of the photon intensities at the peak wavelength of the spectral distributions are shown in Figure 19 where one notes the characteristic 1/T energy dependence of bremsstrahlung for both polarization components especially at large angles of electron incidence. The dependence of photon intensities upon angle of emission (observation) for the peak wavelength is given in Figure 20 where one notes that in the parallel component there is a shift of the maximum to smaller angles (from $\Theta \simeq 30^\circ$ at $\theta_i = 60^\circ$ to $\Theta \simeq 15^\circ$ at $\theta_i = 89^\circ$) as one goes to grazing electron incidence. One would expect this to occur since as the electron incidence is varied the radiation pattern with respect to the electron motion must move accordingly. The shift is smaller for the perpendicular component which is probably due again to the effect of refraction of the photons at the boundary. The essentially $(\cos \theta_i)^{-1}$ dependence of the photon intensity upon the angle of electron incidence is seen in Figure 21 for both polarization components. One

notes the rapid increase in the photon intensity as one approaches grazing electron incidence. In Figure 22 where the azimuthal dependence is plotted one notes that there is a sharp decrease in the parallel component as one moves away from the plane of emission with a minimum being reached at approximately $\Phi = 100^\circ$ after which the intensity gradually rises again. The intensity in the backward direction is smaller than that in the forward direction, clearly illustrating the forward peaking of the small-angle scattering. One further notes that the perpendicular component shows the opposite effect, i.e., a gradual increase in intensity until $\Phi = 80^\circ$ and then a rapid decrease until $\Phi = 180^\circ$. One would probably expect the maximum and minimum to occur at 90° but the effect of refraction of photons at the boundary modifies this, which is evident from the fact that the angle $\Phi = 100$ at the maximum intensity of the parallel component is the supplement of the angle $\Phi = 80$ at the minimum of the perpendicular component.

3. Comparison with Experimental Results

The incentive for the theoretical considerations at arbitrary incidence was provided by the experimental results reported by Von Blanckenhagen *et al.*[88] and expanded by Boersch *et al.*[89] in which they noted an intense peaking of the photon intensity for grazing electron incidence on thick silver targets in the neighborhood of $\lambda = 3470$ Å. These workers analyzed their data into a "bremsstrahlung" component, assumed to be proportional to E^{-1} and a transition radiation component, assumed to be proportional to E. They

concluded from this analysis and from the dependence of the photon intensity on surface conditions that this peaking was due to the excitation and subsequent radiation of surface plasmons. Since the radiation due to transition radiation and that due to bremsstrahlung will experience constructive and/or destructive interference, the validity of the separation of the experimental spectrum by energy analysis alone may be questioned. Hence, for a comprehensive comparison with the experiments of Boersch *et al.*[88] one would prefer to use data before the energy analysis was made. A comparison of the present theoretical results, under the reported experimental geometry, with the results of Boersch *et al.*[88] is shown in Figure 23 (a, theoretical - b, experimental) where one notes the similarity of the appearances of the peaks. The discrepancy between the wavelength at which the theoretical peaking and the experimental peaking occurs may be attributed to possible differences in the optical constants used for the theoretical results and those of the actual experimental material. Huebner *et al.*[81] have reported that the optical constants of silver vary with the experimental procedure of foil preparation. The experimental intensities of Boersch *et al.*[88] are larger than the present theoretical results by approximately a factor of 5. This same factor of 5 is reported by Boersch *et al.*[88] to be present for the bremsstrahlung at normal incidence and may be due to large angle back scattering of electrons which is not considered in the present work, and/or to uncertainties in the value used for $\langle \Theta^2 \rangle$ in the theoretical calculations. Preliminary calculations on the radiative de-excitation of surface plasmons by collisions with impurities or

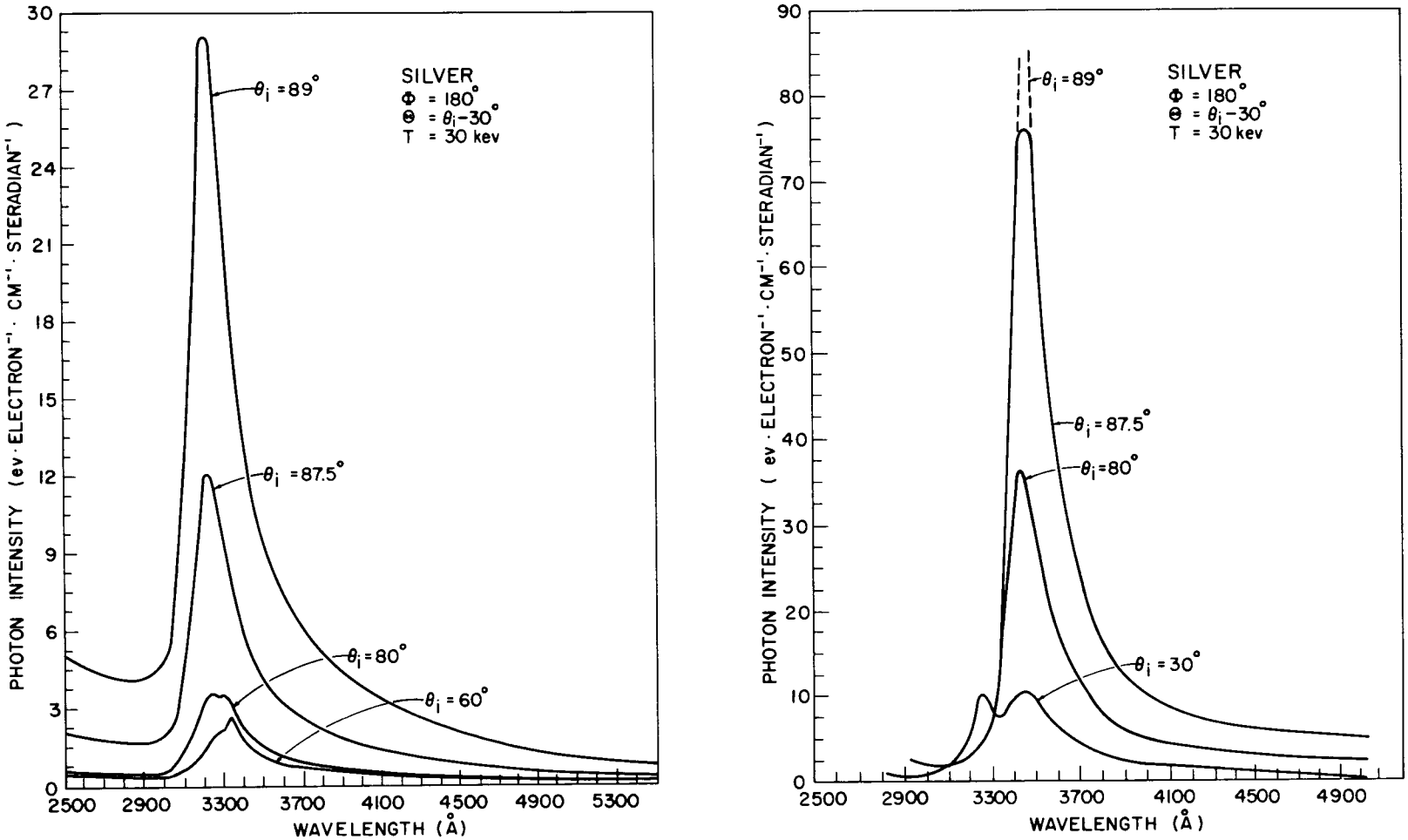

(a) Theory

(b) Experiment

Fig. 23. - Comparison of Photon Intensity vs Wavelength with Experiment - Silver, Arbitrary Incidence

microstructures at the foil surface lead to an $(E \cos^2 \theta_i)^{-1}$ dependence of the intensity of the emitted light. The general trend of the present results on the bremsstrahlung yield leads one to believe that the reported experimental results may be interpreted in terms of the $(\cos \theta_i)^{-1}$ dependence of the bremsstrahlung rather than in terms of the surface plasmon radiation hypothesis. However, the results of Boersch et al.[88] on the dependence of the radiation yield on the conditions of the surface are not predicted by the present work. Obviously, more extensive theoretical considerations on this problem are needed before a definite explanation is possible, but these are beyond the scope of the present work.

B. Conclusions

Theoretical considerations of the radiation emitted from electron irradiated dielectric materials for arbitrary angles of electron incidence have been presented in which one has considered the radiation due to polarization effects of the electron on the dielectric slab (transition radiation) and the scattering of the electron on randomly distributed scattering centers (bremsstrahlung). Comparison of the numerical results thus obtained for normal incidence with the available experiments—although these experiments do not strictly satisfy the theoretical assumptions—show that the agreement for the transition radiation component (parallel polarization) is good for the higher electron energies (T = 100 keV) but not as good at lower energies (T = 25 keV) due to the increased bremsstrahlung effect, being more pronounced for high Z

materials. This leads one to conclude that the underestimate of the bremsstrahlung may be partly due to the uncertainties in the theoretical expression used for the mean square scattering angle $\langle \Theta^2 \rangle$ which of course is critically dependent on the screening parameters and potential functions assumed for the scattering atom, and partly due to the fact that the foils used in the experiments do not satisfy the present theoretical assumptions. Results at grazing electron incidence for silver predict a strong peaking of the bremsstrahlung and would provide an interesting means of studying this radiation in the optical region to perhaps enable one to determine the quantity $\langle \Theta^2 \rangle$ from experimental measurements of the photon intensity of emitted photons from an electron irradiated metal (accompanied by the knowledge of the optical constants n and k of that material). In this manner one can avoid the inherent low intensity of the bremsstrahlung radiation at normal incidence and can observe those photons which are produced near the surface of the material before the electron beam has reached the diffusion stage. Further experimental work with thin foils which satisfy the present theoretical assumptions is certainly desirable.

APPENDIX I

DETERMINATION OF GREEN'S FUNCTION

One solves the wave equation connecting $\vec{\Pi}(\vec{k}, \omega|z)$ with $\vec{J}(\vec{k}, \omega|z)$ by employing the well known Green's function method. Briefly, an equation of the form

$$\frac{d^2\vec{\Pi}(\vec{k},\omega|z)}{dz^2} - \nu'^2\vec{\Pi}(\vec{k},\omega|z) = -\frac{\Lambda}{\epsilon} f(z)\, e^{i\frac{\omega}{v}z} \tag{AI. 1}$$

has the solution

$$\vec{\Pi}(\vec{k},\omega|z) = -\frac{\Lambda}{\epsilon}\int_{-\infty}^{\infty} f(z')\, e^{i\frac{\omega}{v}z'} G(\vec{k},\omega|z-z')\, dz' \tag{AI. 2}$$

where $\vec{G}(\vec{k}, \omega|z-z')$ is a solution of the reduced "unit source" equation

$$\left(\frac{d^2}{dz^2} - \nu'^2\right) G(\vec{k},\omega|z-z') = \delta(z-z_0)\ . \tag{AI. 3}$$

By elementary methods one knows that the solution of Equation (AI. 3) can be written

$$G(\vec{k},\omega|z-z') = A e^{\nu' z}\, St(z'-z) + B e^{-\nu' z}\, St(z-z') \tag{AI. 4}$$

where $St(z'-z)$ is a step function which has the values

$$St(z'-z) = \begin{cases} 0 & z > z' \\ 1 & z < z' \end{cases} \tag{AI. 5}$$

In order that this solution be continuous at the point $z = z'$ one has the

requirement

$$Ae^{\nu' z'} = Be^{-\nu' z'} . \tag{AI. 6}$$

Hence, one can write the solution (AI. 4) as

$$G(\vec{k}, \omega | z-z') = A\left[e^{\nu z} St(z'-z) + e^{-\nu' z + 2\nu' z'} St(z-z')\right] \tag{AI. 7}$$

One can now evaluate the constant A by integrating Equation (AI. 3) to obtain

$$\int_{z'-\epsilon}^{z'+\epsilon} \frac{d^2 G}{dz^2} dz = \int_{z'-\epsilon}^{z'+\epsilon} \delta(z-z') dz = 1 . \tag{AI. 8}$$

This yields

$$A\left(-\nu' e^{-\nu' z'} - \nu' e^{-\nu' z'}\right) = 1 . \tag{AI. 9}$$

Hence one has $A = -e^{-\nu' z'}/2\nu'$ and can write finally

$$G(\vec{k}, \omega | z-z') = -\frac{1}{2\nu'}\left[e^{-\nu'(z'-z)} St(z'-z) + e^{-\nu'(z-z')} St(z-z')\right] \tag{AI. 10}$$

which, employing the properties of the step functions, yields the solution used in Chapter III

$$G(\vec{k}, \omega | z-z') = -\frac{e^{-\nu' |z-z'|}}{2\nu'} . \tag{AI. 11}$$

When, as in Chapter III, $f(z) \neq 0$ for $z < 0$ then one must perform the integration of Equation (AI. 2) over all space. One finds that the solution $\Pi_1(\vec{k}, \omega | z)$ contains a term which must be included with the homogeneous solution of Equation (AI. 1)—applicable to medium 1—to obtain the total

radiation field. Hence one is concerned with an integration of the form

$$\Pi_1(\vec{k},\omega|z) = \frac{\Gamma}{2\nu}\int_{-\infty}^{0} e^{-\nu|z-z'|+i\frac{\omega}{v}z'}\,dz' \tag{AI. 12}$$

which can also be written as

$$\Pi_1(\vec{k},\omega|z) = \frac{\Gamma}{2\nu}\left\{\int_{-\infty}^{z} e^{-\nu|z-z'|+i\frac{\omega}{v}z'}\,dz' + \int_{z}^{0} e^{-\nu|z-z'|+i\frac{\omega}{v}z'}\,dz'\right\}. \tag{AI. 13}$$

In the first integral one has $z' < z$ and $|z - z'| = -(z - z')$ while in the second integral one has $z' > z$ and $|z - z'| = (z - z')$. Then one finds

$$\Pi_1(\vec{k},\omega|z) = \frac{\Gamma}{2\nu}\left\{\frac{e^{-\nu z}e^{(\nu+i\frac{\omega}{v})z}}{(\nu+i\frac{\omega}{v})} + \frac{e^{\nu z}\left(1-e^{-(\nu-i\frac{\omega}{v})z}\right)}{-(\nu-i\frac{\omega}{v})}\right\}. \tag{AI. 14}$$

Simplifying this equation one finds the result

$$\Pi_1(\vec{k},\omega|z) = \frac{\Gamma}{2\nu}\left\{\frac{2\nu\, e^{i\frac{\omega}{v}z}}{\nu^2+\omega^2/v^2} - \frac{e^{\nu z}}{\nu-i\frac{\omega}{v}}\right\}. \tag{AI. 15}$$

Now the first term inside the braces of Equation (AI. 15) represents the transform of the electron's self-field and does not contribute to the radiation field. However one sees that the second term inside the brases does contribute to the radiation field, and hence when employing the Green's function method to obtain a particular solution in medium 1, $z < 0$, one must add the result of the integration in that medium in order to describe the complete radiation field.

APPENDIX II

STATISTICAL AVERAGES

Performing the required integrations in Equations (3.28) over the incident particle's original direction (along the z' axis of Figure 4) one obtains terms of the form

$$\eta_o = C_o \tag{AII.1}$$

$$\eta_1 = C_1 \left| \sum_{=1}^{\infty} \left(e^{-\xi' z'_n} - e^{-\xi' z'_{n-1}} \right) \theta_n \sin \phi_n \right|^2 \tag{AII.2}$$

$$\eta_2 = C_2 \sum_{n=1}^{\infty} \left(e^{-\xi' z'_n} - e^{-\xi' z'_{n-1}} \right) \theta_n^2 \tag{AII.3}$$

and

$$\eta_3 = C_3 \left\{ \sum_{n=1}^{\infty} \left(e^{-\xi' z'_n} - e^{-\xi' z'_{n-1}} \right) \theta_{nx}^2 + \sum_{n=1}^{\infty} \sum_{m=n+1}^{\infty} \theta_{nx} \left(\theta_{mx} - \theta_{m-1,x} \right) \cdot \right.$$

$$\left. \cdot \left(z' - z'_n \right) e^{-\xi' z_n} \right\} \tag{AII.4}$$

where C_o, C_1, C_2, and C_3 are coefficients which are independent of scattering angle or path length. These terms must be averaged according to the probability specified by Equation (3.34). Averaging of the term η_o which does not involve the scattering process yields the term η_o itself. For η_1 one obtains

$$\frac{\langle n_1 \rangle}{C_1} = \prod_{k=1}^{\infty} \int_{z_{k-1}}^{\infty} e^{-\gamma(z'_k - z'_{k-1})} \gamma \, dz'_k \int p(|\vec{\theta}_k - \vec{\theta}_{k-1}|) \, d\vec{\theta}_k \left\{ \sum_{m=1}^{\infty} \sum_{n=1}^{\infty} (e^{-\zeta' z'_n} - e^{-\zeta' z'_{n+1}}) \cdot \right.$$

$$\left. \cdot (e^{-\zeta'^* z'_m} - e^{-\zeta'^* z'_{m+1}}) \, \theta_m \sin\phi_m \, \theta_n \sin\phi_n \right\} \qquad \text{(AII. 5)}$$

Let $s_k = z'_k - z'_{k-1}$, $s_{k-1} = z'_{k-1} - z'_{k-2}$, and so on, then one can write

$$z'_k = s_k + s_{k-1} + \cdots + s_2 + s_1 = \sum_{j=1}^{k} s_j \qquad \text{(AII. 6)}$$

and

$$z'_{k+1} = s_{k+1} + s_k + \cdots + s_2 + s_1 = \sum_{\ell=1}^{k+1} s_\ell \qquad \text{(AII. 7)}$$

which one substitutes into Equation (AII. 5) to obtain

$$\frac{\langle n_1 \rangle}{C_1} = \prod_{k=1}^{\infty} \int_{0}^{\infty} e^{-\gamma s_k} \gamma \, ds_k \int p(|\vec{\theta}_k - \vec{\theta}_{k-1}|) \, d\vec{\theta}_k \left\{ \sum_{m=1}^{\infty} \sum_{n=1}^{\infty} (e^{-\zeta' \sum_{j=1}^{m} s_j} - e^{-\zeta' \sum_{j=1}^{m+1} s_j}) \cdot \right.$$

$$\left. \cdot (e^{-\zeta'^* \sum_{\ell=1}^{n} s_\ell} - e^{-\zeta'^* \sum_{\ell=1}^{n+1} s_\ell}) (\vec{\theta}_m \cdot \hat{\epsilon}_\perp)(\vec{\theta}_n \cdot \hat{\epsilon}_\perp) \right\} \qquad \text{(AII. 8)}$$

where one has used the relationship $\vec{\theta} \cdot \hat{\epsilon}_\perp = \theta \sin\phi$, $\hat{\epsilon}_\perp$ being a unit vector perpendicular to the plane of emission. Consider now a typical term in the angular probabilities, i.e.,

$$I_{mn} = \prod_{k=1}^{\infty} \int p(|\vec{\theta}_k - \vec{\theta}_{k-1}|) \, (\vec{\theta}_m \cdot \hat{\epsilon}_\perp)(\vec{\theta}_n \cdot \hat{\epsilon}_\perp) \, d\vec{\theta}_k \qquad \text{(AII. 9)}$$

which, for $m > n$ is written as

$$I_{mn} = \int p(|\vec{\theta}_1|)\,d\vec{\theta}_1 \int p(|\vec{\theta}_2 - \vec{\theta}_1|)\,d\vec{\theta}_2 \cdots \int p(|\vec{\theta}_m - \vec{\theta}_{m-1}|)\,d\vec{\theta}_m\,(\vec{\theta}_m \cdot \hat{\epsilon}_\perp)(\vec{\theta}_m \cdot \hat{\epsilon}_\perp). \quad \text{(AII. 10)}$$

Now let

$$\begin{aligned} \vec{\alpha}_1 &= \vec{\theta}_m - \vec{\theta}_{m-1} \\ \vec{\alpha}_2 &= \vec{\theta}_{m-1} - \vec{\theta}_{m-2} \\ &\vdots \\ \vec{\alpha}_{r+1} &= \vec{\theta}_{m-r} - \vec{\theta}_{m-r-1} \end{aligned} \quad \text{(AII. 11)}$$

where

$$\vec{\theta}_{m-r-1} = \vec{\theta}_n \,. \quad \text{(AII. 12)}$$

Then adding the terms in Equation (AII. 11) and using Equation (AII. 12) one obtains

$$\vec{\theta}_m = \sum_{q=1}^{m-n} \vec{\alpha}_q + \vec{\theta}_n \quad \text{(AII. 13)}$$

and Equation (AII. 10) is - for m > n.

$$\begin{aligned} I_{mn} = {} & \int p(|\vec{\theta}_1|)\,d\vec{\theta}_1 \int p(|\vec{\theta}_2 - \vec{\theta}_1|)\,d\vec{\theta}_2 \cdots \int p(|\vec{\theta}_n - \vec{\theta}_{n-1}|)\,d\vec{\theta}_n \int p(|\vec{\alpha}_{m-n}|)\,d\vec{\alpha}_{m-n} \cdot \\ & \cdot \int p(|\vec{\alpha}_{m-n+1}|)\,d\vec{\alpha}_{m-n+1} \cdots \int p(|\vec{\alpha}_2|)\,d\vec{\alpha}_2 \int p(|\vec{\alpha}_1|)\,d\alpha_1\,(\vec{\theta}_n \cdot \hat{\epsilon}_\perp) \cdot \\ & \cdot \left[\vec{\alpha}_1 \cdot \hat{\epsilon}_\perp + \vec{\alpha}_2 \cdot \hat{\epsilon}_\perp + \cdots + \vec{\alpha}_{m-n} \cdot \hat{\epsilon}_\perp + \vec{\theta}_n \cdot \hat{\epsilon}_\perp\right]. \end{aligned}$$

The integrations over terms linear in the α's yield zero since positive and negative values are equally probable.

Then one has

$$I_{mn} = \int p(|\vec{\theta}_1|)\, d\vec{\theta}_1 \int p(|\vec{\theta}_2 - \vec{\theta}_1|)\, d\vec{\theta}_2 \cdots \int p(|\vec{\theta}_n - \vec{\theta}_{n-1}|)\, d\vec{\theta}_n\, (\vec{\theta}_n \cdot \hat{\epsilon}_\perp)^2 . \qquad \text{(AII.14)}$$

Now when m = n one has

$$I_{nn} = \int p(|\vec{\theta}_1|)\, d\vec{\theta}_1 \int p(|\vec{\theta}_2 - \vec{\theta}_1|)\, d\vec{\theta}_2 \cdots \int p(|\vec{\theta}_{n-1} - \vec{\theta}_{n-2}|)\, d\vec{\theta}_{n-1} \int p(|\vec{\alpha}_1|)\, d\vec{\alpha}_1 \cdot$$

$$\cdot \left[(\vec{\alpha}_1 \cdot \hat{\epsilon}_\perp)^2 + (\vec{\theta}_{n-1} \cdot \hat{\epsilon}_\perp)^2 + 2 (\vec{\alpha}_1 \cdot \hat{\epsilon}_\perp)(\vec{\theta}_n \cdot \hat{\epsilon}_\perp) \right] \qquad \text{(AII.15)}$$

where one has used $\vec{\theta}_n = \vec{\alpha}_1 + \vec{\theta}_{n-1}$. Neglecting the cross term, which is linear in the quantity α_1 and integration over $d\alpha_1$ will give zero (see page 98), one has

$$I_{nn} = \int p(|\vec{\theta}_1|)\, d\vec{\theta}_1 \int p(|\vec{\theta}_2 - \vec{\theta}_1|)\, d\vec{\theta}_2 \cdots \int p(|\vec{\theta}_{n-1} - \vec{\theta}_{n-2}|)\, d\vec{\theta}_{n-1}\, (\vec{\theta}_n \cdot \hat{\epsilon}_\perp)^2 +$$

$$+ \int p(|\vec{\theta}_1|)\, d\vec{\theta}_1 \int p(|\vec{\alpha}_{n-1}|)\, d\vec{\alpha}_{n-1} \cdots \int p(|\vec{\alpha}_1|)\, d\vec{\alpha}_1\, (\vec{\alpha}_1 \cdot \hat{\epsilon}_\perp)^2 . \qquad \text{(AII.16)}$$

Now the second term in Equation (AII.16) is the average of the projected angle, i.e., $\langle \theta'^2 \rangle$ which can also be written[8] $\langle \theta'^2 \rangle = 1/2\, \langle \theta^2 \rangle$. Hence one has

$$I_{nn} = I_{n-1,n-1} + \tfrac{1}{2} \langle \theta^2 \rangle . \qquad \text{(AII.17)}$$

Now $I_{oo} = 0$, then $I_{11} = 1/2\, \langle \theta^2 \rangle$ and one has the result. $I_{nn} = n/2\, \langle \theta^2 \rangle$; or in the general case

$$I_{mn} = \min(m,n)\, \tfrac{1}{2} \langle \theta^2 \rangle . \qquad \text{(AII.18)}$$

One now writes a typical term in the spatial average as

$$J_{nm} = \int_0^\infty e^{-\gamma s_1} \gamma ds_1 \int_0^\infty e^{-\gamma s_2} \gamma ds_2 \cdots \int_0^\infty e^{-\gamma s_{n+1}} \gamma ds_{n+1} \left[e^{-\zeta'(s_1+s_2+\cdots+s_n)} + \right.$$

$$\left. - e^{-\zeta'(s_1+s_2+\cdots+s_{n+1})} \right] \left[e^{-\zeta'^*(s_1+s_2+\cdots+s_m)} - e^{-\zeta'^*(s_1+s_2+\cdots+s_{m+1})} \right].$$

For n > m one writes this as

$$J_{nm} = \int_\infty^0 e^{-\gamma s_1} (-\gamma ds_1) \int_\infty^0 e^{-\gamma s_2} (-\gamma ds_2) \cdots \int_\infty^0 e^{-\gamma s_{n+1}} (-\gamma ds_{n+1}) \left\{ \exp\left[-(\zeta' + \zeta'^*)(s_1 + \right.\right.$$

$$\left. + s_2 + \cdots + s_m) - \zeta'(s_{m+1} + s_{m+2} + \cdots + s_n) \right] + \exp\left[-(\zeta' + \zeta'^*)(s_1 + s_2 + \cdots + s_{m+1}) + \right.$$

$$\left. - \zeta'(s_{m+2} + s_{m+3} + \cdots + s_{n+1}) \right] - \exp\left[-(\zeta' + \zeta'^*)(s_1 + s_2 + \cdots + s_{m+1}) + \right.$$

$$\left.\left. - \zeta'(s_{m+2} + \cdots + s_n) \right] - \exp\left[-(\zeta' + \zeta'^*)(s_1 + s_2 + \cdots + s_{m+1}) - \zeta'(s_{m+2} + \cdots + s_{n+1}) \right] \right\}$$

which one integrates term by term to obtain

$$J_{nm} = \frac{\gamma^{n-m} \gamma^m}{(\gamma + \zeta')^{n-m} (\gamma + \zeta' + \zeta'^*)^m} + \frac{\gamma^{n-m} \gamma^{m+1}}{(\gamma + \zeta')^{n-m} (\gamma + \zeta' + \zeta'^*)^{m+1}} +$$

$$- \frac{\gamma^{n-m-1} \gamma^{m+1}}{(\gamma + \zeta')^{n-m-1} (\gamma + \zeta' + \zeta'^*)^{m+1}} - \frac{\gamma^{n-m+1} \gamma^m}{(\gamma + \zeta')^{n-m+1} (\gamma + \zeta' + \zeta'^*)^m} .$$

This can be reduced in a simple algebraic manner and one finds, for n > m

$$J_{nm} = \frac{\gamma^n |\zeta'|^2}{(\gamma + \zeta')^{n+1} (\gamma + 2 \operatorname{Re} \zeta')} \left[\frac{\gamma + \zeta'}{\gamma + 2 \operatorname{Re} \zeta'} \right]^m . \tag{AII.19}$$

In the same manner one obtains, for n = m

$$J_{nn} = \frac{\gamma^n |\zeta'|^2 (2)(\gamma + 2 \operatorname{Re} \zeta')}{|\gamma + \zeta'|^2 (\gamma + 2 \operatorname{Re} \zeta')^{n+1}} . \tag{AII.20}$$

Now Equation (AII. 8) can be written in the form

$$\frac{\langle n_1 \rangle}{c_1} = \sum_{m=1}^\infty \sum_{n=1}^\infty I_{nm} J_{nm} = \frac{1}{2} \langle \theta^2 \rangle \sum_{m=1}^\infty \sum_{n=1}^\infty \min(m,n) J_{nm} \tag{AII.21}$$

which becomes

$$\frac{\langle \eta_1 \rangle}{C_1} = \frac{1}{2} \langle \theta^2 \rangle \left\{ \sum_{n=1}^{\infty} \sum_{m=1}^{n-1} m J_{nm} + \sum_{n=1}^{\infty} \sum_{m=n+1}^{\infty} n J^*_{mn} + \sum_{n=1}^{\infty} n J_{nn} \right\}$$

Inserting the values given by Equations (AII. 8) and (AII. 9) one can then evaluate the resulting sums by using the simple binominal relationships[90]

$$\sum_{n=1}^{\infty} n x^n = x(1 + 2x + 3x^2 + \cdots + kx^{k-1} + \cdots +) = x(1-x)^{-2} ; \quad x^2 < 1 \qquad \text{(AII. 22)}$$

and

$$\sum_{n=1}^{\infty} x^{n-1} = (1 + x + x^2 + \cdots + x^{k-1} + \cdots +) = (1-x)^{-1} ; \quad x^2 < 1 \qquad \text{(AII. 23)}$$

to obtain the simple result

$$\frac{\langle \eta_1 \rangle}{C_1} = \frac{\gamma \langle \theta^2 \rangle}{4 \operatorname{Re} \zeta'} \qquad \text{(AII. 24)}$$

but $\gamma \langle \theta^2 \rangle = \langle \Theta^2 \rangle_\ell$ is the mean square scattering angle per unit length. Using Equation (3. 35) and Equation (AII. 3) for η_2, one has

$$\frac{\langle \eta_2 \rangle}{C_2} = \int_0^{\infty} e^{-\gamma z_1'} \gamma dz_1' \int_{z_1}^{\infty} e^{-\gamma (z_2' - z_1')} \gamma dz_2' \cdots \int p(|\vec{\theta}_1|) d\vec{\theta}_1 \int p(|\vec{\theta}_2 - \theta_1|) d\vec{\theta}_2 \cdots$$
$$\cdot \sum_{n=1}^{\infty} (e^{-\zeta' z_n} - e^{-\zeta' z_{n-1}}) \theta_n^2 \qquad \text{(AII. 25)}$$

As before let a typical angular term be given by

$$I_n = \int p(|\vec{\theta}_1|) d\vec{\theta}_1 \int p(|\vec{\theta}_2 - \vec{\theta}_1|) d\vec{\theta}_2 \cdots \int p(|\vec{\theta}_n - \vec{\theta}_{n-1}|) d\vec{\theta}_n \; \theta_n^2$$

which, using substitutions similar to Equation (AII.11) is

$$I_n = \int p(|\vec{\theta}_1|)\, d\vec{\theta}_1 \int p(|\vec{\theta}_2 - \vec{\theta}_1|)\, d\vec{\theta}_2 \cdots \int p(|\vec{\theta}_{n-2} - \vec{\theta}_{n-1}|)\, d\vec{\theta}_{n-2} \int p(|\vec{\alpha}_1|)\, d\alpha_1 \cdot$$

$$\cdot \left[|\vec{\alpha}_1|^2 + |\vec{\theta}_{n-1}|^2 + 2\vec{\alpha}_1 \cdot \vec{\theta}_n \right] . \qquad \text{(AII. 26)}$$

Then neglecting the cross term for the same reason given previously one has

$$I_n = I_{n-1} + \langle \theta^2 \rangle .$$

Now $I_o = 0$, $I_1 = \langle \theta^2 \rangle$ and one obtains the general form

$$I_n = n \langle \theta^2 \rangle \qquad \text{(AII. 27)}$$

A typical spatial term in Equation (AII. 25) is

$$J_n = \int_0^\infty e^{-\gamma s_1} \gamma ds_1 \int_0^\infty e^{-\gamma s_2} \gamma ds_2 \cdots \int_0^\infty e^{-\gamma s_n} \gamma ds_n \left[\exp(-\zeta' \{ s_1 + s_2 + \cdots + s_n \}) + \right.$$

$$\left. - \exp(-\zeta' \{ s_1 + s_2 + \cdots + s_n + s_{n+1} \}) \right]$$

where the substitutions (AII. 6) and (AII. 7) have been used. Equation (AII. 28) can be integrated successively to obtain

$$J_n = \frac{\gamma^n}{(\gamma + \zeta')^n} - \frac{\gamma^{n+1}}{(\gamma + \zeta')^{n+1}} \qquad \text{(AII. 29)}$$

and combining Equations (AII. 27), (AII. 29), and (AII. 25) one has

$$\frac{\langle n_2 \rangle}{c_2} = \langle \theta^2 \rangle \left(1 - \frac{\gamma}{\gamma + \zeta'} \right) \sum_{n=1}^{\infty} n \left(\frac{\gamma}{\gamma + \zeta'} \right)^n . \qquad \text{(AII. 30)}$$

Now using the binomial expansion given by (AII. 22) and simplifying one has

$$\frac{\langle n_2 \rangle}{c_2} = \frac{\gamma \langle \theta^2 \rangle}{\zeta'} = \frac{\langle \theta^2 \rangle_l}{\zeta'} \qquad \text{(AII. 31)}$$

Now the first sum in η_3 is of the same form as that averaged in Equation (AII. 25) except that one now has the projected angle. Hence using (AII. 31) and the relationship $\langle \theta'^2 \rangle = 1/2 \langle \theta^2 \rangle$ one obtains for the average of the first term of η_3

$$\frac{\langle \eta_3 \rangle}{c_3} = \frac{\gamma \langle \theta^2 \rangle}{2\xi'} = \frac{\langle \Theta^2 \rangle_\ell}{2\xi'} \tag{AII. 32}$$

Since one obtains terms of the form $[\langle \theta_{xn} \theta_{xm} \rangle - \langle \theta_{xn} \theta_{xm-1} \rangle]$ the average of the second sum in η_3 yields zero. Performing all of the required averages in the manner described above and combining terms one obtains Equations (3. 35) and (3. 38).

LIST OF REFERENCES

1. G. F. Barker (ed.), Röntgen Rays: Memoirs by Röntgen, Stokes, and J. J. Thomson (Harper and Brothers, New York, 1899).

2. D. L. Webster, Bull. Nat. Res. Council 1, 427 (1920).

3. H. A. Kramers, Phil. Mag. 46, 836 (1923).

4. N. F. Mott, Proc. Roy. Soc. (London) 118, 542 (1928).

5. G. Temple, Proc. Roy. Soc. (London) 121, 673 (1928).

6. A. Sommerfeld, Ann. Physik 11, 257 (1931).

7. H. Bethe and W. Heitler, Proc. Roy. Soc. (London) 146, 83 (1934).

8. J. D. Jackson, Classical Electrodynamics (John Wiley and Sons, Inc., New York, 1962), Chapters 13 and 15.

9. R. L. Gluckstern, M. H. Hull, Jr., and G. Breit, Phys. Rev. 90, 1026 (1953).

10. R. L. Gluckstern and M. H. Hull, Jr., Phys. Rev. 90, 1030 (1953).

11. H. Kulenkampf, M. Scheer, and E. Zeitler, Z. Physik 157, 275 (1959).

12. H. A. Bethe, M. E. Rose, and L. P. Smith, Proc. Am. Phil. Soc. 78, 573 (1938).

13. E. J. Williams, Proc. Roy. Soc. (London) 169, 531 (1939).

14. S. Goudsmit and J. L. Saunderson, Phys. Rev. 57, 24 (1940).

15. H. S. Snyder and W. T. Scott, Phys. Rev. 76, 220 (1949).

16. H. W. Lewis, Phys, Rev. 78, 526 (1950).

17. G. Molière, Z. Naturforsch. 3a, 78 (1948).

18. H. A. Bethe, Phys. Rev. 89, 1256 (1953).

19. G. Molière, Z. Naturforsch. 2a, 133 (1947).

20. B. P. Nigam, M. K. Sundaresan, and Ta-You Wu, Phys. Rev. 115, 491 (1959).

21. R. H. Dalitz, Proc. Roy. Soc. (London) A206, 509 (1951).

22. W. G. Simon, Phys. Rev. 136, B410 (1964).

23. R. D. Reed and J. S. Nodvik, Phys. Rev. 135, B199 (1964).

24. A. O. Hanson, L. H. Lanzl, E. M. Lyman, and M. B. Scott, Phys. Rev. 84, 634 (1951).

25. I. Gol'dman, Soviet Phys.—JETP 11, 1341 (1960).

26. I. V. Andreev, Soviet Phys.—JETP 19, 1188 (1964).

27. R. H. Ritchie, J. C. Ashley, and L. C. Emerson, Phys. Rev. 135, A759 (1964).

28. I. M. Frank, Soviet Phys.—Usp. 4, 740 (1962).

29. I. M. Frank and Ig. Tamm, Dokl. Akad. Nauk SSSR 14, 109 (1937).

30. P. A. Cerenkov, Dokl. Akad. Nauk SSSR 2, 451 (1934).

31. Eve Curie, Madame Curie (Heinemann, London, 1941).

32. L. Mallet, C. R. Acad. Sci. (Paris) 183, 274 (1926).

33. L. Mallet, C. R. Acad. Sci. (Paris) 187, 222 (1928).

34. L. Mallet, C. R. Acad. Sci. (Paris) 188, 445 (1929).

35. S. I. Vavilov, Dokl. Akad. Nauk SSSR 2, 457 (1934).

36. P. A. Cerenkov, Dokl. Akad. Nauk SSSR 3, 413 (1936).

37. P. A. Cerenkov, Dokl. Akad. Nauk SSSR 14, 101 (1937).

38. P. A. Cerenkov, Dokl. Akad. Nauk SSSR 14, 105 (1937).

39. P. A. Cerenkov, Phys. Rev. 52, 378 (1937).

40. Ig. Tamm, Zh. Fiz. SSSR 1, 439 (1939).

41. V. L. Ginsburg, Zh. Fiz. SSSR 2, 441 (1940).

42. J. V. Jelley, Cerenkov Radiation and Its Applications (Pergamon Press, London, 1958).

43. G. Beck, Phys. Rev. 74, 795 (1948).

44. G. M. Garibian, Soviet Phys.—JETP 6, 1079 (1958).

45. E. Rudberg, Proc. Roy. Soc. (London) A127, 111 (1930).

46. E. Rudberg and J. C. Slater, Phys. Rev. 50, 150 (1936).

47. D. Bohm and D. Pines, Phys. Rev. 82, 625 (1951).

48. D. Pines and D. Bohm, Phys. Rev. 85, 338 (1952).

49. D. Bohm and D. Pines, Phys. Rev. 72, 609 (1953).

50. D. Pines, Phys. Rev. 92, 626 (1953).

51. D. Bohm and E. P. Gross, Phys. Rev. 75, 1851 and 1864 (1949).

52. R. A. Ferrell, Phys. Rev. 101, 554 (1956).

53. L. Marton and L. B. Leder, Phys. Rev. 94, 203 (1954).

54. D. Pines, Rev. Mod. Phys. 28, 184 (1956).

55. R. H. Ritchie, Phys. Rev. 106, 874 (1957).

56. R. A. Ferrell, Phys. Rev. 111, 1214 (1958).

57. R. H. Ritchie and H. B. Eldridge, Phys. Rev. 126, 1935 (1962).

58. I. Frank and V. Ginsburg, J. Phys. (USSR) 9, 353 (1945).

59. G. A. Askar'ian, Soviet Phys.—JETP 3, 613 (1955).

60. Ia. B. Fainberg and N. A. Khizhniak, Soviet Phys.—JETP 5, 720 (1957).

61. G. M. Garibian, Soviet Phys.—JETP 8, 1003 (1959).

62. V. E. Pafomov, Soviet Phys. —JETP 5, 1074 (1957).

63. V. E. Pafomov, Soviet Phys. —JETP 6, 829 (1958).

64. G. M. Garibian and G. A. Chalikian, Soviet Phys. —JETP 8, 894 (1959).

65. G. M. Garibyan, Soviet Phys. —JETP 10, 372 (1960).

66. K. A. Barsukov, Soviet Phys. —JETP 10, 787 (1960).

67. G. M. Garibian, Izv. Akad. Nauk Ser. Fiz.-Mat. Nauk Arm. SSR 11, 7 (1958).

68. N. A. Korkhmazyan, Izv. Akad. Nauk Ser. Fiz.-Mat. Nauk Arm. SSR 11, 87 (1958)

69. G. M. Garibyan, Soviet Phys. —JETP 12, 237 (1961).

70. S. P. Kapitza, Soviet Phys.—JETP 12, 954 (1961).

71. M. L. Ter-Mikaelyn and A. D. Gazazyan, Soviet Phys. —JETP 12, 1183 (1961).

72. E. A. Kaner and V. M. Yakovenko, Soviet Phys. —JETP 15, 330 (1962).

73. J. C. Ashley and R. H. Ritchie, J. Appl. Phys. 35, 2313 (1964).

74. J. A. Stratton, Electromagnetic Theory (McGraw-Hill, Inc., New York, 1941).

75. H. Margenau and G. M. Murphy, The Mathematics of Physics and Chemistry (D. Van Nostrand Co., Inc., Princeton, 1961), 2nd edition, Section 12.10.

76. H. Jeffreys and B. S. Jeffreys, Methods of Mathematical Physics (University Press, Cambridge, 1950), 2nd edition, p. 503.

77. P. M. Morse and H. Feshbach, Methods of Theoretical Physics (McGraw-Hill, Inc., New York, 1953).

78. Shin-R Lin, Phys. Rev. 133, A065 (1964).

79. W. J. Byatt, Phys. Rev. 104, 1298 (1956).

80. F. C. Bauer, H. Rutishauser, and E. Stiefel, Proc. Sym. Appl. Math. 15, 199 (1963).

81. R. H. Huebner, E. T. Arakawa, R. A. MacRae, and R. N. Hamm, Jr., J. Am. Opt. Soc. 54, 1434 (1964).

82. H. Ehrenreich and H. R. Philipp, Phys. Rev. 128, 1622 (1962).

83. R. S. Minor, Ann. Physik 10, 581 (1903).

84. R. Philip, Opt. Acta 7, 49 (1960).

85. L. C. Emerson, E. T. Arakawa, R. H. Ritchie, and R. D. Birkhoff, "Emission Spectra of Electron Irradiated Foils," ORNL-3450 (July 30, 1963).

86. D. C. Hammer, E. T. Arakawa, L. C. Emerson, and R. D. Birkhoff, "Optical Emission from Electron Irradiated Thin Gold Foils," ORNL-3468 (August 26, 1963).

87. See Reference 85, p. 147.

88. P. Von Blanckenhagen, H. Boersch, D. Fritsche, H. G. Seifert, and G. Sauerbrey, Phys. Letters 11, 296 (1964).

89. H. Boersch, P. Dobberstein, D. Fritzsche, and G. Sauerbrey (private communication).

90. C. D. Hodgman (ed.), C. R. C. Standard Mathematical Tables (Chemical Rubber Publishing Co., Cleveland, 1960), 12th edition, p. 370.

INTERNAL DISTRIBUTION

1. Biology Library
2-4. Central Research Library
5. Reactor Division Library
6-7. ORNL-Y-12 Technical Library Document Reference Section
8-57. Laboratory Records Department
58. Laboratory Records, ORNL R. C.
59-83. R. H. Ritchie
84-108. R. D. Birkhoff
109. E. T. Arakawa
110. L. C. Emerson
111. R. N. Hamm
112. H. H. Hubbell, Jr.
113. G. S. Hurst
114. W. H. Jordan
115. C. E. Larson
116. H. G. MacPherson
117. K. Z. Morgan
118. D. R. Nelson
119. H. C. Schweinler
120. M. J. Skinner
121. J. L. Stanford
122. A. M. Weinberg
123. G. M. Fair (consultant)
124. J. C. Frye (consultant)
125. E. P. Odum (consultant)
126. R. L. Platzman (consultant)
127. H. O. Wyckoff (consultant)
128. J. B. Hurst (consultant)

EXTERNAL DISTRIBUTION

129-153. H. J. Howe, Jr., Radiation Safety Section, Industrial Hygiene and Safety Division, Argonne Nat'l. Laboratory, Argonne, Illinois
154. W. G. Holliday, Dept. of Phys., Vanderbilt University, Nashville, Tennessee
155. F. Abeles, Institut d'Optique, Paris, France
156. W. V. Bouldin, Dept. of Physics, Vanderbilt University, Nashville, Tennessee
157. J. C. Ashley, Marshal Space Flight Center, Huntsville, Alabama
158. W. T. Pinkston, Dept. of Physics, Vanderbilt University, Nashville, Tennessee
159. N. T. Barr, Division of Biology and Medicine, USAEC, Washington, D. C.
160. M. J. Berger, National Bureau of Standards, Division 403, Washington, D. C.
161. H. Boersch, I. Physikalischen Institut der Technischen Universitat, Berlin, Germany
162. W. Brandt, Department of Physics, New York University, New York 3, New York
163. C. J. Calbick, Bell Telephone Laboratories, Murray Hill, New Jersey
164. R. M. Chaduhri, High Tension and Nuclear Research Laboratory, Church Road, Government College, P. O. Box 701, Lahore, W. Pakistan
165. B. T. Chertok, National Bureau of Standards, Washington, D. C.
166. J. P. Davey, Cambridge University, Dept. of Physics, Cavendish Laboratory, Cambridge, England

167. W. D. Deeds, Department of Physics, University of Tennessee, Knoxville, Tennessee
168. H. Ehrenreich, Physics Department, Harvard University, Cambridge, Massachusetts
169. Mlle. D. Fabre, CNRS, Laboratories de Bellevue, Bellevue, France
170. U. Fano, National Bureau of Standards, Washington, D. C.
171. R. A. Ferrell, Physics Department, University of Maryland, College Park, Maryland
172. H. A. Fowler, Electron Physics Section, National Bureau of Standards, Washington, D. C.
173. D. C. Hammer, NASA, Lewis Research Center, Cleveland, Ohio
174. W. R. Hunter, U.S. Naval Research Laboratory, Washington 25, D. C.
175. W. C. H. Joiner, Westinghouse Electric-Aerospace Division, Box 746, Baltimore, Maryland
176. J. Kastner, Argonne National Laboratory, Argonne, Illinois
177. H. Kanter, Aerospace Corporation, Los Angeles, California
178. O. H. McMahan, Physics Department, Texas Western College, El Paso, Texas
179. C. A. Klein, Raytheon Company, Waltham 54, Massachusetts
180-181. C. W. Litton, ARL(ARX), Wright-Patterson AFB, Ohio
182. S. A. Lough, Division of Biology and Medicine, USAEC, Washington, D. C.
183. R. P. Madden, National Bureau of Standards, Washington 25, D. C.
184. L. Marton, National Bureau of Standards, Washington, D. C.
185. H. Mayer, Physikalishes Institut des Technischen Hoshschule, Clausthal, Germany
186. Earl W. McDaniel, School of Physics, Georgia Institute of Technology, Atlanta, Georgia
187. H. Mendlowitz, National Bureau of Standards, Atomic Physics Division, Washington, D. C.
188. K. P. Miyake, Institute for Optical Research, Kyoiku University, Tokyo, Japan
189. A. H. Nielsen, Department of Physics, University of Tennessee, Knoxville, Tennessee
190. A. Otto, II. Physikalisches Institut der Universitat Munchen, Munchen, 13, Germany
191. H. R. Philipp, General Electric Research Laboratory, P. O. Box 1088, Schenectady, New York
192. J. C. Phillips, Department of Physics, University of Chicago, Chicago, Illinois
193. D. Pines, Department of Physics, University of Illinois, Urbana, Illinois
194. C. J. Powell, National Bureau of Standards, Washington, D. C.
195. J. J. Quinn, R.C.A. Laboratories, Princeton, New Jersey
196. H. Raether, Institut fur Angewandte Physik der Universitat, Hamburg, Germany

197. O. P. Rustgi, Electromagnetics Lab Research Department, Northrup Space Laboratories, 1111 E. Broadway, Hawthorne, California
198. S. Robin, Faculte des Sciences, Rennes, France
199. P. Rouard, Faculte des Sciences, Laboratoire de Physique Generale, Marseille, France
200. J.A.R. Samson, Geophysics Corporation of America, Bedford, Mass.
201. T. Sasaki, College of General Education, University of Tokyo, Komaba, Tokyo, Japan
202. G. Sauerbrey, Physikalische-Technischev Bundensanstalt, Berlin-Charlottenburg, Germany
203. P. Schmüser, Institut fur Angewandte Physik der Universitat, Hamburg, Germany
204. J. A. Simpson, National Bureau of Standards, 312 Riley St., Falls Church, Virginia
205. W. Steinmann, II. Physikalisches Institut der Universitat, Munchen, Munchen 13, Germany
206. E. A. Stern, University of Maryland, Department of Physics, College Park, Maryland
207. J. B. Swan, Department of Physics, University of Western Australia, Nedlands, Western Australia
208. Nils Swanson, National Bureau of Standards, West 103, Washington 25, D.C.
209. E. A. Taft, General Electric Research Laboratory, P. O. Box 1088, Schenectady, New York
210. J. Thomas, Dept. of Public Health, Yale University, New Haven, Connecticut
211. Ye-Yung Teng, Department of Physics and Astronomy, University of Maryland, College Park, Maryland
212. H. J. Watson, Brown Engineering Co., Huntsville, Alabama
213. G. L. Weissler, University of Southern California, Department of Physics, Los Angeles, California
214. P. R. Wessel, U. S. Naval Ordnance Laboratory, Silver Spring, Maryland
215. P. A. Wolff, Bell Telphone Laboratories, Murray Hill, New Jersey
216. R. W. Wood, Division of Biology and Medicine, USAEC, Washington, D.C.
217. S. Yamaguchi, Department of Physics, Tokyo Metropolitan University, Setagaya-Ku, Tokyo, Japan
218. R. L. Schumaker, Physics Department, Texas Western College, El Paso, Texas

219-220. Health Physics Fellowship Office, Oak Ridge Institute of Nuclear Studies, Oak Ridge, Tennessee

221. Research and Development Division, AEC, ORO

222-236. Division of Technical Information Extension